DOMINANT AND CONTEXT-SPECIFIC CONTROL OF ENDODERMAL ORGAN ALLOCATION BY PTF1A

By

Spencer G. Willet

Dissertation

Submitted to the Faculty of the

Graduate School of Vanderbilt University

in partial fulfillment of the requirements

for the degree of

DOCTOR OF PHILOSOPHY

in

Cell and Developmental Biology

December, 2014

Nashville, Tennessee

Approved:

Guoqiang Gu, Ph.D.

Roland W. Stein, Ph.D.

Michelle Southard-Smith, Ph.D.

Christopher V. E. Wright, D.Phil.

ACKNOWLEDGEMENTS

I would like to thank my mentor, Chris Wright; my thesis committee – Roland Stein, Michelle Southard-Smith, and Guoqiang Gu; members of the Wright lab; the Department of Cell and Developmental Biology and the Program in Developmental Biology; and my parents and sisters. Special thanks to Ray MacDonald, Anne Grapin-Botton, and Mark Magnuson for sharing mouse reagents with me pre-publication and making this thesis possible.

TABLE OF CONTENTS

Page

LIST OF FIGURES

CHAPTER I

INTRODUCTION

The definitive endoderm gives rise to the epithelial lining of the digestive, respiratory, and urogenital tracts and associated organs. Processes such as gas exchange, food digestion, nutrient absorption, and waste removal functionally depend on these endodermal tissues. Congenital defects, chronic disease states, and metaplasia within endodermal tissues cause significant challenges to human health worldwide. Careful study of the developmental processes that lead to the formation of endodermal organs can help the generation of new treatments for these disease conditions. One potential emerging treatment for these conditions involves the generation of functional differentiated cell types from pluripotent cell sources (via in vitro directed differentiation) to replace damaged or non-functional tissues. The basis for this type of treatment is a sophisticated understanding of the development of endodermal organs, from the pluripotent stem cell stage into the properly terminally differentiated cell types.

The pancreas is an endodermally derived organ with two major functional compartments, exocrine and endocrine. The exocrine pancreas, composed of acinar and duct cells, secretes and carries digestive enzymes (acinar cells) and bicarbonate (duct cells) into the duodenum to aid in food digestion and de-acidify contents released from the stomach. The endocrine pancreas is composed of five principal cell types – alpha (glucagon-secreting), beta (insulin), delta (somatostatin), epsilon (ghrelin), or PP (pancreatic polypeptide) – arranged in islets of Langerhans that regulate metabolism by secreting hormones into the bloodstream. Loss or dysfunction of the β-cell in the endocrine pancreas causes the disease diabetes. Both type I and type II diabetes result in the inability to generate sufficient insulin, which is secreted by the β-

cell to regulate blood sugar levels. In type I diabetes, β-cells are destroyed by auto-immune attack leading to a complete lack of insulin-producing cells in the patient's pancreas. Type II diabetes generally develops due to insulin resistance in peripheral tissues. Type II diabetes patients have insulin-producing β-cells, but cannot produce enough insulin to properly regulate blood sugar levels. The disease incidence of type II diabetes is rapidly increasing in the western world due to poor diet and lack of exercise, such that there is a significant need for better, longer-lasting treatments for diabetes.

As mentioned above, one still-hypothetical treatment for diabetes is to replace lost or dysfunctional pancreatic β-cells with new β-cells to bolster the production of insulin. Treatment of diabetes with bona fide β-cells has many potential benefits over the current, most broadly used treatment for diabetes – patient-monitored insulin administration. Insulin is only one factor that is produced by β-cells that impacts overall health. By supplying functional β-cells, they would contain all these necessary molecular components (c-peptide, amylin, etc.) in addition to insulin. β-cells also would respond to changes in blood sugar levels in a more physiological manner compared to the blunt insulin doses given by the patient. Supplying functional cell types to patients would also eliminate the need for a motivated patient to properly monitor blood sugar levels to control the disease. In addition to learning how to generate new sources for functional β-cells, the status of autoimmune attack in type I diabetes patients and lifestyle changes in type II diabetes patients will still need to be addressed before these treatments can be a successful therapy for patients.

Cadaveric islets, replication of pre-existing β-cells, transdifferentiation of other cell types into β-cells, or generating new β-cells from pluripotent cell sources are all potential ways of providing the patient with a fresh complement of functional β-cells. Given the scarcity of

cadaveric islets and how difficult it is to genetically modify cells within the human body in a clinically relevant manner, the generation of β-cells from pluripotent cell sources, such as human embryonic stem (hES) cells and induced pluripotent stem (iPS) cells, is perhaps the most promising way to generate new functional β-cells for clinical use.

The generation of functional β-cells from pluripotent cell sources is a complex developmental biology problem. The most common-sense way to generate a β-cell from a pluripotent cell source is to transition the pluripotent cells through developmental states mimicking those found during embryogenesis leading to the generation of β-cells. Known developmental progenitor states that lead to the generation of β-cells, from earliest to latest, include definitive endoderm, regionalized posterior foregut, pancreatic progenitors, pancreatic endocrine progenitors, and finally, committed and differentiated pancreatic β-cells. Even the most advanced directed-differentiation protocols fail to produce large numbers of functional, glucose-responsive β-cells. Instead these protocols generate low numbers of non-functional, multi-hormonal pancreatic endocrine cells (Kroon et al., 2008). The inability to generate large numbers of functional β-cells is likely due to our incomplete knowledge of the important cues required during various developmental stages to generate a functional β-cell. Another problem with current studies is that they solely focus on the generation of β-cells. It may be necessary to generate the entire islet as organoids, including other endocrine cell types and support cells like the neural crest and pancreatic mesenchyme in order to generate fully functional β-cells.

Careful genetic studies using developmental models is one way to further our understanding of the factors that can deterministically trigger the correct series of progenitor-precursor-differentiated transitions that eventually lead to functional, mature pancreatic β-cells. The main focus of my thesis is to understand the role of the transcription factor Ptf1a in the

acquisition of organ identity and in the control of cell fate choice during pancreas organogenesis. Ptf1a is a basic helix-loop-helix transcription factor that is specifically expressed within pancreatic progenitors during early endodermal development. In subsequent stages, Ptf1a expression is maintained within multipotent progenitor cells in the growing pancreatic bud and, later, in all developing acinar cells (Krapp et al., 1998). Ptf1a is one of the components of a trimeric transcriptional activator complex, PTF1, which also contains a canonical E-protein (E12, E47, HEB) and the downstream mediator of Notch signaling, RBPJk (also referred to as CSL) (Beres et al., 2006).

Both Ptf1a expression and its interaction with RBPJκ are necessary for pancreatic specification: endodermal progenitors almost completely fail to be specified to the pancreatic lineage and become productively incorporated into the multipotency progenitor programs of adjacent organ primordia such as the bile duct and intestine in these conditions (Kawaguchi et al., 2001; Masui et al., 2008). Ptf1a is also required to determine interneuron cell types in other non-endoderm organ systems including the retina, cerebellum, and spinal cord. In the absence of Ptf1a in these organs, cells that would normally adopt Ptf1a-controlled inhibitory interneuron cell fates differentiate into other neural cell lineages. For example, in the cerebellum, Ptf1a is required to specify GABAergic interneurons from the ventricular zone. In the absence of Ptf1a, these cells adopt an excitatory (glutamatergic) cell fate (Glasgow et al., 2005; Hoshino et al., 2005; Fujitani et al., 2006). Misexpression of Ptf1a in various model organisms has addressed the complementary issue: to what degree can Ptf1a dominantly control cell identity (Huang et al., 2008; Jusuf et al., 2011; Lelièvre et al., 2011). Ectopic expression of Ptf1a in retinal progenitor cells showed that Ptf1a is sufficient to determine the horizontal and amacrine cell fates (both of these cell types are lost in the absence of Ptf1a) over ganglion and photoreceptor cell fates.

The knockout phenotype of Ptf1a, and the expression pattern of Ptf1a during later pancreas development, implicates Ptf1a as an important specifier of cell identity during many stages of pancreas development. In the results sections of my thesis, I will detail the generation and use of genetic systems to modify or eliminate the expression of Ptf1a during pancreatic specification and organogenesis to explore its instructive role in these processes. To provide context for the role of Ptf1a during pancreatic development, the next portion of this introduction will detail the specification and regionalization of definitive endoderm, which gives rise to all gut-derived organs in the adult.

Endodermal Specification

The definitive endoderm is formed by the ingression of epiblast cells through the primitive streak of the gastrulation-stage mouse embryo. Egressing endodermal progenitor cells incorporate into (and displace most of) the visceral endoderm, a single-layered epithelium beneath the epiblast, by single-cell intercalation (Kwon et al., 2008). The first epiblast cells to enter the primitive streak give rise to medial and lateral anterior endoderm (and mesoderm), while progenitors that enter the primitive streak at later stages give rise to more posterior endoderm (Lawson et al., 1986; Lawson and Schoenwolf, 2003). By the end of gastrulation, the definitive endoderm is a single-layered epithelial sheet residing on the outside of the embryo. Some visceral endoderm progenitors are retained within definitive endoderm and may give rise to a small portion of embryonic (as opposed to extraembryonic – the fate of most of the displaced visceral endoderm) structures (Kwon et al., 2008). Near the completion of gastrulation, the endodermal sheet becomes shaped into pockets at the anterior and posterior end of embryo: the foregut and hindgut pockets, respectively. The endodermal tube is completed by the caudal and rostral spread, respectively, of the foregut and hindgut pockets – zippering has

been suggested as an appropriate term for this process, similar to the neural tube. As a whole, the formation of a nascent endodermal cylinder, growth of the lateral plate mesoderm, and the turning of the mouse embryo transform the endoderm from a simple sheet on the outside of the embryo to an internal tube (Fig. 1.1).

Endodermal Regionalization

The following description of endodermal specification, regionalization, and differentiation will thematically emphasize the coordination of these processes by the sequential activation of transcription factors, as these molecules were the focus of my thesis. Less will be presented about the specific detailed roles of individual signaling molecules, although there will be some description of these factors when relevant to describing the expression or behavior of transcription factors.

During definitive endoderm specification (for a detailed review see, Grapin-Botton and Constam, 2007) a highly evolutionarily conserved gene regulatory network controlled by transcription factors (such as Mixl1, Sox17, Foxa2, Gata4/6, and Eomes) is enacted to ensure the segregation of the endodermal progenitors from mesodermal progenitors and promote endodermal progenitor survival (Hart et al., 2002; Kanai-Azuma et al., 2002; Ang and Rossent, 1994; Sasaki and Hogan, 1993; Morrisey et al., 1998; Jacobsen et al., 2002; Russ et al., 2000).

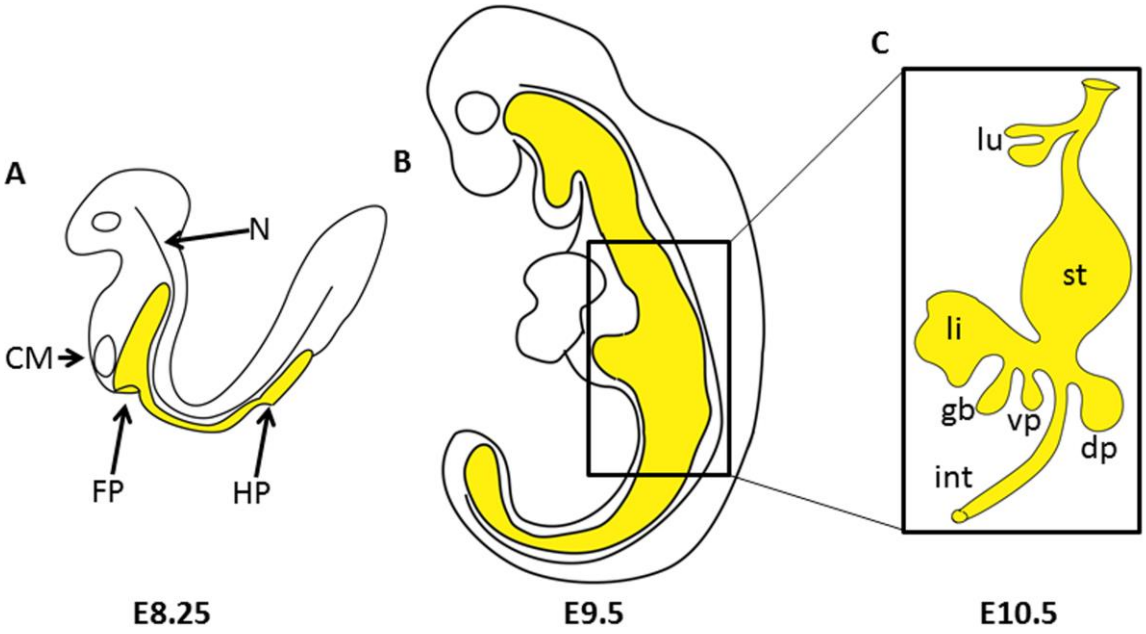

Figure 1.1 Morphogenetic changes in the endoderm during development. Endoderm is yellow in all schematics. (A) In the E8.25 embryo, the endoderm forms two pockets at the respective anterior and posterior end of the embryo. "Zippering" of the endodermal sheet changes the endoderm into a gut tube. Endodermal progenitors are always in close contact with different [as discussed] mesodermal tissues. The ventral foregut is (transiently?) located close to the cardiac mesoderm (CM, arrow), while the dorsal foregut is in proximity to the notochord (N, arrow). FP, foregut pocket; HP, hindgut pocket (B) E9-9.5 embryo. Budding of many endodermal organs starts around E9.5. (C) E10.5 posterior region of the foregut. By E10.5, many organ buds are proliferating substantially and growing into the surrounding mesenchyme. lu, lung; li, liver; vp, ventral pancreas; dp, dorsal pancreas; gb, gall bladder; int, intestine.

During later stages of endodermal development, many of these transcription factors have important roles in endodermal development. A good example of the way in which these genes are reiteratively used is *Sox17*. *Sox17* is essential for endoderm formation, and is expressed throughout the early definitive endoderm (Kanai-Azuma et al., 2002). During subsequent developmental stages, *Sox17* expression recedes from rostral and caudal endodermal derivatives and becomes restricted to the prospective posterior ventral foregut that will go on to produce the extra hepatic biliary system (EHBS) and ventral pancreas. Using *Foxa3*^{Cre} to conditionally remove *Sox17* function during endodermal regionalization causes defects in the specification of the gall bladder and cystic duct (Spence et al., 2009). Gata4 and Gata6 are also an example of transcription factors that are initially expressed throughout the definitive endoderm before becoming restricted to specific regions of the developing endoderm. Gata4 and Gata6 become restricted to the posterior foregut and have important roles in liver, pancreas and stomach development (Jacobsen et al 2002, Watt et al., 2007; Carrasco et al., 2012; Xuan et al., 2012). In contrast, other genes such as Foxa2 maintain broad expression throughout the endoderm from its initial formation and through the processes of regionalization, with important roles in the organogenesis of most endodermal organs (for review see, Friedman and Kaestner, 2006). Foxa2 has been shown to act as a pioneer factor. Pioneer factors bind to and open chromatin, allowing other regionally-expressed factors to access DNA and coordinate assembly of gene regulatory networks.

The regional identity of the endoderm is thought to be influenced by the cues that endodermal progenitors receive from their post-gastrulation environment. This environment includes mesodermal tissue, which is capable of influencing gene expression in the endodermal progenitors, ultimately stimulating the acquisition of regional competence states that

promote/restrict the downstream organ identities. The type of mesodermal tissue that endodermal progenitors are located next to depends on their anterior-posterior and dorsal-ventral location in the gut tube.

The endodermal gut tube is generally divided into three regions along the anterior-posterior axis of the embryo: foregut, midgut, and hindgut. Now moving directly to the main focus of this thesis, the *Ptf1a*-expressing pancreatic progenitors arise from a particular region of the posterior foregut. The posterior foregut also gives rise to the posterior stomach, anterior duodenum, liver, gall bladder, and EHBS. The anterior foregut produces the endodermal derivatives that extend from the oral endoderm down to but not including the posterior-most antral stomach (in anterior to posterior sequence): salivary gland, pharynx, thyroid, parathyroid, thymus, lung, trachea, esophagus, forestomach, and glandular stomach. The midgut gives rise to the small intestine, and the hindgut produces the large intestine and urogenital tract.

As mentioned above, after formation of the nascent gut tube, many important transcription factors become regionally expressed within the endoderm, often with spatiotemporally dynamic patterns. *Sox2* and *Cdx2* are expressed in the most rostral and caudal endoderm, respectively, during early regionalization (Fig. 1.2). During subsequent development, *Sox2* expression spreads posteriorly such that it marks the entire anterior endoderm from the prospective oral endoderm up to and including the posterior stomach. *Cdx2* spreads anteriorly to mark the posterior endoderm that encompasses the region extending from the ano-rectal junction to and including the duodenum (Sherwood et al., 2009). Genetic manipulation of either *Sox2* or *Cdx2* indicates that both are important for maintaining the regional identity of the endoderm. Inactivation of either gene causes massive changes in cell identity within their respective expression domains. Complete knockout of *Sox2* in the early endoderm has not been

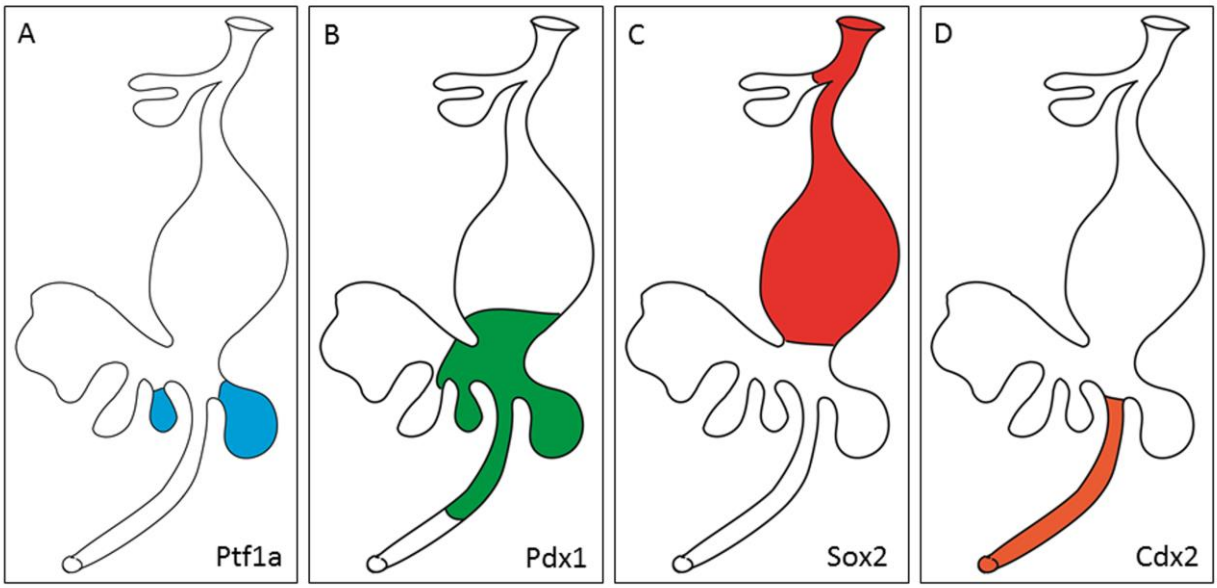

Figure 1.2 Schematic representations of the expression domains of various fate-instructive transcription factors in the E10.5 foregut endoderm. The approximate expression domains are: (A) *Ptf1a*: restricted to the dorsal and ventral pancreatic buds. (B) *Pdx1*: regionally expressed in the posterior foregut including the area producing the posterior stomach, anterior duodenum, pancreatic buds, and proximal EHBS. (C) *Sox2*: expressed throughout the anterior foregut extending from the prospective oral endoderm to the glandular stomach. *Sox2* is not expressed in the lung bud at this stage, but it is expressed in the proximal lung and trachea at later stages of development. (D) *Cdx2*: expressed throughout the posterior derivatives of the endoderm including the anterior duodenum (orange). More posterior endoderm tissues such as the posterior small intestine and large intestine are not shown.

characterized because Sox2 global null mutants die during gastrulation and tools to conditionally inactivate Sox2 have not been widely available. Ongoing projects in the Wright lab are *Sox17*$^{GFP.Cre}$ to conditionally inactivate *Sox2* in the early endoderm. Lowering the gene dosage of *Sox2* causes mis-specification of the esophagus (Que et al., 2007). In these *Sox2* hypomorphic animals, the esophagus epithelium fails to establish a stratified squamous phenotype and adopts a more trachea-like phenotype. Loss of *Cdx2* completely transforms the small intestine into a squamous cell state similar to the esophagus or rectum (Gao et al., 2009), indicating that Sox2 is required to maintain intestinal identity and prevent posterior endodermal progenitors from adopting other non-intestinal progenitor states.

The posterior foregut is located between the endodermal expression territories of *Sox2* and *Cdx2*. It can be generally identified by the expression domain of *Pdx1* (Fig 1.2). *Pdx1* expression is first detected within two distinct domains in the dorsal and ventral posterior foregut. Over developmental time, *Pdx1* expression spreads anterior and posterior such that it overlaps the most posterior extent of *Sox2* expression and anterior extent of *Cdx2* expression. In total, *Pdx1* expressing progenitors give rise to the prospective antrum (posterior or caudal stomach), anterior duodenum, pancreas, and EHBS. While the liver is derived from the posterior foregut, these progenitors probably never express *Pdx1*. Within the posterior foregut, the dorsal and ventral progenitor domains are located in drastically different environments. Dorsal posterior foregut progenitors – which give rise to the dorsal pancreas, posterior stomach, and anterior duodenum – are initially in close contract with the notochord until E9.5 (E, embryonic day; essentially equivalent to "days post coitum") when it is displaced by the formation and medial movement of the dorsal aorta. Activin and FGF signals produced from the notochord are thought

to suppress Shh signaling in the posterior foregut to allow *Pdx1* expression in this dorsal domain (Hebrok et al., 1998). Tissue recombination experiments in chicken embryos showed that in the absence of the notochord tissue, the *Shh* expression domain in the endoderm expanded and led to reduced *Pdx1* expression in the prospective posterior foregut (Kim et al., 1997). Similarly, Inactivation of *Patched*, a negative regulator of Shh signaling, also led to a loss of *Pdx1* expression at E9.0-9.5 likely through expansion of the *Shh* expression domain (Hebrok et al., 2000). Inhibiting Shh signaling in chicken embryos using cyclopamine treatment led to the expansion of pancreatic progenitors but did not appreciably alter the *Pdx1* expression domain (Kim et al., 1998), indicating that Shh signaling may be more directly involved in limiting pancreas specification than setting the spatial boundaries of the Pdx1 expression domain.

In contrast to the dorsal posterior foregut, the ventral posterior foregut gives rise to the liver, pancreas, and EHBS. This progenitor pool is transiently in close contact with the cardiac mesoderm and septum transversum mesenchyme. Both of these tissues produce FGF as a key regulator of the specification of the pancreas, EHBS, and liver, with the amount of FGF signaling influencing organ fate. Higher levels or longer duration of FGF signaling promotes liver specification over pancreas and EHBS (Bort et al., 2004). During development of posterior ventral foregut organs, the liver is specified from the common progenitor pool first. Liver progenitors can be identified by the exclusive expression of Hnf4α. After liver specification, the EHBS and ventral pancreas remain as a common primordium expressing both *Pdx1* and *Sox17*. By E10.5, the *Sox17*-expressing progenitors (gall bladder and cystic duct progenitors) and *Pdx1*-expressing progenitors (ventral pancreas and common bile duct progenitors) separate into distinct organ anlagen (Fig 1.3). Separation of the gall bladder from the ventral pancreas is

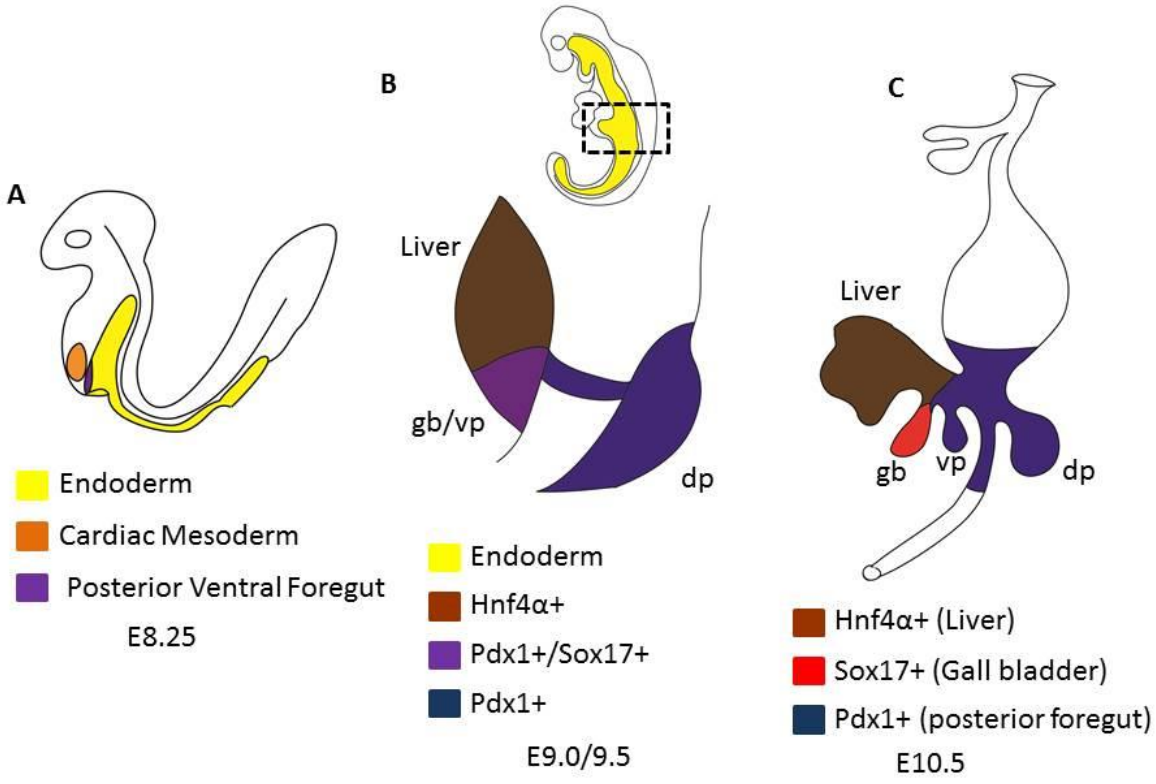

Figure 1.3 Morphological changes in the ventral posterior endoderm. E8.25 foregut endoderm. The prospective liver, ventral pancreas, and EHBS are derived from a common progenitor pool. FGF ligands are produced by the adjacent cardiac mesoderm and high levels of FGF signal in posterior ventral foregut specify the liver, while lower levels of signal specify the pancreas/EHBS. (A) E9.5 posterior foregut. By E9.5, the liver is specified and Hnf4a+ hepatoblasts invade the adjacent mesenchyme (brown). The ventral pancreas and gall bladder still exist as a common progenitor pool (purple). (B) E10.5 posterior foregut. By E10.5, the gall bladder (red) and ventral pancreas (blue) have formed separate organ primodia.

thought to occur by *Sox17*-driven *Hes1* expression in the gall bladder that suppresses *Pdx1* and *Ptf1a* (Spence et al., 2009).

Pancreatic Budding and Specification

Pancreatic progenitors first become morphologically apparent when they begin to protrude, into the surrounding mesenchyme, from the Pdx1-positive posterior foregut endoderm around E8.5 to E9.0. Prior to budding there are a number of factors expressed in early endodermal progenitors that are essential in order to access the pancreatic fate and initiate pancreatic organogenesis. For the purpose of this introduction, I will focus below on the intrinsic factors in the endoderm that help build the pancreatic gene regulatory network. I will specifically focus on the signaling pathways and transcription factors that are involved in the regulation of the transcription factors Ptf1a and Pdx1. One observation from my thesis research is that the $Ptf1a^{+}Pdx1^{+}$ co-expression state can initiate the self-assembly of the pancreatic program, suggesting that this co-expression state is an essential intermediate state for the proper execution of the pancreatic program.

Hnf1b, *Onecut1* (a.k.a. *Hnf6*), and *Mnx1* are all expressed prior to the more regionally restricted expression of *Pdx1* in the posterior foregut. Inactivation of *Hnf1b*, *Onecut1*, or *Mnx1* leads to profound consequences on pancreatic specification and budding, partly derived from their effects on expression of *Pdx1* and *Ptf1a*, two key regulators of pancreatic development. In the absence of *Hnf1b*, progenitors (correctly) begin to express *Pdx1* and *Mnx1* in a localized manner in the dorsal pancreatic bud region, but fail to expand in number. The ventral pancreatic bud does not form in *Hnf1b* homozygous null mutants. Progenitors within the respective regions of the normal prospective pancreatic buds fail to express *Ptf1a*, and thus, are not specified to the

pancreatic fate (Haumaitre et al., 2005). *Onecut1* is required to regulate *Pdx1*. *Pdx1* expression is reduced and delayed in *Onecut1* mutants, leading to hypoplastic pancreatic buds (Jacquemin et al., 2003). In *Mnx1* null mutants, budding and specification of the dorsal pancreas is lost, but ventral pancreas budding and specification is largely unaffected. In the remaining dorsal pancreatic region, *Pdx1* is not properly upregulated. In contrast, *Pdx1* expression in the ventral pancreatic bud is unaffected – and the ventral pancreas develops relatively normally, albeit with altered endocrine cell specification (Li et al., 1999; Harrison et al., 1999). The phenotype of *Mnx1* mutants indicates that there are different transcriptional regulatory cascades operating in the dorsal and ventral pancreas that are required for budding and specification. The differential requirement of *Mnx1* in the dorsal and ventral pancreatic buds is likely due to the distinct developmental ontogeny of dorsal and ventral progenitors described above.

In addition to the transcription-factor genes mentioned in the paragraph above, *FoxA*, *Gata4*, *Gata6*, *Prox1* and *Sox9* are all expressed in the posterior foregut prior to pancreatic specification. The direct role of these factors in pancreatic budding and specification has not been addressed, often because of early embryonic lethality of the global null mutants. Some of these factors, such as Foxa1, Foxa2, Gata4, and Gata6 have been conditionally inactivated using *Foxa3*^{Cre} [Tg(Foxa3-cre)1Khk]. *Foxa3*^{Cre} activates around E8.25 to E8.5, about the same time as *Pdx1* expression is initiated in the posterior foregut. While *Foxa3*^{Cre} is a usefully tool for the conditional inactivation in the endoderm, the late activation time-window of *Foxa3*^{Cre} may reveal a different phenotype when compared to an earlier endoderm-specific inactivation using Cre-drivers like *Sox17*^{GFPCre}. *Foxa1* and *Foxa2* double-knockout using *Foxa3*^{Cre} causes a complete loss of *Pdx1* expression, indicating that the FoxA family is crucial for maintaining *Pdx1* expression in pancreatic endoderm (Gao et al., 2008). *Gata4*/*Gata6* double-knockout using

Foxa3^{Cre} also causes a significant reduction of *Pdx1* expression in pancreatic endoderm (Xuan et al., 2012; Carrasco et al., 2012). The function of *Prox1* and *Sox9* in pancreatic specification has only been conditionally addressed using *Pdx1*^{Cre}, which activates even later than *Foxa3*^{Cre}. Conditional knockout of *Sox9* or *Prox1* leads to hypoplastic pancreatic buds because there is failure to promote proliferation and survival of early pancreatic progenitors (Seymour et al., 2012; Wang et al., 2005). In the absence of *Sox9*, pancreatic progenitors start to express hepatic genes (such as α-fetoprotein and albumin), indicating that *Sox9* is actively suppressing alternative organ programs during pancreatic development.

Pdx1 is expressed throughout the posterior foregut and is required for the proper development of the antral stomach, duodenum, and common bile duct, in addition to the pancreas. Although activation of *Pdx1* expression is often, incorrectly, used diagnostically as a specific indicator of pancreatic budding and specification, it is not explicitly required for either. In the absence of Pdx1, both pancreatic buds form and begin to protrude from the posterior foregut, but fail to expand any further. By the end of development there is only a small dorsal bud rudiment containing very limited differentiation of acinar and endocrine cells. No ventral rudiment can be found (Jonsson et al., 1994; Offield et al., 1996).

The transcription factors Ptf1a (Fig 1.2), Nkx6.1, and Nkx2.2, which have pancreatic progenitor-specific expression in the endoderm, start to be expressed between E9 and E9.5. Although *Nkx2.2* and *Nkx6.1* have early pancreas-specific expression, neither gene is required for pancreatic specification (their roles will be described later). In contrast, Ptf1a has an important role in this process. Both the dorsal and ventral pancreatic buds still form when Ptf1a is globally deleted, but the ventral pancreatic bud fails to be maintained and relatively rapidly seems to disappear completely. By the end of gestation, only a tiny dorsal rudiment remains that

completely lacks pancreatic acinar cells, although it does contain duct and endocrine cells (Krapp et al., 1998; Kawaguchi et al., 2002). Lineage-tracing studies with a ROSA26^{YFP} reporter in animals heterozygous for the *Ptf1a*^{Cre} knock-in – which is also a null allele – revealed that lineage-traced cells are restricted to pancreatic lineages and that the progeny of Ptf1a-positive cells give endocrine, duct, and acinar cell lineages in the pancreas. Lineage tracing cells in animals homozygous for the *Ptf1a*^{Cre} revealed that cells that would otherwise be committed to pancreatic lineages adopt an intestinal and EHBS progenitor state and go on to differentiate into representative cell types including the stem cell compartment within those organs (Kawaguchi et al. 2002). Because *Ptf1a* expression is maintained in wild-type animals in developing and adult acinar cells, and Ptf1a null mutants completely lack acinar cells, *Ptf1a* is thought to be one of the master regulatory factors of the acinar lineage.

Given the pancreas-restricted expression of *Ptf1a*, the factors that control the expression of *Ptf1a* would provide insight into the pancreatic specification process. There is currently a very limited understanding of the factors that control the spatial and temporal extent of *Ptf1a* expression in the endoderm. In embryos lacking endothelial cells (*Flk1* global null embryos), the expression of *Ptf1a* is initiated in the ventral pancreatic bud but not the dorsal pancreatic bud (Yoshitomi and Zaret, 2004). It remains to be discovered what factor(s) are secreted from the endothelial cells that promote dorsal bud expression of *Ptf1a*.

While we have some understanding of the targets of Ptf1a in the acinar-cell lineage, we do not have a firm grasp of the targets of Ptf1a during pancreatic specification. One proposed target is *Mnx1* (Thompson et al., 2012). Because *Mnx1* is expressed in the endoderm prior to *Ptf1a*, and *Mnx1* is not essential for ventral pancreas specification (described above), it is unclear if *Mnx1* is a critical target of *Ptf1a*. Another potential direct target in the early pancreas is the

Notch ligand *Delta* (*Dll1*). *Delta* expression in the pancreatic epithelium is completely abrogated in *Ptf1a* null mutants. In *Dll1* mutant mice, the pancreatic buds are hypoplastic in part due to decreased proliferation of early multipotent progenitors because of reduced *Ptf1a* expression (Ahnfelt-Rønne et al., 2012).

Epithelial Apical-Basal Polarization and Plexus Formation

At the beginning of the early multipotent progenitor cell (MPC) stage, the pancreatic bud is a pseudo-stratified columnar epithelium with little or no apical-basal polarization (Fig 1.4 A,B). Apical-basal polarization of a few pioneer cells and the spreading of such cell polarity to surrounding cells leads to the formation of microlumens (Fig 1.4 C). The microlumens expand through the recruitment of adjacent polarized epithelial cells, and the process of merging with other microlumens forms a complex tubular network (Kesavan et al., 2009; Villasenor et al., 2010) (Fig 1.4 D). This tubular network can be thought of as resembling the epithelial plexus state of the developing vascular system. It represents a developmental process of tube formation and organ outgrowth that is distinct from branching morphogenesis of other organs such as the lung. The generation of a plexus state produces tubular structures containing distant tip and trunk progenitor domains (Fig 1.4 E).

In parallel with the dynamic morphological reorganization of the pancreatic buds to a plexus state are large-scale changes in the gene expression patterns of various regions of the epithelium. Due the focus on Ptf1a in this thesis, I will highlight the changes that occur in the expression of Ptf1a during compartmentalization. At the onset of pancreatic development, Ptf1a is expressed organ-wide. During polarization, Ptf1a expression becomes restricted to the tip domain. Tip cells are in close contact with the basement membrane and mesenchyme

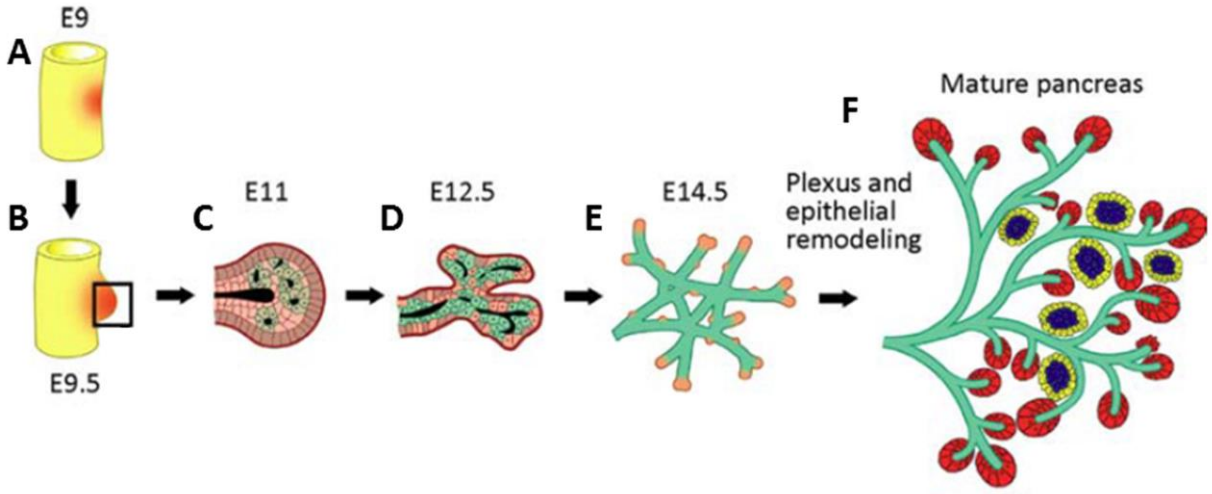

Figure 1.4 Schematic representations of morphological changes of the pancreatic epithelium during development. (A) Permissive signals from the notochord (activin and FGF) along with proper expression of several transcription factors (Hnf1b, Mnx1, Onecut1, Foxa1, Foxa2, Gata4, Gata6) in the pre-pancreatic endoderm lead to the establishment of region (red) in the dorsal foregut endoderm the expresses both Pdx1 and Ptf1a. (B) The early pancreatic progenitors protrude from the foregut endoderm into the surrounding pancreatic mesenchyme. (C) The early pancreatic dorsal bud is pseudostratified columnar epithelium. Cell within the epithelium have no apical-basal polarization. Apical-basal polarization occurs in a few pioneering cells and spreads to surrounding cells to generate microlumens. (D) Microlumens coalesce to generate an epithelial plexus. (E) Within the epithelial plexus are two distinct progenitor populations, tip (pink) and trunk (green) cells. During early pancreatic development, both of these progenitors give rise to all pancreatic cell types. By late plexus state, tip cells are committed to the acinar cell lineage and trunk cells give rise to endocrine and ductal cells. The dense plexus state is thought to be a niche that supports the efficient specification of endocrine cells. As the plexus remodels into the more simplified tubular network (epithelial tree) in the mature pancreas, the ability to generate endocrine cells is lost. (F) The final morphology of the mature pancreas. Acinar cells (red) produce and secrete digestive enzymes to aid in food digestion. Duct cells secrete bicarbonate and carry acinar and duct secretions to the common bile duct and then on to the duodenum. these contents enter the duodenum. Islets are distributed through the pancreatic organ. β-cells (blue) form the core of the islet, while alpha and other endocrine cells (yellow) predominantly occupy a mantle location. Adapted with permission from Pan and Wright, 2013.

surrounding the epithelium. It is thought the mesenchyme may help establish the unique gene expression patterns and progenitor behavior of tip cells through juxtacrine signaling. Trunk cells, which constitute the core of the dense plexus, maintain expression of a different set of genes from the tip domain, including genes such as *Nkx6.1*, *Sox9*, and *Hnf1β*.

Transcription factors, such as *Ptf1a* and *Nkx6.1*, have been shown to have an important role in establishing the divergent expression characteristics of the tip and trunk domain. *Nkx6.1* and *Ptf1a* mutually repress each other's expression. Constitutive misexpression of Nkx6.1 throughout the epithelium causes repression of Ptf1a and the loss of tip cell character. The resulting epithelium adopts a trunk progenitor cell state. Misexpression of Ptf1a throughout the pancreas suppresses Nkx6.1 and turns the epithelium exclusively into tip cell-like progenitors. These data suggest a model where Ptf1a and Nkx6.1 affect the acquisition of tip or trunk cell states through directly or indirectly repressing the other cell state. Whether a cell in the pancreatic epithelium adopts a tip or trunk cell state could be triggered by signals that promote the maintenance of Ptf1a or Nkx6.1. Notch signaling in pancreatic progenitors, which could be modulated by Ptf1a through competition for RBPJk, could shift the equilibrium of the Ptf1a-Nkx6.1 cross-repressive loop to generate different cell states. The proximity of cells to the pancreatic mesenchyme might also influence the Ptf1a-Nkx6.1 expression status by promoting tip cell marker instead of trunk markers.

Lineage tracing tip cells using the Cpa1 or Ptf1a promoter demonstrated that tip cells give rise to a significant number of duct, endocrine, and acinar cells up until E12.5 (Zhou et al., 2007; Pan et al., 2013). After E12.5, tips are essentially committed to the acinar cell lineage. Likewise, lineage-tracing trunk cells using the Sox9 or Hnf1b promoter indicates that trunk cells can give

rise to acinar, duct, and endocrine cells up until E13.5 (Kopp et al., 2011; Solar et al., 2009). After E13.5, trunk cells become a bipotent progenitor population that gives rise to duct and endocrine cells. After the main endocrine specification phase, Hnf1b-positive cells are committed to the ductal lineage (Solar et al., 2009).

The current model of multipotent progenitor behavior during pancreas development, based on available lineage-tracing data, is that the early pancreatic buds are full of a homogenous population of multipotent progenitors (that is, fully capable of giving rise to all three pancreatic cell lineages). Because of the compartmentalization of the pancreatic epithelium, multipotent progenitors allocate to the tip and trunk domains and become lineage-restricted. Multipotentiality is thought to remain due to the asynchronous nature of early multipotent progenitors committing to the tip or trunk progenitor domains. It is also possible that at the interface of the tip and trunk domain cells can readily transition between a tip and trunk cell state and adopt that population's progenitor behavior.

Plexus Resolution and Differentiation

The stages of pancreas development covered in this introduction so far have encompassed the processes of specification, apicobasal polarization, and patterning of the pancreatic epithelium that lead to the generation of a dense epithelial plexus composed of spatially segregating pools of tip and trunk progenitor cells. I have also described that tip and trunk progenitors have different propensities to give rise to the differentiated cell types of the mature pancreas. Tip cells largely give rise to acinar cells while the trunk domain gives rise to the endocrine and ductal lineages (Zhou et al., 2007; Pan et al., 2013; Kopp et al., 2011; Solar et al., 2009). The generation of the dense plexus state is thought to produce the tissue environment, or niche, for the efficient production of endocrine progenitor cells that are born from the epithelium,

delaminate, and go on to cluster and form the islets of Langerhans in the mature pancreas. Currently, it unclear what are the exact properties of the dense plexus state that promote efficient endocrine cell birth. As the epithelial plexus resolves into a simplified tubular network (Fig 1.4 F), the ability to generate large numbers of endocrine progenitors is lost and the remaining cells become ductal cells. It is interesting to note that β-cells seem to be made most efficiently from pancreatic epithelium in the dense plexus state. Other endocrine cell types like the alpha cell are made prior to the dense plexus state, while delta and PP cells are made as the plexus begins to resolve to the duct (after delaminated endocrine cells have all left).

Endocrine precursors cells produced from the trunk progenitor cells during this stage of development are determined by high levels of the transcription factor Ngn3 (Gu et al., 2002). Following the scattered, transient induction of Ngn3, these progenitors delaminate from the trunk domain epithelium and coalesce with other endocrine progenitors to form endocrine progenitor cords. Because they likely never really break through the basal lamina, these endocrine cords, bound by N-cadherin as opposed to E-cadherin in their preceding epithelial state, remain 'spread along' and in relatively close association with the epithelium that by this stage is becoming the almost mature ductal network. The endocrine cords are also in proximity to the intrapancreatic vasculature, which tends to mimic the pattern of the ductal epithelial tree, as expected because of the capillary bed that must develop within the islets. These endocrine cords then remodel into a structure like beads-on-a-string and during subsequent development they break off to form the mature islets with a β-cell core with a mantle of other endocrine cell types. While the controlling the commitment of individual endocrine cell lineages is an important facet of pancreas development, I will not spend time detailing this topic. These processes are extensively detailed in Pan and Wright, (2011).

When tip cell multipotentiality is lost, these cells become converted to lineage-committed pro-acinar cells by essentially E12.5 or so. The residual multipotency detected by Pan et al. (2013) and others may reflect the asynchronous nature of the maturation of the epithelium to the trunk-tip compartmentalization state, with some regions completing this process much later than others. Coinciding with the MPCs to pro-acinar transition of tip cells is an important alteration in the molecular character of the PTF1 complex. During the early MPC stage, the PTF1 complex comprises the basic helix-loop-helix transcription factor Ptf1a, an E-box partner (HEB, E12, or E47), and RBPJκ (Beres et al., 2006). As tip cells transition to lineage-committed acinar cells, a direct the PTF1-κ (Ptf1a and RBPJκ) complex is *RBPJL*, a Notch-independent paralog of *RBPJκ*. As RBPJL levels rise, the PTF1 complex incorporates RBPJL to replace RBPJκ (Masui et al., 2010). PTF1-J (Ptf1a and RBPJL) is thought to coordinate and maintain a transcriptional gene regulatory network of acinar cells through (auto)regulation of *RBPJL*, *Ptf1a*, and a number of key transcription factors such as *Gata4*, *Nr5a2*, and *Mist1* (Holmstrom et al., 2011; Hale et al., 2014; Xuan et al., 2012; Pin et al., 2001).

Genetic Tools that Allow Manipulation of Key Instructive Molecules

The genetic tools that are used in Chapter III and IV of this thesis rely on the use of Cre/loxP technology to manipulate genomic DNA *in vivo*. For an extensive review of the many capabilities of DNA recombinases in mouse genetics see Branda and Dymecki (2004). Cre recombinase is a type I topoisomerase that catalyzes the excision of DNA located between two 34 bp motifs (13 bp palindromic sequences with an 8 bp internal spacer) called loxP sites. Some forms of Cre recombinase described in this thesis are ligand-activatable. In the CreER fusion protein, Cre recombinase is held in the cytoplasm until addition of tamoxifen, which binds to CreER allowing it enter the nucleus and act on DNA. In my thesis research, I used a variety of

Cre drivers ($Sox17^{GFPCre}$, $Tie1^{Cre}$, $EIIA^{Cre}$, and $Ptf1a^{CreER}$) that produce Cre in specific embryonic tissues. When these Cre drivers are combined with floxed conditional null alleles (such as $Ptf1a^{flox}$ –described in Chapter IV) or lineage-tracing reporters (such as *ROSA26* alleles described in Chapter III and IV), one can achieve gene inactivation or activation, or lineage reporting that is short-lived or indelibly carried within the progeny of parent cells in which Cre was active.

Another component of the genetic system used in Chapter III of this thesis is the tetracycline-inducibility system, which allows on-off control of gene expression in eukaryotic cells. tTA and rtTA are modified forms of the *tetA E. coli* gene that contain the DNA-binding domain of *tetA* and the transcriptional activation domain of VP16. In the presence of tetracycline analogs such as doxycycline (preferred tetracycline analog for use in mammalian systems due to low toxicity), tTA and rtTA are able to bind to the *tet* operator sequences on responder genes, leading to either repression (tTA; Tet-Off) or activation (rtTA; Tet-ON) of gene expression. In order to use this system in the mouse, alleles that express tTA/rtTA (driver alleles) and respond to tTA/rtTA (tetO allele - responder allele) must be generated. Responder alleles contain a gene cassette controlled by tandem repeats of the tet operon attached to a minimal promoter.

When combined with Cre/loxP technology, such tTA or rtTA systems can achieve spatiotemporally controlled gene activation. With my own specific case as the example (as used in Chapter IV), $ROSA26^{rtTA.IRES.EGFP}$ is a Cre-activatable, tetracycline-driver allele. After Cre-mediated recombination in the chosen cell type, all progeny from the parent cell express rtTA from the "constitutively active" ROSA26 promoter. In the presence of doxycyline, rtTA binds to and activates expression of the gene encoded in a *tet* responder allele. By crossing

ROSA26$^{rtTA.IRES.EGFP}$ to various Cre-driver alleles, I was able to control the cell lineage of expression via the spatial expression profile of the Cre allele, or gain temporal control by varying the timing of doxycycline administration, on the production of Ptf1a from the *tet* responder allele.

Aims of the Dissertation Research

This thesis is comprised of three main research areas, all dealing with the manipulation of key instructive molecules during development. I designed experiments to test: (1) the sufficiency of Ptf1a to determine organ identity during mammalian endodermal development, examining how progenitor competence and commitment changes during development, (2) the role of Ptf1a in controlling progenitor cell state and differentiation in the pancreatic epithelium, and (3) generate antibody reagents to validate mouse genetic tools.

While several publications have reported on the role of signaling molecules and transcription factors in endodermal patterning and organogenesis through gene knockout, very few studies have assayed the potency of transcription factors as dominant controllers of entire organ re-specification during mammalian development. In my first area of research for my thesis, I have designed a transient Ptf1a misexpression system allowing the interrogation of cell re-specification at early organ-allocation and terminal differentiation stages. The results of these experiments are reported in Chapter III (Dominant Control of Endodermal Organ Allocation by the Pancreatic Transcription Factor Ptf1a).

For the second project, I generated novel genetic tools to examine the function of Ptf1a in tip MPCs during pancreas development. Previously published experiments have established that Ptf1a is sufficient to divert cells from trunk type specification, competitively working against Nkx6.1 (Schaffer et al., 2010). Using new tools, we hoped that our experiments would address

the reciprocal question of whether Ptf1a is required to maintain the tip MPC state. The results of these experiments are reported in Chapter IV (The Role of Ptf1a in Tip Cells of the Developing Pancreatic Epithelium).

In a third sub-project, I generated novel GST-Cre and GST-mCherry fusion proteins to produce new Cre and mCherry antibodies. Validating the expression patterns of DNA recombinases and fluorescent proteins used in genetic tools is important to make rigorous conclusions, and we hoped that these antibodies could be used to accomplish this goal. The results of these experiments are reported in Chapter V (Antibodies to Detect Cre and mCherry Protein Localization).

CHAPTER II

MATERIALS AND METHODS

Mouse Strains

Mice were maintained at Vanderbilt University Medical Center according to institutional protocols. $Sox17^{GFPCre}$ (Choi et al., 2012), $Tie1^{Cre}$ (Gustafsson et al., 2000), $Ptf1a^{CreER}$ (Pan et al., 2013), $EIIA^{Cre}$ (Lakso et al., 1996), Flp^{E} (Rodriguez et al., 2000), $Pdx1^{CreEarly}$ (Gu et al., 2000), $ROSA26^{rtTA.IRES.EGFP}$ (Belteki et al., 2005), and $ROSA26^{YFP}$ (Srinivas et al., 2001) were previously described. The details of the $tetO^{Ptf1a.IRES.LacZ}$ allele will be provided in an upcoming publication from Dr. Raymond MacDonald, UTSW. Briefly, the tetO allele was generated by random transgenesis. It is driven by seven repeats of tet operator linked to the CMV minimal promoter. The Ptf1a gene cassette connected to the tet operator contains the 3' UTR, intron, and exons from the endogenous Ptf1a locus. The 5' UTR was replaced by the *Xenopus laevis* β-globin gene, and the 3' UTR was truncated to remove its polyadenylation signal (Hale et al., 2005) allowing fusion to an optimized Internal Ribosomal Entry Site (IRES) (Kim et al., 1992). The IRES is connected to a *lacZ* reporter with a nuclear localization signal. *lacZ* has the 3'UTR from the bovine growth hormone gene to improve mRNA stability and polyadenylation. The 5' HS4 insulator from the chicken β-globin gene (Pikaart et al., 1998) flanks the transgene. The generation of the *Ptf1a* floxed allele will be described in Chapter 4. All mouse strains were genotyped by PCR amplification of genomic DNA purified from protease digests of tail snip or ear punch tissue.

Doxycycline and Tamoxifen Administration

The low dose regimen that worked effectively in my studies meant that it was critically important to weight out doxycycline and tamoxifen accurately, and an analytical balance (4 decimal point accuracy). Doxycycline in water (5.0 mg/mL) was administered by intraperitoneal injection, at 10.0 µg/g body weight. Doxycycline was also prepared in drinking water, at 2.0 mg/mL. Mice given doxycycline in the drinking water were deprived of other fluids to encourage drinking of the doxycycline solution. It is common practice to include an artificial sweetener to doxycycline solution because of its bitter taste, but I found that this made no difference. Doxycycline in the drinking water was kept in light-protective bottles and replaced every 48 to 72 hours. Tamoxifen was dissolved in pharmaceutical grade corn oil (Welch, Holme & Clark Co., Inc.; at 30.0 mg/mL), and administered by intraperitoneal injection at 3.0 mg per pregnant dam of normal weight (obese mice must be dosed differently).

Fixation and Preparation of Mouse Embryos and Tissues for Sectioning

Early postnatal and embryonic tissue was obtained from naturally mated mice, with noon on the day of the vaginal plug defined as 0.5 days post coitum (d.p.c.), or as mostly referred to in this thesis, embryonic day (E) 0.5. After euthanasia and dissection in ice-cold PBS, embryonic and perinatal tissue was fixed (4% freshly made paraformaldehyde, 4°C; never more than 8 hrs old) for between 1 to 4 hours, with longer times for older stages (1 hour for E10.5, 2 hours for E12.5, 4 hours for E18.5). Embryos and tissues were prepared for cryosectioning by washing in ice-cold PBS following fixation, then sucrose-equilibrated (30%, 4°C, overnight), and embedded by standard procedures straight into OCT compound (Tissue-Tek, Sakura). Cryosections were cut on a standard Leica cryostat at 10 microns (µm) per section.

Embryos or dissected tissues were prepared for paraffin embedding by washing in ice-cold PBS following fixation, and placed in 70% ethanol at 4°C until embedded was started. Tissues in 70% ethanol were dehydrated through an ethanol/water series (80% ethanol, 1 hour; 90%, 1 hour; 95%, overnight; 100%, 2 hours) on a rocking table and placed in Histo-Clear (National Diagnostic; a non-toxic replacement for xylene-based embedding) for 2 hours. Tissues were transferred from Histo-Clear to a 50% Histo-Clear, 50% paraffin wax (Paraplast Plus, Fisher Scientific) mixture for 1 hour at 60°C followed by 3 consecutive 100% molten wax washes at 60°C for 45 minutes each. After the last 100% wax step, tissues were mounted in standard plastic peel away molds at a traditional wax embedding station and then "wax-glued" onto a plastic cassette for sectioning. Paraffin sections were cut on a standard Leica microtome (Lecia RM2135), 10 microns per section. Sections were floated on warm water bath, picked up on glass slides and dried on a slide warmer overnight. All sections were placed on Superfrost Plus pre-cleaned glass slides (Fisher Scientific). Tissue sections stick to Superfrost Plus slides electrostatically without need for additional adhesives such as poly-L-lysine.

Hematoxylin and Eosin Staining

Paraffin sections on glass slides were prepared for hematoxylin and eosin staining by going through a standard dewaxing and rehydration series (Histo-Clear, 100% ethanol, 90% ethanol, 70% ethanol, 50% ethanol, and distilled water) for 3 minutes each. Slides were then immersed in hematoxylin (Harris Modified Hematoxylin, Fisher Scientific) for 30 seconds to 2 minutes. Length of staining depends on the stage and type of tissue (the best results in my hands were to stain early postnatal stage tissues for 30 seconds to 1 minute and adult tissues for approx. 1-2 minutes). Slides were then rinsed in running distilled water for 5 minutes and dipped in acidified alcohol (980 mL 70% ethanol mixed with 20 mL stock concentrated hydrochloric acid

(stock 12 M; 240 mM final concentration). Acidified alcohol de-stains hematoxylin and changes the color of the stain from deep red/purple to brown/light brown. Acidified alcohol can be used to completely de-stain hematoxylin if left in the solution for a long period time. After acidified alcohol treatment, slides were rinsed in distilled water and dipped in 1 g/L sodium bicarbonate, which changes the hematoxylin stain from brown to blue. Any lightly basic solution can replace sodium bicarbonate in this protocol. Slides were transferred from sodium bicarbonate to distilled water and then immersed in 95% ethanol. Slides were then dipped into eosin (Accustain Eosin Y solution Alcoholic, Sigma-Aldrich). It is important to determine empirically the period of eosin staining for each stage and tissue. Eosin can be de-stained by rinsing slides in fresh 95% ethanol or by rinsing slides through 95% ethanol, distilled water, and 1 g/L sodium bicarbonate (basic solutions de-stain eosin). After achieving the appropriate eosin-staining intensity, slides were placed back in 95% ethanol, dehydrated, and cover-slip mounted in toluene-based permanent mounting medium (Permount SP15-100; Fisher Scientific).

Section-based Immunohistochemistry

Paraffin sections on glass slides were prepared for DAB (3, 3'-diaminobenzidine) staining by going through a standard dewaxing and rehydration series (100% Histo-Clear, 100% ethanol, 90% ethanol, 70% ethanol, 50% ethanol, and distilled water). After being placed in distilled water for some time, endogenous peroxidase was quenched for 15 minutes at room temperature with 1.5% hydrogen peroxide in methanol. Slides were then rinsed in distilled water and permeabilized in 0.2% Triton X-100 in PBS. Antigen retrieval was performed for all the nuclear antigens (transcription factors) reported in this thesis, by heating slides for 2 minutes in 10 mM sodium citrate, pH 6.0 (1000 watt microwave, 100% power). Upon bring the retrieval solution to a boil in the microwave, the solution is microwaved for 10 minutes at 20% power. Following

permeabilization or permeabilization and antigen retrieval, slides section were isolated using a pap pen and were blocked for 2 hours (5% serum with 0.2% Triton X-100 in PBS; the species of this serum was concordant with the species of the secondary antibody; for example, secondary antibodies raised in donkey were blocked with normal donkey serum). Primary antibodies were incubated overnight at 4°C in blocking solution. Slides were washed 5 times, for 5 min each, in PBS containing 0.2% Triton X-100. Next, biotinylated secondary antibody diluted 1:200 in blocking solution was incubated on slides for 30 minutes at room temperature. Slides were washed in 0.2% Triton X-100 in PBS, and then incubated in avidin/biotin/peroxidase complexes (Vectastain ABC Kit, Vector Labs) diluted in blocking solution for 30 minutes at room temperature. Next, DAB substrate (Metal Enhanced DAB Substrate Kit, Thermo Scientific) was added. While DAB substrate incubated on the slides, slides were visualized periodically and briefly under brightfield on a dissecting scope until desired staining intensity was achieved. Staining was then quickly quenched by immersing slides in distilled water. Following DAB staining, slides could be counter-stained with a variety of histological stains, including hematoxylin and eosin. DAB-stained slides were dehydrated and cover-slip mounted in Permount.

Section-based Immunofluorescence

Cryosections were washed in PBS, permeabilized in 0.2% Triton X-100 in PBS, and blocked for 1 hour (5% serum in PBS; as above, serum species altered according to secondary antibody). Primary antibodies were incubated overnight at 4° in blocking solution. For indirect immunofluorescence, secondary antibodies were incubated for 1 hour at room temperature in PBS. For avidin-biotin amplification, prior to adding the biotinylated secondary antibody (1 hour, in blocking solution), sections were blocked with an avidin-biotin blocking kit (Vector

labs). Streptavidin-conjugated secondary antibodies were incubated for 1 hour at room temperature in PBS. For Tyramide™ signal amplification (TSA; Perkin Elmer), the fluorescent TSA reagent (1:1000) was prepared in the TSA diluent and incubated on the slides for 10 minutes. For all immunofluorescence techniques, slides were mounted with Prolong Gold anti-fade with DAPI [2-(4-amidinophenyl)-1H-indole-6-carboxamidine; Invitrogen]. Slides were sealed with nail polish.

Whole-mount immunofluorescence

Embryos were fixed whole with 4% freshly made paraformaldehyde at 4°C for between 1 to 4 hours (for E10.5: 1 hour), and then gut and associated tissues were dissected from the whole embryo, and blocked for 2 hours in 1x PBS containing 0.5% Tween-20 and 20% serum. Primary or secondary antibody incubations were overnight at 4° in PBS with 0.5% Tween-20 and 10% serum. Tissue was then dehydrated and cleared in BABB (benzyl alcohol: benzyl benzoate, 1:2) for imaging.

Microscopy

Brightfield images of tissue morphology were obtained with an Olympus DP-72 digital camera on an Olympus SZX12 microscope. Brightfield images of histology and chromogenic staining were photographed using an Aperio (Leica) whole-slide scanning. Fluorescent images were captured using a Zeiss LSM 510 Meta or Olympus FV-1000 confocal microscope. Imaging of whole-mount immunofluorescence was performed on a Zeiss LSM 510 Meta confocal microscope and images were analyzed with Image J (NIH). Whole-mount immunofluorescence max projections were produced using Image J with dust and scratches noise reduction processed in Photoshop (Adobe). Noise reduction was applied to experimental and control embryos.

DNA preparation for transient transgenics

Plasmid DNA from a midi- or maxi-prep was cut to remove the plasmid backbone, run out on low melt temperature (LMT) agarose gel, and purified ethanol precipitation. Gel purified DNA was phenol, phenol/chloroform extracted and ethanol precipitated. For additional purity, precipitated DNA was run on an Elutip column (Schleicher & Schuell), and eluted in high salt, before ethanol precipitation according to the manufacturer's protocol, and re-suspended in Tris-EDTA (10 mM TRIS, .1 mM EDTA) DNA concentration was determined by a spectrophotometer before provided to the ES cell core.

Antigen selection and cloning of Cre and mChery GST fusion proteins

Hydrophilic regions of Cre and mCherry were determined by the Hopp-Wood hydrophobicity-plotting algorithm to potential generate highly soluble antigens for immunization. Hydrophilic regions of Cre and mCherry that showed no homology to other relevant proteins, including other DNA recombinases and fluorescent proteins were inserted in-frame into pGEX-KG (Smith and Johnson, 1998) at the 3' end of GST, after the glycine linker sequence. The glycine linker sequence promotes autonomous folding of GST and the antigen and provides a steric gap for the antigen to move independent of GST. Plasmids were transformed into *E. coli* strain JM109. JM109 *E. coli* have a cell wall defect that makes soluble proteins easier to recover after sonication. Protein production described in greater detail in Chapter V. Soluble protein was collected and bound to (batch-style incubation) glutathione-sepharose beads. GST-containing proteins, batch incubated, were loaded into small columns plugged with glass wool for washing and elution steps. GST-fusion proteins were eluted with

excess reduced glutathione and high protein factions were run on 10% SDS-PAGE gels. SDS-PAGE gels were stained with Coomassie Brilliant Blue G-250 (Sigma-Aldrich).

Southern blotting

Southern blotting was performed by standard sodium hydroxide transfer onto PVDF membrane. Southern blot probes were radiolabeled with P^{32-}incorporated ATP. For a detailed protocol of alkaline transfer, please consult Molecular Cloning, A Laboratory Manual, second edition (Sambrook, Fritsch, and Maniatas).

CHAPTER III

DOMINANT CONTROL OF ENDODERMAL ORGAN ALLOCATION BY THE PANCREATIC TRANSCRIPTION FACTOR PTF1A

Introduction

This chapter is a modified version of a published article (Willet et al., 2014). The journal, *Development*, grants permission for reproduction within doctoral candidate thesis.

Embryonic endodermal patterning directs naïve progenitors toward regionalized competence states and the subdivision into appropriately located organ-specific progenitors. Orderly analysis of the gene regulatory logic that resolves organ-specific identities would yield critical insight into the first steps of organogenesis. Understanding how gene regulatory networks stabilize cell fates could also be relevant to the mechanisms underlying disease states or organ/tissue metaplasia, often considered to be associated with de-differentiation and reversion to more primitive progenitor-like states (an example related to diabetes: Talchai et al., 2012).

Also pertinent is the reciprocal interaction between endoderm and mesoderm: during later development, the mesoderm has been connected to important roles in endodermal survival and patterning (Morrisey and Hogan, 2012; Pan and Wright, 2011). It is less clear at earlier specification stages what the role of either tissue is in enforcing the differentiated state of the partner tissue. It is uncertain how and when the endoderm-adjacent mesoderm is specified towards a particular organ character, and the degree to which the regionalized endoderm directly

instructs that outcome. Local mesoderm-endoderm codependency could be significant in building and maintaining normal organ functions.

Transcription factors (TFs) are potent directors of cell-intrinsic gene regulatory networks. Despite knowledge of early-acting and regionally expressed endodermal TFs, it is often unclear how such gene regulatory networks interact with each other, presumably often in mutually repressive and auto-regulatory feedforward loops, to select target genes that promote or restrict progenitor competence associated with the formation of each organ.

Loss-of-function or gene-dosage studies on key TFs (e.g., Sox2, Sox17, Ptf1a, Cdx2) have revealed roles in specifying regional and organ-specific progenitor character in the endoderm. In some cases, removing or reducing their function causes endodermal progenitors to acquire another region or organ identity (Que et al., 2007; Gao et al., 2009; Spence et al., 2009; Kawaguchi et al., 2002). Limited studies address in detail their role in deterministically controlling progenitor behavior, especially in comprehensively switching organ fates. Combining necessity and sufficiency tests could help understand how organ territories are defined, how endoderm-mesoderm communication occurs, and how gene dysregulation leads to aberrant epithelial maintenance.

The pancreas is initiated from separate domains in the posterior dorsal and ventral foregut endoderm. The basic helix-loop-helix TF Ptf1a is expressed within endoderm throughout the pancreatic bud progenitors, subsequently within the growing tips of the branched epithelium, and finally in their subsequently derived acinar cells (Krapp et al., 1998; Kawaguchi et al., 2002; Zhou et al., 2007; Masui et al., 2007). In the early MPC (multipotent progenitor cell), Ptf1a is part of a complex, PTF1, with a canonical E-protein (E12, E47, or HEB) and the nuclear

mediator of Notch signaling, RBPJκ. As multipotent cells transition to acinar-lineage-restricted fates, increased expression of RPBJL, a Notch-independent RBPJκ paralog, replaces RBPJκ in PTF1 (Masui et al., 2007). Thus, two types of PTF1, PTF1-J and PTF1-L, promote pro-pancreatic multipotency or acinar gene-regulatory networks, respectively.

Previous work in *Xenopus* tested Ptf1a as a dominant instructor of pancreas fate (Afelik et al., 2006; Jarikji et al., 2007), but left open questions, including the temporal and spatial windows during which such effects can be elicited, and the completeness of conversion. Particularly important issues include the duration of ectopic Ptf1a required for tissue conversion, and the effect on other genes that supposedly act together with Ptf1a as upper-level regulators of the cascade that regionally specifies pancreatic MPC and moves them to fully differentiated cells. Moreover, it is essential to understand these issues in the mammalian embryo.

We therefore addressed the potency of Ptf1a as a single TF in dominantly instructing organ fate in mammalian endoderm. Transient endodermal Ptf1a misexpression caused a coherent change in the TF expression domains in the endoderm, including broad, rapid expansion of Pdx1 expressed from its endogenous locus, and recruitment of other pancreatic-progenitor identifier genes. Early transient Ptf1a stably converted pancreas-adjacent endoderm that normally forms the glandular stomach, extra hepatic biliary system, and rostral-most duodenum into pancreatic tissue comprising its full complement of cell fates, including endocrine cells. Altering the timing of Ptf1a misexpression defined the developmental period over which dominant respecification of the endoderm became switched from early multipotent to lineage-restricted acinar transformation. We also defined a period in which endoderm and endoderm-associated mesoderm displayed interdependent specification programs.

Prior to the work described below, I used a 4.5 kb Pdx1 promoter fragment to drive Ptf1a misexpression during endodermal development. The Pdx1 promoter fragment in this transgene should drive persistent expression of Ptf1a from the time the Pdx1 promoter is first activated (around E8.25 to E8.5) (Gannon et al., 2001). This transgene was used by Schaffer et al., (2010) to generate transient transgenic embryos to drive Ptf1a misexpression throughout pancreas development. They noticed areas of pancreatic respecification within the stomach and duodenum. The size and location of the respecified tissues were highly variable.

To confirm the results obtained by the Sander lab, I generated transient transgenic embryos and analyzed them at E14.5 for pancreatic lineage markers. Consistent with the results from the Sander lab, I also noticed highly variable respecificaiton of the stomach and duodenum within the Pdx1 expression domain. We attributed the highly variable respecification to mosaic expression of the transgene. Ectopic pancreatic progenitors that were found maintained Ptf1a expression and expressed acinar cell markers (Amy and Cpa1). These ectopic progenitors did not express pancreatic endocrine (Insulin) or trunk markers (Sox9 and Nkx6.1). Due to the highly mosaic expression of the transgene and acinar cell nature of the respecified progenitors that were analyzed, I pursued the genetic system described in this chapter that would allow tighter control over the timing and duration of Ptf1a expression.

Results

Transient endodermal Ptf1a misexpression

Transient endodermal Ptf1a misexpression, or Ptf1a^{EDD} [endoderm] used a three-allele system: *Sox17*^{GFPCre} pan-endodermal Cre driver; *ROSA26*$^{rtTA.IRES.EGFP}$, which Cre-dependently expresses the reverse tetracycline transactivator (rtTA) and green fluorescent protein (EGFP); and tetO$^{Ptf1a.IRES.lacZ}$, expressing Ptf1a and beta-galactosidase (βgal) in the presence of rtTA and doxycycline (Fig. 3.1A). Single doxycycline injections produce pulsed Ptf1a expression. *Sox17* is essential for endoderm formation, and is expressed throughout the early definitive endoderm (Kanai-Azuma et al., 2002). Analysis of a *ROSA26* reporter with an independent *Sox17*-Cre allele (Engert et al., 2009) indicated recombination starting as early as E7.5, with the *ROSA26* promoter maintaining extensive endodermal expression until at least E16.5. Our own monitoring of EGFP expressed from *ROSA26*$^{rtTA.IRES.EGFP}$ at E10.5 and E12.5 showed recombination broadly throughout the endoderm and endothelium, with the *ROSA26* promoter equivalently active during the test windows used herein (not shown). Therefore, variable response to doxycycline-induced Ptf1a^{EDD} cannot be attributed to shutting down of the rtTA expression system. Appropriate system behavior was also validated by post-doxycycline pan-endodermal βgal (e.g., Fig. 3.1D). Ectopic Ptf1a in trigenic animals was only activated in endoderm and endothelium in the presence of doxycycline (not shown); we rule out endothelial effects below. Controls were largely *Sox17*^{GFPCre}; *ROSA26*$^{rtTA.IRES.EGFP}$ littermates, or non-littermate non-doxycycline-treated triple transgenics, which were phenotypically equivalent to wild type.

To estimate the kinetics of Ptf1a^{EDD} misexpression, we analyzed Ptf1a at various stages after single E9.5 doxycycline injections. By 24 hours (E10.5), βgal and Ptf1a were induced in

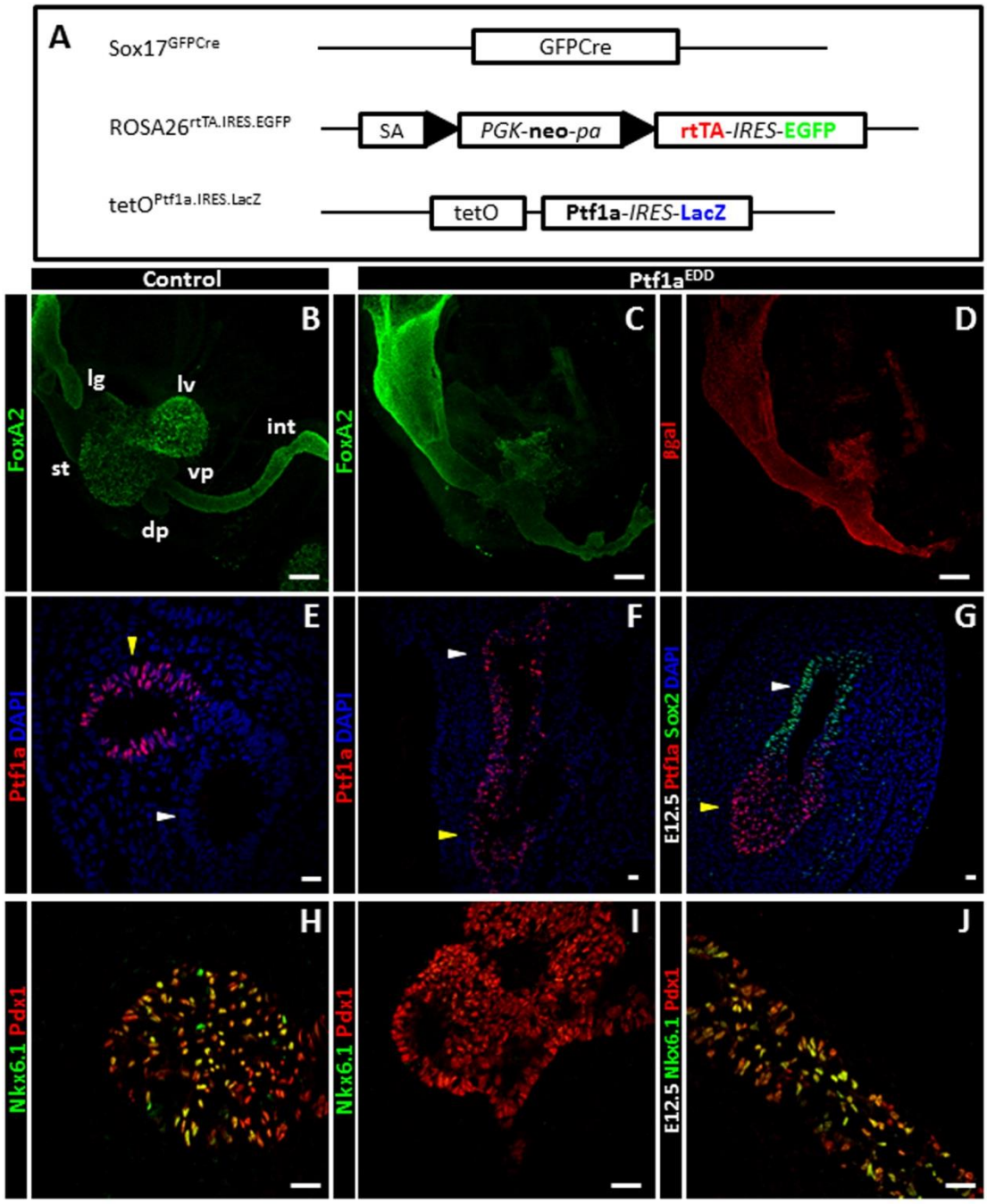
A
Sox17GFPCre
GFPCre
ROSA26rtTA.IRES.EGFP
SA
PGK-neo-pa
rtTA-IRES-EGFP
tetOPtf1a.IRES.LacZ
tetO
Ptf1a-IRES-LacZ
Control
Ptf1aEDD
B
C
D
FoxA2
FoxA2
βgal
lg
lv
int
st
vp
dp
E
F
G
Ptf1a DAPI
Ptf1a DAPI
E12.5 Ptf1a Sox2 DAPI
H
I
J
Nkx6.1 Pdx1
Nkx6.1 Pdx1
E12.5 Nkx6.1 Pdx1

Figure 3.1. Conditional endodermal Ptf1a misexpression (Ptf1a^{EDD}). All E10.5 tissues except (G, J). (A) Ptf1a^{EDD} **system**. Black triangles, loxP sites. (B,C) Morphologies of control and Ptf1a^{EDD} endoderm; whole-mount immunolabeling (maximum-intensity projection), pan-endodermal Foxa2. (D) *tetO* allele activation by βgal immunolabeling. (E) Control endodermal Ptf1a was in pancreatic progenitors (dorsal pancreas, yellow arrowhead; intestine, white arrowhead). (F) Ptf1a^{EDD} embryos showed pan-endoderm Ptf1a at E10.5, including regions normally devoid of expression (e.g., anterior stomach progenitors: white arrowhead). (G) 72 hrs (E12.5) after initiating Ptf1a^{EDD}, Ptf1a^{+} tissue was more restricted, with an anterior boundary within prospective stomach (posterior, anterior stomach: yellow, white arrowheads). (H) Control E10.5 embryo, Nkx6.1/Pdx1 co-production in dorsal pancreatic anlage. (I) With Ptf1a^{EDD}, Nkx6.1 was suppressed in the pancreatic buds, but (J) by E12.5, was restored to normal levels (dorsal bud shown). Bars: B-D, 100 μm; E-J, 20 μm. dp, dorsal pancreas; vp, ventral pancreas; st, stomach; lv, liver; lg, lung; int, intestine.

endoderm and endothelium (Fig. 3.1D-F), essentially with uniform foregut endoderm coverage (Fig. 3.1D). Endodermal cells broadly recognized and functionally responded to Ptf1a^{EDD}. There were widespread alterations in tissue morphology associated with dominant re-regionalization of the germ layer, described below (Fig. 3.2). E10.5 embryos showed variable absence of overt organ buds (Fig. 3.1D), and slight retardation in forming lung buds, which always became distinct again by E12.5 (not shown). Anterior endoderm showed wide suppression in Sox2 level, described below. By 72 hours (E12.5), in addition to its presence in many pancreatic bud cells, Ptf1a was observed in tissue representing the region normally turning into stomach (Fig. 3.1G) and anterior duodenum. In this region at this stage, any Ptf1a was likely derived from the endogenous locus, because Ptf1a was no longer observed in more anterior foregut such as Sox2^{+} prospective anterior stomach (Fig. 3.1G) or esophagus (not shown). Extinguished Ptf1a in these regions suggests a limited window of exogenous Ptf1a^{EDD}.

Titrating the timing and level of doxycycline was required for eliciting coherent tissue responses to Ptf1a^{EDD}. In preliminary findings, prolonged Ptf1a^{EDD} via doxycycline in the drinking water caused pervasive malformations and embryo death between E10.5-11.5, and similarly with single 1.0 mg injections, leading to the low-level scheme (~0.25 mg/female) that caused short-lived Ptf1a^{EDD} and profound tissue-conversion. Within the pancreas buds, Ptf1a^{EDD} temporarily disturbed the normal marker combinations of early pro-pancreatic MPC status. Normally, Nkx6.1 is widely expressed in pancreatic progenitors at E10.5 (Fig. 3.1H), and slightly later (E11.5-12.5) becomes restricted to the trunk domain (i.e., absent from prospective pro-acinar tip domains) of the pancreatic epithelium. Mutual repression between *Ptf1a* and *Nkx6.1* has been reported, with Ptf1a from a Pdx1 promoter/enhancer transgene strongly suppressing *Nkx6.1* (Schaffer et al., 2010). Our observation of temporary Nkx6.1 suppression

(n=3) provides further indirect evidence for transient Ptf1a^{EDD}. Analysis 24 hours after E9.5 doxycycline administration showed strong Nkx6.1 suppression within pancreatic bud MPC (Fig. 3.1I). We speculate that endogenous Ptf1a added to Ptf1a^{EDD} was greater than in normal pancreatic MPC thus suppressing *Nkx6.1*, and that the post-doxycycline decline in Ptf1a^{EDD} restored the Nkx6.1^{+} state (n=3; for 72 hours post-doxcycyline, Fig. 3.1J). We propose that the post-doxycycline decline led to lower level, normally regulated Ptf1a from its endogenous locus, allowing the foregut endoderm either to restore normal pancreatic MPC specification, or undergo pro-pancreatic conversion with intermediate acquisition of a pro-pancreatic state.

Ptf1a^{EDD} broadly expands the Pdx1^{+} endodermal territory and pro-pancreatic regulatory network

We next examined alterations in early regional foregut endodermal gene expression. *Pdx1* and *Ptf1a* are the best-known markers linked to pancreatic MPC specification (Zhou et al., 2007; Pan et al., 2013). *Pdx1* expression at E10.5 normally marks endoderm representing the dorsal and ventral pancreatic buds, caudal-most stomach, rostral duodenum, and a portion of the extra-hepatic biliary system (EHBS) (Fig. 3.2A). Endodermal *Ptf1a* is restricted to the developing pancreas within this territory. Both genes are required for proper pancreatic outgrowth and differentiation (Jonsson et al., 1994; Offield et al., 1995; Holland et al., 2002; Krapp et al., 1998; Kawaguchi et al., 2001). In Ptf1a^{EDD} embryos at E10.5, the region of Pdx1^{+} cells was reproducibly and greatly expanded into the more rostral endoderm and caudal ventral foregut (n=6; Fig. 3.2B). We reproducibly observed clear suppression of Sox2 in Ptf1a^{EDD} anterior endoderm in whole-mounts (n=5; Fig. 3.2B, Fig. 3.3) or multiple independent side-by-

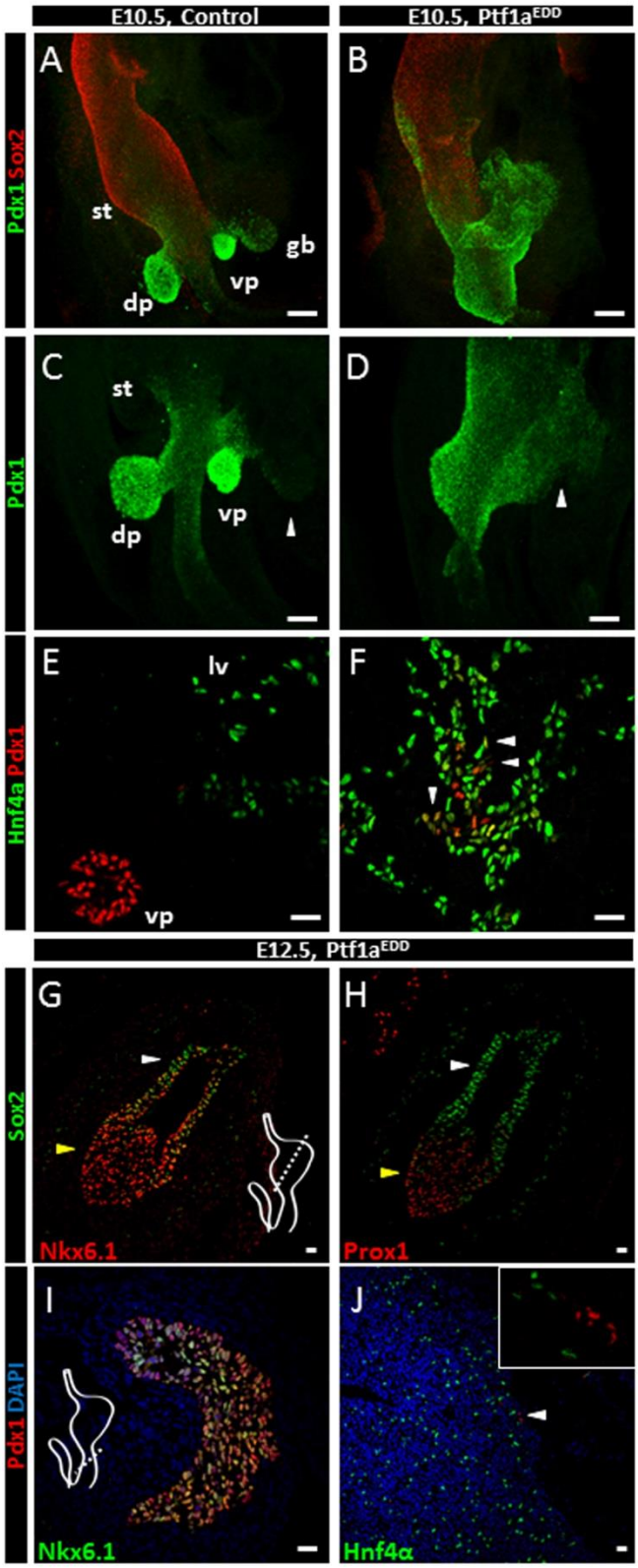
E10.5, Control
E10.5, Ptf1a^EDD
A
B
Pdx1 Sox2
st
gb
vp
dp
C
D
Pdx1
st
vp
dp
E
F
lv
Hnf4a Pdx1
vp
E12.5, Ptf1a^EDD
G
H
Sox2
Nkx6.1
Prox1
I
J
Pdx1 DAPI
Nkx6.1
Hnf4α

Figure 3.2. Expansion of Pdx1 and early pancreatic MPC markers. Ptf1a^{EDD} induced at E9.5, analysis 24 (E10.5) or 72 (E12.5) hrs post-injection. (A-D) Whole-mount immunolabeling: Pdx1, Sox2. (A) Pdx1 and Sox2 differentially marked foregut endoderm, with co-production in posterior stomach. (B) Pdx1^{+} domain greatly expanded by Ptf1a^{EDD}. (C) Low-level Pdx1 detected in a sub-region of control gall bladder (arrowhead). (D) Ptf1a^{EDD} broadly expanded the Pdx1^{+} territory into posterior ventral foregut (arrowhead). (E) Control Pdx1 was not co-expressed with hepatoblast marker Hnf4α. (F) Ptf1a^{EDD} embryos, many Hnf4α^{+} hepatoblasts expressed low levels of Pdx1 (arrowheads: example cells). (G,H) By E12.5, Nkx6.1 (G) and Prox1 (H) were detected within presumptive posterior stomach (co-labeled with Sox2) under Ptf1a^{EDD} (yellow, white arrowheads: posterior, anterior stomach). (I) Ectopic Nkx6.1 expression within what normally would become anterior duodenum. (J) Pdx1 signal was not maintained within the definitive liver of E12.5 embryos from E9.5 Ptf1a^{EDD}; few Pdx1^{+} cells were found within the liver anlage (arrowhead). Inset: a different embryo showing a few groups of Pdx1^{+} cells adjacent to Hnf4α^{+} cells. Approximate sectional plane indicated in (G,H,I). Bars: A/B, 100 µm; C/D, 50 µm; E-J, 20 µm. gb, gall bladder.

side section analyses (not shown). For unknown reasons, the posterior Pdx1 expansion was limited and patchy. Despite widespread endodermal activation of *ROSA26*$^{rtTA.IRES.EGFP}$, the tetO$^{Ptf1a.IRES.lacZ}$ allele was poorly activated in the prospective mid/hindgut (Fig. 3.4). Accordingly, Cdx2 expression and general histology was normal in the rostral-most remaining small intestine in our postnatal Ptf1a^{EDD} analysis (not shown). This situation prevents rigorous conclusions regarding effects of Ptf1a^{EDD} in posterior endoderm, and we therefore focus on the rostral-most duodenum and regions located rostral and ventral to it.

Because *Sox17* is also expressed within endothelial cells, it was important to address effects of endothelial Ptf1a misexpression on endodermal patterning. We misexpressed Ptf1a using the endothelial *Tie1*^{Cre} driver (Gustafsson et al., 2001) in *Tie1*^{Cre}; *ROSA26*$^{rtTA.IRES.EGFP}$; tetO$^{Ptf1a.IRES.lacZ}$ embryos. Endothelial Ptf1a, with the same injection regimen as *Sox17*^{Cre}-based Ptf1a^{EDD} at E9.5, did not change the *Pdx1* expression domain at E10.5 (n=3; Fig. 3.5), or affect other regional (Nkx6.1, Pdx1) expression patterns at E12.5 (data not shown). Therefore, Ptf1a must be endodermally delivered to cause repatterning and organ conversion. We cannot, however, rule out the possibility that endothelial Ptf1a somehow supported or synergized with the Ptf1a^{EDD} phenotype; but we note that other endodermal Cre drivers do not offer the timing and broad endodermal characteristics, are substantially mosaic, or expressed in other key tissues known as essential in patterning the embryo.

The posterior ventral foregut produces liver, EHBS (extra hepatic biliary ducts, gall bladder) and ventral pancreas (McCracken and Wells, 2012). The presumptive ventral pancreas and gall bladder are distinguishable by *Sox17* expression, which becomes progressively restricted to the gallbladder anlage (Spence et al., 2009), and *Pdx1*. At 10.5, the ventral pancreas bud displays uniformly high Pdx1, while the gall bladder primordium shows lower, variable levels of Pdx1,

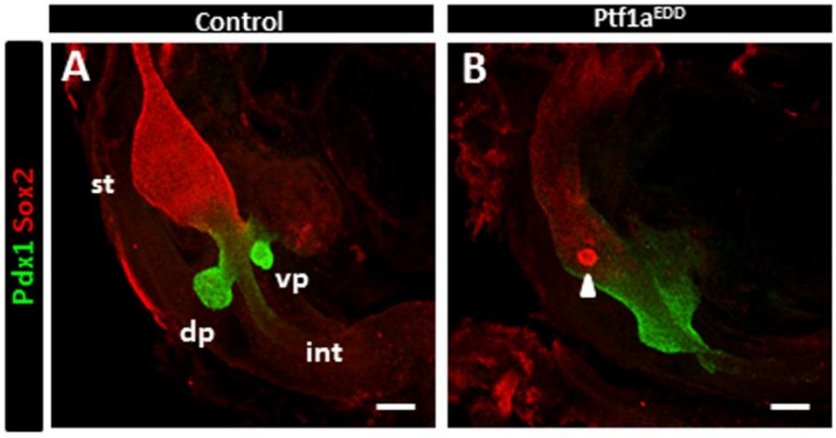

Figure 3.3: Broad foregut endoderm suppression of Sox2 levels following Ptf1a^{EDD}. *(A,B)* Maximum-intensity projection of a confocal z-stack. *(A)* In control embryos, Sox2 marks anterior foregut endoderm and Pdx1 the posterior foregut endoderm. *(B)* In addition to an expanded Pdx1^{+} domain following Ptf1a^{EDD} (see Fig. 2), we observed Sox2 suppression throughout the foregut endoderm. Arrowhead in *(B)* indicates a presumed area of Sox2^{+} endoderm that escaped ROSA26$^{rtTA.IRES.EGFP}$ recombination (this area lacked any Ptf1a expression), such that this level, in side-by-side comparison to control whole mounts, was similar to the normal foregut endodermal signal, allowing direct estimation of the reduced level in all of the surrounding Ptf1a^{EDD} tissue. This suppression was temporary, as shown in Fig. 2. Scale bars: 100 µm. Abbreviations: dp, dorsal pancreas; vp, ventral pancreas; st, stomach; int, intestine.

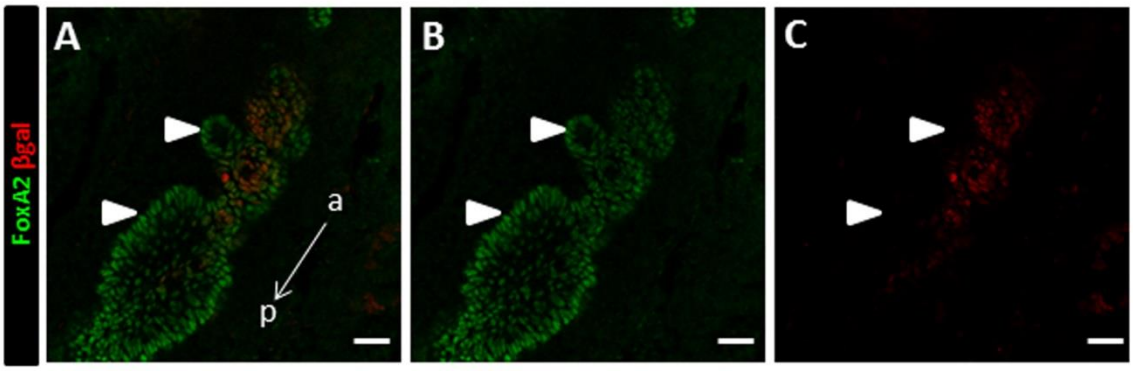

Figure 3.4: Poor tetO allele activation in posterior endoderm. *(A)* Individual optical section of E10.5 Ptf1a^{EDD} midgut after doxycycline administration at E9.5. Foxa2 marks all endoderm progenitors while βgal indicates activation of the tetO$^{Ptf1a.IRES.LacZ}$ allele. In contrast to the near-ubiquitous activation of the tetO allele in the foregut (see Fig. 1), not all Foxa2^{+} cells *(B)* expressed βgal *(C)* in the midgut or hindgut (indicated by arrowheads). In the absence of ectopic Ptf1a in these more posterior tissues, we cannot currently interpret their capacity to be respecified as pancreatic cell types. Scale bars, 25 μm.

which are shortly thereafter reduced further; i.e., the $Pdx1^+$ domain seems to recede towards the ventral pancreas (Fig. 3.2C). With $Ptf1a^{EDD}$, the $Pdx1^+$ territory was vastly expanded ventrally, and uniformly high within the posterior ventral foregut, suggesting that Pdx1 was ectopically expressed throughout the EHBS primordia and a substantial portion of the nearby liver anlage (n=6 individual embryos; Fig. 3.2D). To verify ectopic *Pdx1* activation in hepatoblasts, we tested for co-production of Pdx1 and the hepatoblast marker Hnf4α, which normally define complementary domains (n=3; Fig. 3.2E). $Ptf1a^{EDD}$ embryos showed many co-producing cells in ventral foregut endoderm (Fig. 3.2F). In $Ptf1a^{EDD}$ embryos analyzed at E12.5, no distinct gall bladder or EHBS could be found, consistent with the idea that their progenitors had been respecified and joined a common state with the ventral pancreatic bud (n=6). Serial-section analysis failed to show ectopic $Pdx1^+$ cells at E12.5 within the distinct liver domain, indicating resolution of the early mixed pancreas/liver state as the tissue moved into liver differentiation (Fig. 3.2J). We cannot rule out that some Ptf1a-expressing hepatoblasts or forestomach progenitors did undergo respecification and move physically into adjacent respecified domains. We addressed a potential cell-death explanation below. The cell migration issue would require early specification-marker-driven and temporally specific lineage tracing by non-Cre methods (because we used Cre to activate $Ptf1a^{EDD}$), which are currently unavailable.

We tested if $Pdx1^+Ptf1a^+$ endodermal progenitors induced by $Ptf1a^{EDD}$ expressed other pancreatic MPC markers. In normal E10.5-12.5 endoderm, Nkx6.1 specifically marks pancreatic progenitors (Pedersen et al., 2005), and therefore was not expressed in control $Pdx1^+$ stomach or duodenum (not shown). Analyzing $Ptf1a^{EDD}$ embryos at E12.5, we observed co-production of Nkx6.1 within the $Pdx1^+Ptf1a^+$ presumptive posterior stomach (n=6; Fig. 3.2G). We reproducibly detected similar expansion of Prox1, another influential pancreatic progenitor TF

not normally expressed in the prospective stomach (n=3; Fig. 3.2H). Nkx6.1 was also ectopically expressed in the domain that would normally produce anterior duodenum (Fig. 3.2I). We examined whether proliferative expansion of pancreatic progenitors contributed to the spatial expansion of pancreatic markers in Ptf1a^{EDD} embryos. We presume that replacement of stomach progenitors by hyper-proliferative pancreatic progenitors would also involve loss of progenitors for other organ territories. In Ptf1a^{EDD} embryos at E10.5, we were unable in this analysis to use pancreas-specific markers such as Ptf1a, which was expanded throughout the endoderm, or Nkx6.1 (temporarily suppressed). Given that the vast expansion of Pdx1 occurs acutely following Ptf1a^{EDD}, we examined E10.5 Ptf1a^{EDD} embryos by extensive sectional analysis for regional alterations in proliferation using phospho-histone H3 (chosen over, for example, Ki67 or BrdU labeling, because of the high proliferation rate of cells in all tissues over these stages of organogenesis). We also tested for increased apoptosis (cleaved caspase-3) within the Pdx1^{+} domain. We detected no regional alterations in proliferation or apoptosis that could explain the expansion in the Pdx1^{+} domain as spreading of cells from the normal pancreatic domain (not shown).

These combined alterations in progenitor markers suggest that Ptf1a^{EDD} initiated a dominant effect on the posterior foregut, initially activating expression of Pdx1, a principal component of the pro-pancreatic MPC gene regulatory network, from its endogenous locus and much more widespread than normal. The expression of other pro-pancreatic MPC regulatory-network members was recruited to the remaining Ptf1a^{+}Pdx1^{+} region (more rostral regions withdrawing from this condition), stabilizing a pro-pancreatic condition in what would normally have become the prospective glandular stomach, anterior duodenum, and EHBS.

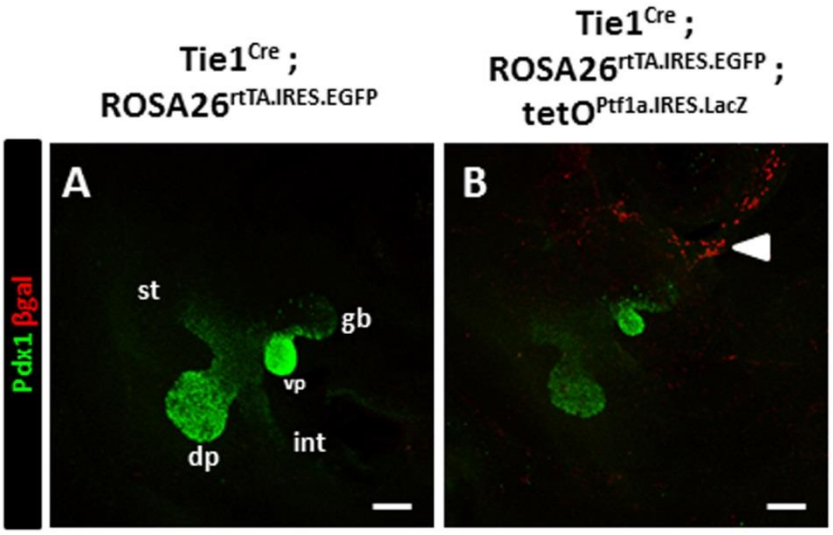

Figure 3.5: Endothelial misexpression of Ptf1a does not expand the endodermal Pdx1+ territory. *(A)* E10.5 Tie1^{Cre}; ROSA26$^{rtTA.IRES.EGFP}$ (control) maximum intensity projection of the posterior foregut. Pdx1 was restricted to its normal expression domain: pancreatic buds, posterior stomach, anterior duodenum, and a portion of the EHBS. *(B)* E10.5 *Tie1*^{Cre}; *ROSA26*$^{rtTA.IRES.EGFP}$; tetO$^{Ptf1a.IRES.LacZ}$ (trigenic misexpression) maximum intensity projection of the posterior foregut following doxycycline administration at E9.5. In *Tie1*^{Cre}-trigenic embryos, the tetO allele was activated within endothelial cells (expression of βgal) but not endoderm. Arrowheads indicate endothelial βgal expression. The maintenance of the normal expression domain of Pdx1 with this method indicates that endodermal Ptf1a production was required for the regionalized pancreas-conversion effects reported here. Scale bars, 100 μm. Scale bars: A, B, 100 μm. Abbreviations: dp, dorsal pancreas; vp, ventral pancreas; st, stomach; int, intestine; gb, gall bladder.

Respecified pancreas-adjacent endoderm produces differentiated pancreatic cell types

To test if Ptf1a^{EDD} initiated a complete conversion to pancreatic tissue, misexpression was initiated at E9.5 and tissues analyzed at E18.5/P0 when differentiation programs are clearly distinguishable. While some aspects of pancreas differentiation are discernible mid-gestation, the programs in stomach and intestine acquire many cell-type-specific characteristics only at later gestation and peri/postnatally. Ptf1a^{EDD} pups were stillborn (likely caused by deficits in endothelial tissues), but otherwise equivalent in size to the various controls described above.

The gross anatomy of foregut endodermal organs (e.g., Fig. 3.6 for lung) was normal except in the posterior foregut (described below), and cellular differentiation was largely normal in the lung and forestomach in Ptf1a^{EDD} pups. Because Ptf1a^{EDD} pups were stillborn, their lungs did not inflate, but there was appropriate differentiation of proximal and distal lung, and extensive endothelial coverage of terminal airways (Fig. 3.6). The Ptf1a^{EDD} forestomach contained multiple layers of Sox2^{+} cells (Fig. 3.7). These data indicate that despite ectopic Ptf1a expression and effects on Sox2, the lung resisted Ptf1a-mediated respecification and the normal differentiation program was reasserted. While the lack of forestomach-specific markers limited our depth of analysis, we conclude that the forestomach and lung were not grossly diverted from their normal organ identities, albeit suffering possible modest alterations in terminal differentiation.

Abnormalities in embryos/pups from E9.5 Ptf1a^{EDD} (n=6) included disrupted gastrointestinal tract continuity at the stomach-duodenum junction, an abnormal shape and color of the stomach (Fig. 3.8B,D), and lack of a morphologically obvious EHBS (Fig. 3.8C,E).

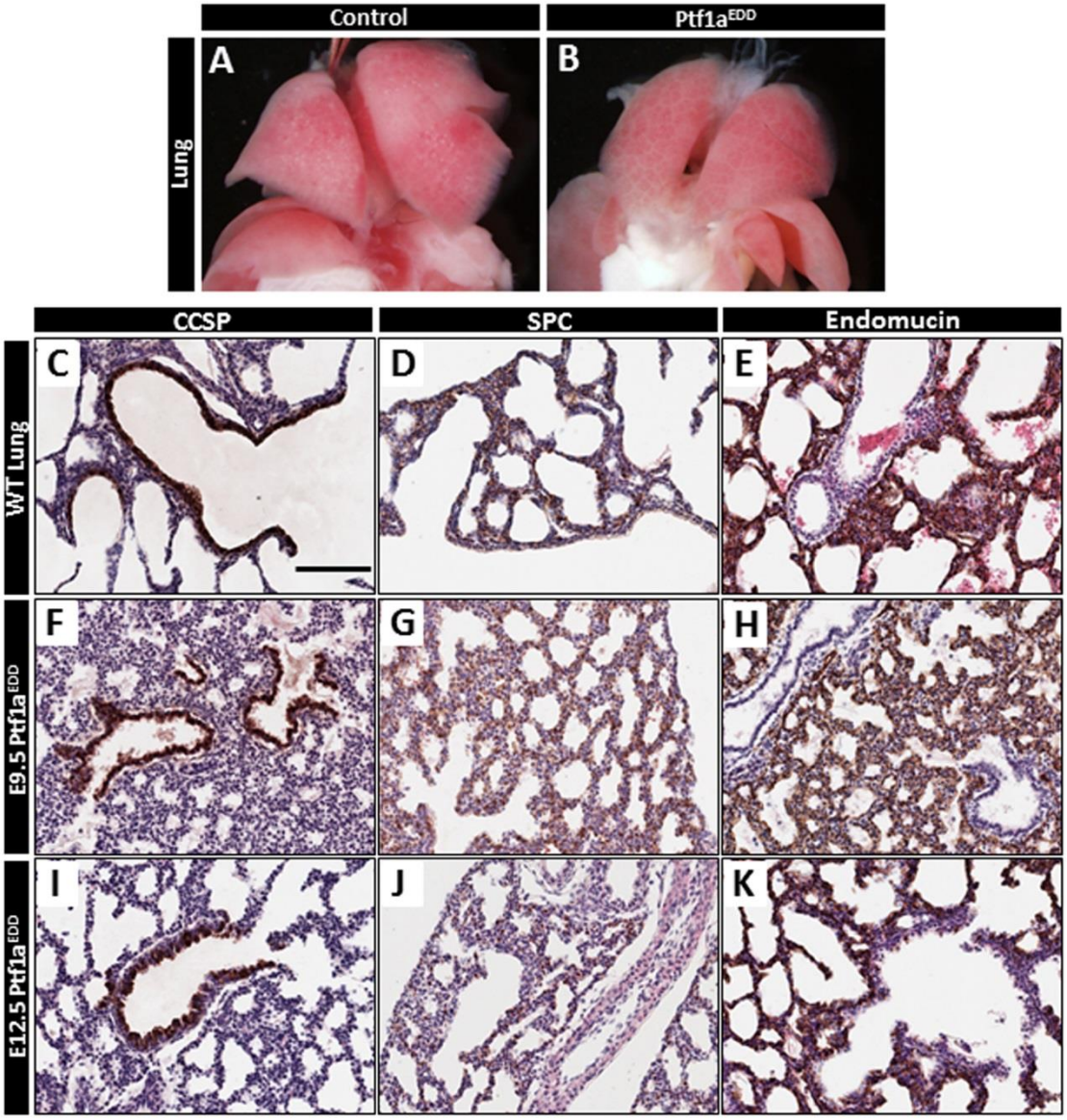

Figure 3.6: Following endodermal Ptf1a misexpression, the lung maintains normal organ identity. *(A,B)* Organ morphology of control *(A)* and Ptf1a^{EDD} *(B)* lung at P0 after doxycycline administration at E9.5. The lungs in Ptf1a^{EDD} embryos were grossly equivalent to control embryos except that Ptf1a^{EDD} lungs were not inflated (animals are stillborn). The completeness of lung development at P0 was tested by the production of terminal differentiation markers and endothelial cells. *(C,F,I)* CCSP (Clara cell secreted protein) marks Clara cells in the small airways of the lung. *(D,G,J)* SPC (Surfactant protein C) marks type II alveolar epithelial cells. *(E,H,K)* Endothelial cells were detected by the pan-endothelial marker Endomucin. The level and distribution of all markers were comparable between control and Ptf1a^{EDD} tissue. These results suggest that lung differentiation proceeds largely unchanged following early-stage Ptf1a^{EDD}. Scale bars: A and B, 1 mm; C-K, 50 µm.

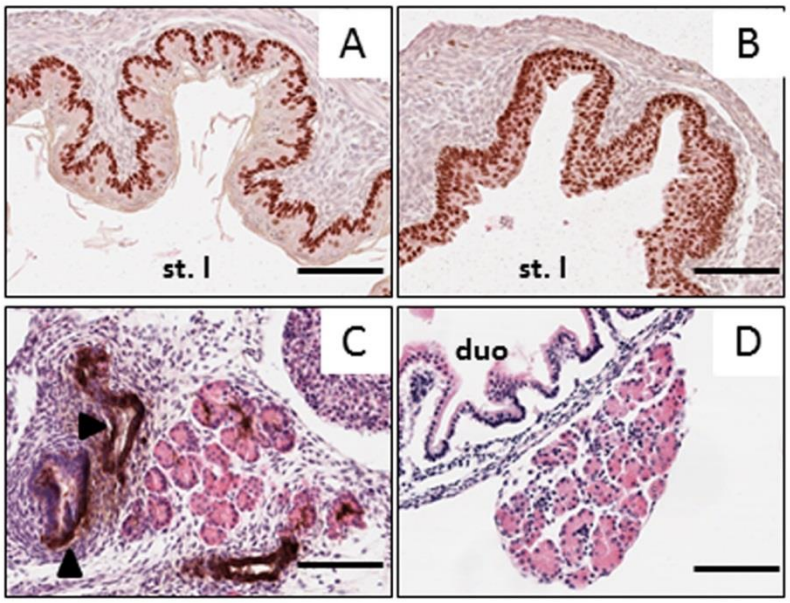

Figure 3.7: Additional histological analysis of Ptf1a^{EDD} initiated at E9.5. *(A)* Immunohistochemical detection of Sox2 in control P0 forestomach tissue (brown). Sox2 production was restricted to the basal layer of the forestomach. *(B)* Detection of Sox2 in Ptf1a^{EDD} P0 forestomach tissue showed an expansion to multiple layers of the forestomach epithelium, and the tissue was lacking an apparently lacking superficial keratinized layer. *(C)* Large caliber DBA-reactive ducts (brown) adjacent to pancreas tissue that may resemble a stranded residual portion of the proximal EHBS (arrowheads). *(D)* Histological example of a patch of pancreas tissue in Ptf1a^{EDD} pups located between the coelomic epithelium and submucosa of the small intestine. Scale bars, A-D 50 µm. Abbreviations: st. l, stomach lumen; duo, duodenum.

Pancreatic acini, the predominant pancreatic cell type, are visually distinguishable by their opacity and characteristic cauliflower-like tissue structure. The posterior stomach in Ptf1a^{EDD} pups contained tissue externally resembling pancreatic acinar cells (Fig. 3.8B,D). The morphology, size, and position of the dorsal pancreas were visually normal. The ventral pancreas resided near the break between the posterior stomach and blind end of the rostral-most duodenum (Fig. 3.8D). The postnatal and adult mouse stomach comprises three distinct domains (Lee et al., 1982). The most rostral forestomach is overall typified by a pseudo-stratified keratinized epithelium. Caudal to forestomach lies the glandular stomach, divided into the corpus and antrum. Both domains have columnar epithelial morphology (Fig. 3.8F) but different cell types. Parietal and chief cells are derived only from the corpus, while the antrum contains mucus-secreting cells. Essentially replacing the entire glandular stomach epithelium in Ptf1a^{EDD} pups were cells indistinguishable from pancreatic acini by morphology and H&E staining (large eosinophilic cells) (Fig. 3.8G,H). It appeared as if pancreatic tissue had replaced the entire glandular stomach (Fig. 3.8H,I,J).

In normal animals, the mesoderm surrounding the stomach (Fig. 3.8F) is distinct from the mesoderm at the pancreas. Stomach-associated mesoderm becomes multi-layered, including submucosa and muscularis layers between the coelomic and endodermal epithelia. This normal stomach-associated mesoderm was absent next to the ectopic pancreas in the posterior stomach of Ptf1a^{EDD} pups. The ectopic pancreas was closely apposed to coelomic epthelium, and the mesoderm was characteristically pancreatic, with pervasive interdigitation amongst the ectopic differentiated epithelial tissue (Fig. 3.8H). These data support the conclusion that following early conversion of the endoderm that would have formed the prospective stomach, anterior duodenum, and EHBS into pancreatic MPC, there was region-appropriate dominant instruction

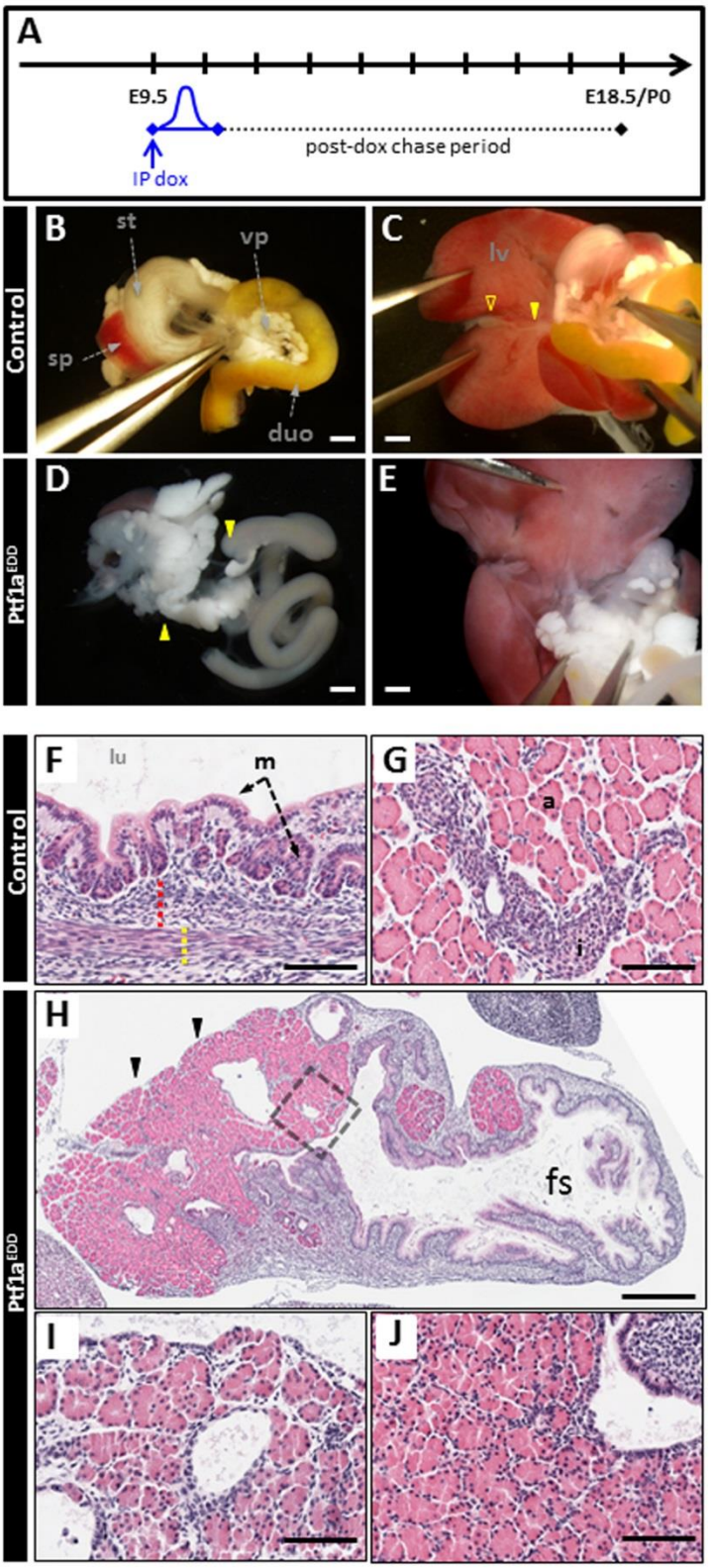
A
E9.5
E18.5/P0
post-dox chase period
IP dox
Control
B
st
vp
sp
duo
C
lv
Ptf1a EDD
D
E
Control
F
lu
m
G
a
i
Ptf1a EDD
H
fs
I
J

Figure 3.8. Pancreatic cells replacing glandular stomach, anterior duodenum, EHBS. (A) Set-up: E9.5 doxycycline transiently pulsed ectopic Ptf1a^{EDD}, analysis at E18.5/P0. (B,C) Morphology of control stomach, duodenum (B), extra-hepatic biliary system (EHBS; C). Closed or open arrowheads in (C): cystic duct, gall bladder. (D) With Ptf1a^{EDD}, pancreatic acinar cells found within posterior stomach. Stomach and intestine were disconnected (yellow arrowheads). (E) Distal EHBS was absent. (F) H&E staining, control glandular stomach. Dashed lines: submucosa (red), muscularis layers (yellow). (G) H&E-stained control pancreas. (H) Glandular stomach in Ptf1a^{EDD} embryos replaced with pancreatic acini. The thick mesenchymal layer normally surrounding glandular stomach was absent adjacent to ectopic pancreas (arrowheads). (I) Close-up from (G). (J) Additional image, Ptf1a^{EDD} glandular stomach. Bars: B-E, 1 mm; F, G, I, J, 50 µm; H, 500 µm. sp, spleen; duo, duodenum; lu, stomach lumen; m, mucosa; a, acini; i, islet; fs, forestomach.

of the overlying mesoderm cell fate. The visual lack of EHBS or anterior duodenum was corroborated by systematic serial-section analysis of Ptf1a^{EDD} tissue, which found no evidence for distal EHBS tissue types (gall bladder, cystic duct) or structures of the anterior duodenum, including the pyloric connection to stomach or the Brunner's glands normally found at the rostral-most collar region of the duodenum. Ptf1a^{EDD} tissue contained some large DBA-reactive ducts adjacent to the liver, and somewhat posterior to the pancreas-converted stomach, which could have represented a fragment or partially formed segment of the normal proximal EHBS (Fig. 3.7). Small patches of pancreas tissue were found between the coelomic epithelium and submucosa along a limited portion of the small intestine (Fig. 3.7). From this morphological and histological evidence, we infer that transient Ptf1a^{EDD} at E9.5 caused glandular stomach, anterior duodenum, and distal EHBS progenitors to become developmentally re-specified into pancreas. The fate switch of gut-tube endodermal progenitors, and change in character of the associated adjacent mesoderm, led to a break in stomach-intestine continuity and loss of a complete EHBS.

Ectopic pancreas tissue replacing the glandular stomach contains endocrine cell types

We focused in the next analysis on the stomach-associated ectopic pancreas, because we were unable to distinguish between the true ventral pancreas and pancreas tissue that had become continuous with it but was derived from the Ptf1a^{EDD}-converted EHBS or rostral duodenum. To determine the extent of pancreas conversion, we serially sectioned the entire foregut from three Ptf1a^{EDD} pups, using molecular markers to identify gastric and pancreatic cell types on a majority of these sections to ensure detailed tissue coverage. Parietal cells are restricted to glands of the corpus and are marked by high HK-ATPase, while epithelium of the corpus and antrum is generally marked by GSII lectin (*Griffonia Simplicifolia* Lectin II). Thus, GSII/HK-ATPase

double-positive glands identify corpus (Fig. 3.9A) and GSII^{+}/HK-ATPase^{-} glands signify antrum. Ptf1a^{EDD}-converted posterior stomach contained only minuscule, scattered GSII^{+}/HK-ATPase^{+} or GSII^{+}/HK-ATPase^{-} areas. Fig. 4B deliberately shows one of those remaining areas, with the overwhelming majority of cells within the posterior stomach expressing pancreatic acinar-specific amylase (Fig. 3.9B).

Pancreatic endocrine and duct cells were present within the ectopic pancreas. Pancreatic endocrine cells are generally synaptophysin^{+}, while duct cells are DBA-lectin-reactive (Fig. 3.9C). Epithelial endocrine cells in the stomach normally distribute as single cells, while most endocrine cells in the pancreas cluster into the often-large islets of Langerhans, with insulin signifying pancreatic identity (Fig. 3.9E). Consistent with the idea that early, transient Ptf1a^{EDD} did not deflect normal pancreatic organogenesis in a major way, immunodetection and histological examination showed that islet-cell representations and clustering in the 'endogenous pancreas' after E9.5 Ptf1a^{EDD} were equivalent to normal controls. Within the ectopic pancreas replacing the glandular stomach, we found synaptophysin^{+} cells, both clustered and dispersed, and DBA^{+} duct cells. Dispersed endocrine cells were much more numerous than those organized into scattered, loosely organized clusters (typified by Fig. 3.9D), but were reproducibly present throughout the ectopic pancreas (see also Fig. 3.10). All endocrine cells were single-hormone-positive, and expressed insulin, glucagon or somatostatin (Fig. 3.9F). Insulin^{+} cells within the ectopic pancreas expressed Pdx1 and Nkx6.1; criteria for equivalence to normal beta cells (Fig. 3.9H, I). These cells are too few for isolation and physiological testing of their maturity and glucose-responsiveness. The morphological, histological, and molecular analysis supports the conclusion that transient Ptf1a^{EDD} at E9.5 caused functional respecification of the prospective stomach into multipotent pancreatic progenitors that were then capable of deriving all pancreatic

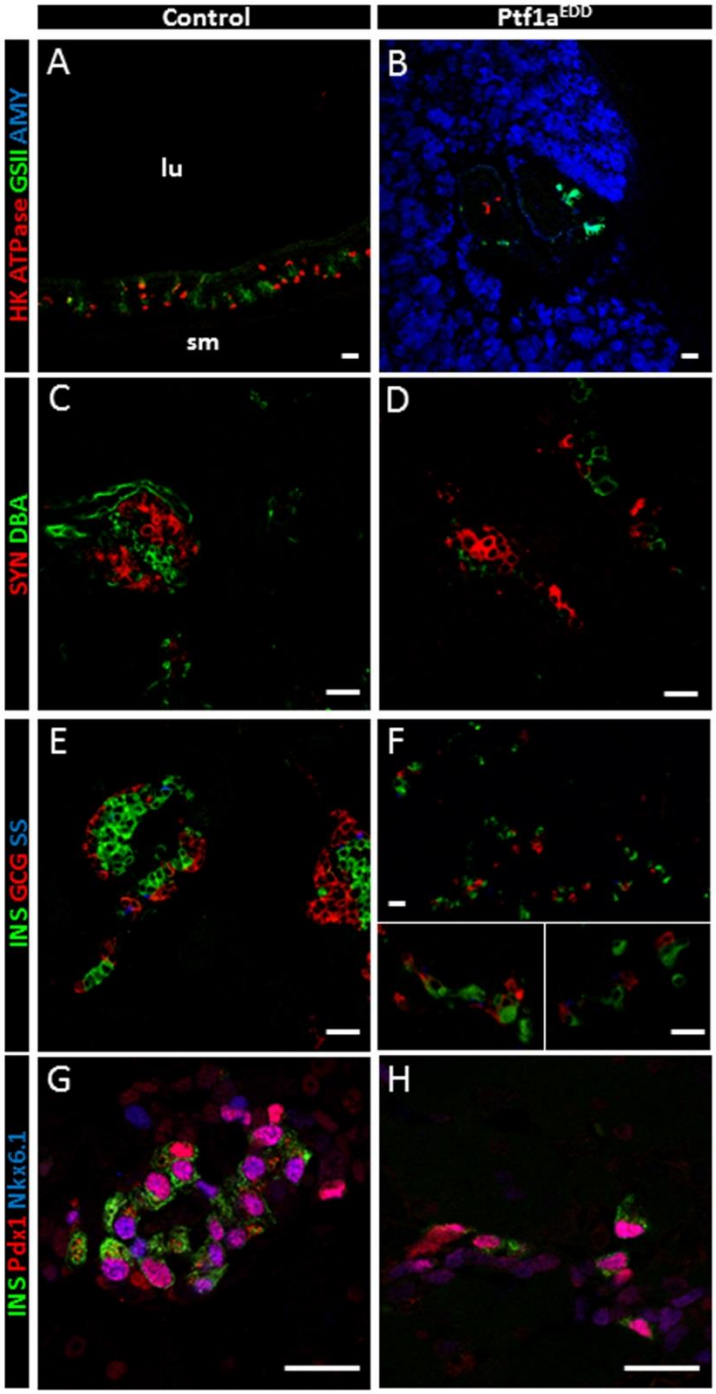
Control
Ptf1a^EDD
HK ATPase GSII AMY
A
lu
sm
B
SYN DBA
C
D
INS GCG SS
E
F
INS Pdx1 Nkx6.1
G
H

Figure 3.9. Ectopic pancreas contains endocrine and exocrine cells. [Doxycycline at E9.5, analysis at E18.5/P0.] (A) Control corpus glands reacted with GSII lectin and expressed HK-ATPase, but not pancreatic acinar amylase. (B) With Ptf1a^{EDD}, most posterior stomach cells expressed amylase but not stomach markers. (C) Normal pancreas, clustered synaptophysin^{+} endocrine cells (islets) and DBA-reactive duct cells. (D) Ptf1a^{EDD}-converted stomach with synaptophysin^{+} cell clusters, DBA-reactive ducts. (E) Endocrine cells expressing insulin, glucagon, somatostatin. (F) Ptf1a^{EDD}-converted stomach contained numerous single-hormone-positive endocrine cells for insulin, glucagon, somatostatin (insets – additional endocrine clusters in Ptf1a^{EDD} tissue). Somatostatin^{+} cells were far fewer than glucagon^{+} or insulin^{+} cells. (G) Insulin-producing normal β-cells were Pdx1^{+}, Nkx6.1^{+}. (H) Insulin^{+} cells within Ptf1a^{EDD}-converted stomach were also Pdx1^{+}/Nkx6.1^{+}. Bars: A-H, 20 μm. sm, submucosa.

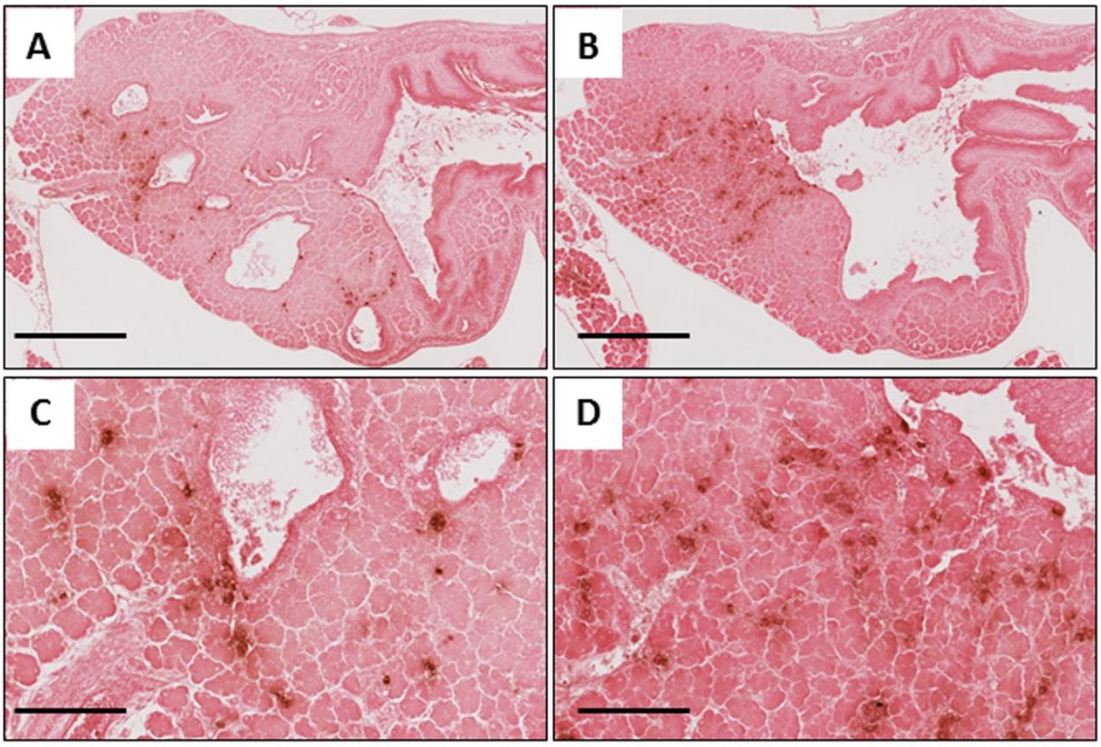

Figure 3.10: Additional histological analysis of endocrine cells in the Ptf1a^{EDD} glandular stomach. *(A,B)* Representative images, immunohistochemical detection of insulin (brown) on P0 Ptf1a^{EDD}-converted glandular stomach tissue after doxycycline administration at E9.5. Insulin-positive cells are distributed throughout the tissue as clusters and more scattered cells. *(C, D)* Higher magnifications A and B. All tissues are counter-stained with eosin. Scale bars: A and B, 1 mm; C and D, 200 µm.

lineages. Possibly, the Ptf1a^{EDD}-induced conversion from an epithelial naïve gut tube to bud-like pre-pancreatic tissue (from section analysis of E12.5 embryos; data not shown) reduced the number and organization of endocrine cells within the ectopic pancreas.

Certain non-pancreatic progenitors maintain competence for Ptf1a-mediated respecification

Given the striking re-specification of glandular stomach, anterior duodenum and EHBS, we tested if their competence to respond to Ptf1a^{EDD} became more restricted over developmental time. Tissue gathered after doxycycline injection at E10.5 (n=6) or E11.5 (n=7) was similar to the E9.5 Ptf1a^{EDD} situation, with pancreatic acinar cells located throughout the glandular stomach. The rostral-most end of the small intestine seemed closer to the posterior stomach compared to E9.5 induction, suggesting loss of less intestinal tissue, but the stomach-intestine connection was still interrupted by pancreas tissue (Fig. 3.11B,D). The distal EHBS was still absent under E10.5 or E11.5 Ptf1a^{EDD} (Fig. 3.11C,E).

Ptf1a^{EDD} initiated at E12.5 (n=5) still caused substantive replacement of the majority of the glandular stomach with pancreatic acini (Fig. 3.11F). This stage of Ptf1a^{EDD} was the first at which the continuity of the gastrointestinal tract at the stomach-intestine junction was no longer interrupted, and the distal EHBS was morphologically apparent (Fig. 3.11G). Sectional analysis revealed that the entire EHBS was replaced with pancreatic acini surrounding a central duct (Fig. 5H). Although the overall gross morphology of the intestine appeared normal, serial sectioning of Ptf1a^{EDD} tissue revealed a few small patches of pancreatic acinar cells scattered within the anterior duodenum (Fig. 3.11I).

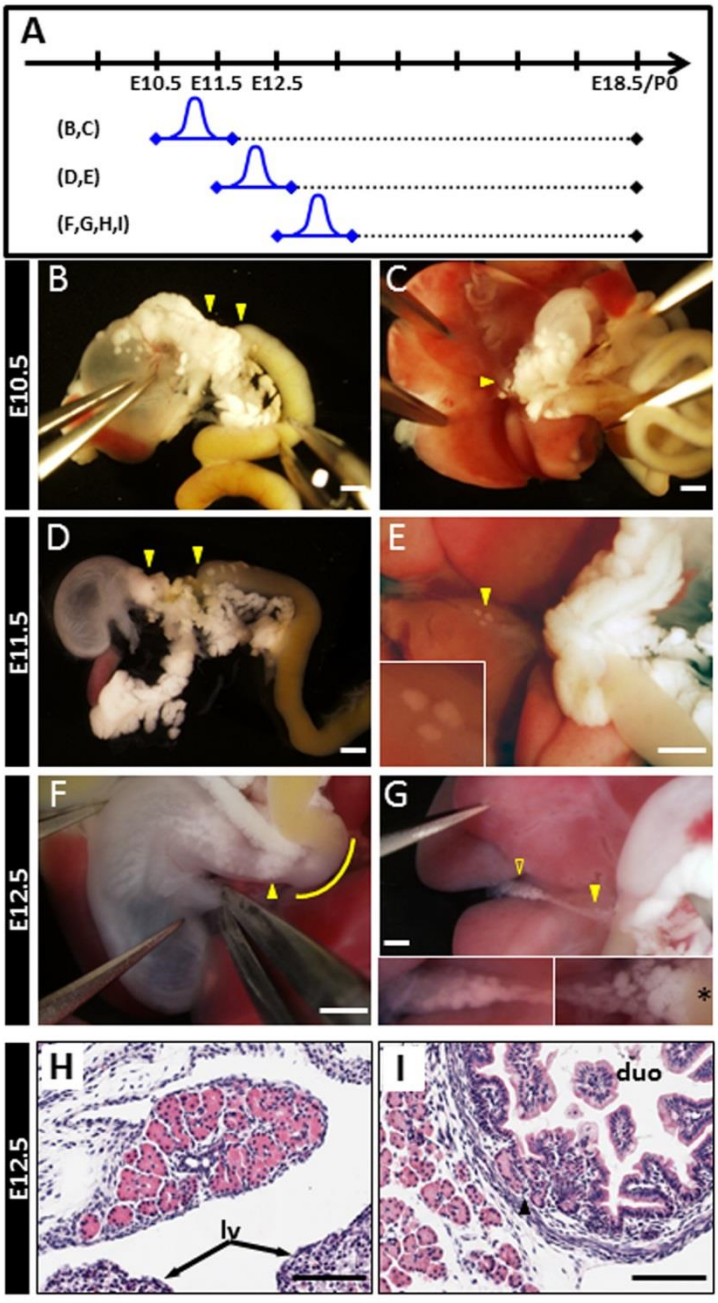
A
E10.5 E11.5 E12.5
E18.5/P0
(B,C)
(D,E)
(F,G,H,I)
E10.5
B
C
E11.5
D
E
E12.5
F
G
*
E12.5
H
lv
I
duo

Figure 3.11. Posterior foregut anatomical alterations after shifting the Ptf1a^{EDD} window. (A) Ptf1a^{EDD} induced at E10.5, E11.5, or E12.5, and analyzed at E18.5/P0. (B,C) Morphology of stomach, duodenum (B), EHBS (C) after E10.5 Ptf1a^{EDD}. (B) Posterior stomach replaced by pancreas tissue, with disconnected blind-ended intestinal tube. Arrowheads: pancreatic tissue present in this location. (C) Definitive EHBS structures were absent (arrowhead and data not shown). (D,E) Similar alterations with E11.5 Ptf1a^{EDD}. (E) Tissue from a separate animal, focused on continued lack of EHBS, but presence (arrowhead; close-up in inset) of several small patches of acinar clusters. (F-I) E12.5 Ptf1a^{EDD}. (F) Pancreatic tissue still replaced much of the glandular stomach (arrowhead); definitive acini are shown in Fig. 6. Stomach and duodenum were now connected (yellow line). (G) EHBS structures were apparent, but showed conversion of most of its endodermal epithelium to acini. Insets: close-ups of both ends, centered on the two yellow arrowheads. Right panel, tissue at the intestinal junction (asterisk). (H) Histology showed this "EHBS" to comprise pancreatic acini surrounding a central duct. (I) Pancreatic cells were also scattered within intestinal tissue (arrowhead). Bars: B-G, 1 mm; H, I, 50 μm.

We compared the morphological and molecular responses to Ptf1a^{EDD} initiated at E10.5, E11.5, or E12.5, with reference to the E9.5 data, by thorough serial-section analysis of three pups per stage. The extent of pancreas replacement within the glandular stomach with Ptf1a^{EDD} instigated at E10.5 or 11.5 was almost equivalent to the E9.5 Ptf1a^{EDD} effect. In the limited regions not showing pancreas conversion, the normal thickened glandular stomach mesenchyme was present, but was otherwise pancreas-type elsewhere (Fig. 3.12A, B). After Ptf1a^{EDD} at E12.5, replacement of the glandular stomach with pancreatic acini was substantial, but becoming much more focal. There was a universal maintenance of stomach mesenchymal character with Ptf1a^{EDD} at any point from E12.5 onward (Fig. 3.12C, D).

Formation of pancreatic acinar tissue following Ptf1a^{EDD} at E10.5, E11.5, or E12.5 occurred throughout the glandular stomach, including the corpus (amylase expression interspersed with GSII^{+}/HK-ATPase^{+} glands) (Fig. 3.12E,F). After Ptf1a^{EDD} at E10.5 or E11.5, insulin^{+} cells within the ectopic pancreas tissue in the glandular stomach were rare, and not found in clusters (Fig. 3.12G). No insulin^{+} cells were detected within the converted stomach with Ptf1a^{EDD} initiated at E12.5 (Fig. 3.12H) or thereafter.

In summary, the endodermal progenitors of the glandular stomach (corpus, antrum), anterior duodenum, and EHBS retained the ability, until at least E12.5, to convert to pancreas tissue under Ptf1a^{EDD} challenge. Between E9.5 and E12.5, the conversion transitioned from complete (whole pancreas) tissue-level replacement to progressively more focal and single-lineage (acinar) cell types. The completeness of pancreatic respecification with E9.5 Ptf1a^{EDD}, as scored by all pancreatic lineages, including insulin^{+} endocrine cells, diminished significantly

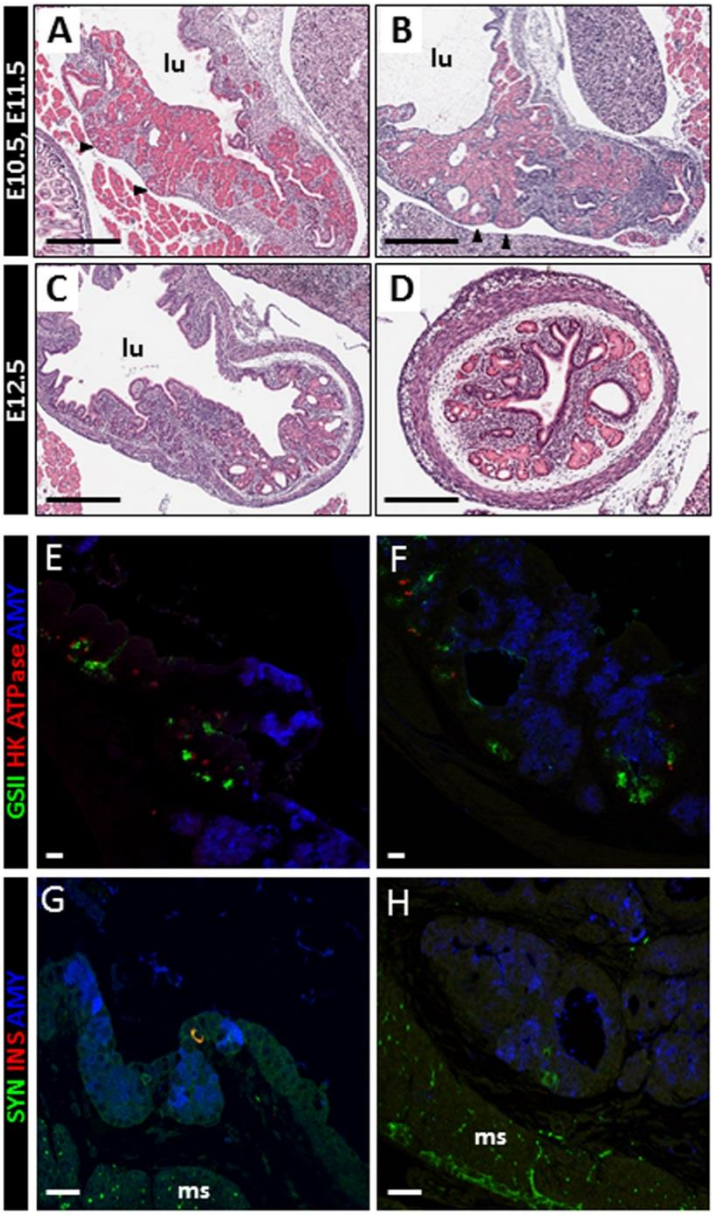

Figure 3.12. Temporal competence of Ptf1a^{EDD} respecification. Ptf1a^{EDD} at E10.5, E11.5, or E12.5; analysis at E18.5/P0. (A,B) Posterior stomach with E10.5 (A) or E11.5 (B) Ptf1a^{EDD}. Pancreatic acinar-like cells replaced the columnar epithelium. Normal stomach-type mesenchyme was absent adjacent to ectopic pancreas (arrowheads). (C,D) E12.5 Ptf1a^{EDD}: pancreatic acini still largely replaced glandular stomach epithelium (C,D: anterior, posterior stomach), but stomach mesenchyme had its normal phenotype adjacent to ectopic pancreas. With (E) E10.5 or (F) E12.5 Ptf1a^{EDD}, pancreatic acini were found next to HK-ATPase^{+} corpus glands. (G) With E11.5 Ptf1a^{EDD}, pancreatic endocrine cells in converted tissue were unclustered and much less prevalent than with E9.5 Ptf1a^{EDD}. Very few insulin+ cells were detected. (H) E12.5 Ptf1a^{EDD}, no insulin^{+} cells were detected. Single, dispersed, synaptophysin^{+} cells were detected, but normal stomach also contains endocrine cells. Extensive analysis of Ptf1a^{EDD} stomach showed transformations were to pancreatic acini. Bars: A-C, 250 µm; D, 100 µm; E-H, 20 µm.

by E10.5 and E11.5. By E12.5, respecification was less robust than earlier Ptf1a^{EDD}, and was wholly acinar-like. With Ptf1a^{EDD} between E9.5 and E11.5, the mesoderm over the glandular stomach, anterior duodenum, and EHBS apparently received instruction from the respecified endoderm to adopt a pancreatic mesodermal character. By E12.5, the fate of the overlying mesoderm in the intestine and glandular stomach was fixed in its original state.

Discussion

Regional susceptibility to dominant Ptf1a-based endodermal conversion to pancreas

Transcription factors can control cell-lineage decisions, dominantly reprogram differentiated cells to pluripotency, or cause direct reprogramming between differentiated cell types. Our work on the organ-switching potential of Ptf1a begins to address the competitive interplay between the transcriptional regulatory networks that pattern the early mammalian posterior foregut endoderm. Under the classical specification–commitment–differentiation paradigm, we focused on the issue of if, how, and when endodermal regions become "irrevocably allocated" to specific organ fates. Our study tested if the endoderm has regional variation in the open-ness to transcription-factor-induced fate switching, or variable response over time, as the organ anlagen begin to build their internal tissue-specific gene regulatory networks. The previous studies on endoderm were mostly focused on how TFs and extracellular signals interact to control differentiation within a particular gut-tube-derived organ, with pioneering work relevant to our studies centered on the decision of posterior foregut endoderm to become liver or pancreas (for example, see Wandzioch et al., 2009).

Previous studies in frog embryos (Afelik et al., 2006; Jarikji et al., 2007) suggested that Ptf1a can divert early endoderm within the *Pdx1* (*XlHbox8* in frogs) territory towards pancreas fate, but our study takes critical further steps: (1) The doxycycline-inducible system expresses unmodified Ptf1a. (2) We find early-stage endoderm competent to switch organ fates completely, forming all pancreatic lineages. There is a competence switch to lineage-restricted acinar transformations at later stages. (3) We define the responsive tissues in more detail: responsive progenitor domains include those outside the endogenous *Pdx1* expression domain (for example, not only stomach antrum but also corpus, and the entire EHBS). (4) The differential sensitivity of mammalian tissue to the correct type of Ptf1a-based switching stimulus brings the endoderm-patterning focus closer to human relevance. (5) We show clearly that Ptf1a triggers expression of principal early-acting ('first tier') members of the pro-pancreatic gene regulatory network, from their endogenous loci, and in particular the rapid and broad activation of *Pdx1* expression, including far outside of its normal territory. (6) We study the organ-conversion process in terms of early-stage alterations in the regionalized expression of other transcriptional regulatory proteins, as well as the final cell/tissue differentiation phenotype, leading to our conclusion that certain tissues are resistant to conversion, despite the broad activation of *Pdx1* expression – which in a few embryos extended even up into the vicinity of the lung bud (n=2; not shown). Longer term Ptf1a misexpression also lead to the expression of acinar cell markers (Cpa1) in endothelial cells (n=1; not shown). Future studies could explore the effects of longer term Ptf1a misexpression on the non-respecified organs like the lung and endothelial cells. Potentially, even if Ptf1a misexpression does not activate the endogenous Ptf1a and Pdx1 promoters in these cell populations, Ptf1a may be able to alter the epigenetic status of the promoters/enhancers that control these genes.

Our system showed differential effects after transiently expressing this fate-triggering factor at various stages of development. Temporal changes in the progenitor response to the same factor help inform on the dynamics of epithelial competence during embryogenesis. For example, inducing Ngn3 activity at different stages of pancreas development caused changes in endocrine cell-fate choice (Johansson et al., 2007). Also, altering BMP and TGFβ signaling in the posterior foregut produced different effects on pancreas specification over time (Wandzioch et al., 2009). An important component in our system was the transient $Ptf1a^{EDD}$; too much ectopic Ptf1a, or for too long, caused early embryo death, likely from unresolvable tissue confusion or dysfunction. The transient expression allows exogenous Ptf1a to act on endogenous loci during a narrow developmental window, and we infer that the absence of continued exogenous Ptf1a allowed proper sequential self-assembly of gene regulatory networks from the endogenous genes. Endoderm farther from the pancreas, such as the prospective forestomach-esophagus and liver, also displayed Ptf1a-induced ectopic Pdx1 production. But, in the farthest reaches, the expanded Ptf1a/Pdx1 co-positive territory subsequently underwent substantial retreat (most likely by extinguishing expression, not large-scale cell migration or apoptosis), with restoration of those territories' original organogenesis programs.

Endodermal Progenitor Competence

The potency of Ptf1a to induce, rapidly, a much broader domain of expression of *Pdx1*, from its endogenous locus, indicates a tight interdependence between these two genes. Both genes represent primary ("first tier") regulators of pro-pancreatic MPC character (Burlison et al., 2008; Kawaguchi et al., 2002; Krapp et al., 1998; Jonsson et al., 1995; Offield et al., 1995; Thompson et al., 2012). We speculate that acquiring a stable $Ptf1a^{+}Pdx1^{+}$ co-positive state, at a

particular stage of organ development, is an efficient feed-forward method of specifying and then committing to the pancreatic fate. A pair-wise threshold-dependent activation switch would be an attractive way of gating entry to specific organ commitment states. Such a relationship could explain the ability of Nkx2.1 and Pax8 can by ectopic induction (although less transient than in our case) stimulate formation of apparently genuine thyroid follicles in vitro from mouse ES cells (Antonica et al., 2012). The rapid activation of *Pdx1* by Ptf1a induction and generation of a feed-forward loop is supported by evidence for *Ptf1a* and *Pdx1* inter- and auto-regulation (Gerrish et al., 2001; Gerrish et al., 2004; Marshak et al., 2000; Masui et al., 2007; Oliver-Krasinski et al., 2009; Wiebe et al., 2007). Possibly, activation of endogenous *Ptf1a* involves its auto-regulatory enhancer (ARE) (Masui et al. 2008), and after activation the production of endogenous Ptf1a should help keep the *Ptf1a* locus active. Potentially, the ARE is accessible to exogenous Ptf1a even at late stages, as cells in the prospective glandular stomach – perhaps epigenetically and functionally related to pancreatic acinar cells – retained competence at E15.5 to initiate focal, acinar-only differentiation (data not shown). The direct downstream target genes of Ptf1a causing respecification of stomach, duodenum, and EHBS, but not other endodermal regions, are unclear. Our working model, however, is that Ptf1a/Pdx1 establish a 'first tier' trigger of the pancreatic GRN, and that in tissues that are competent to fully stabilize their auto- and cross-regulatory interactions, they then dominantly subvert other regional organ programs. This competency state includes the ability to utilize the "second tier" pro-pancreatic genes (Nkx6.1, Mnx1, Prox1, and so forth).

A side-issue relates to the effects of early Ptf1a^{EDD} on the endogenous pancreas. The transient suppression of Nkx6.1 by Ptf1a^{EDD}, an incorrect state with respect to normal pancreatic bud MPC, was reversed by E12.5, likely related to post-doxycycline reduction of exogenous

Ptf1a. After cells exited from this transitional state, endogenous pancreas differentiation proceeded essentially normally. Later stage Ptf1a^{EDD}, however, appeared to promote acinar-cell fates over endocrine and ductal cell fates, we propose via suppressing epithelial Nkx6.1 and Sox9, as reported by Schaffer et al. (2010). Future studies are aimed at exploring if the acute effects of Ptf1a misexpression in the endogenous pancreas change over time.

In resistant progenitor populations, such as the more distant anterior endoderm, Ptf1a^{EDD} seems unable to initiate or sustain the expression from endogenous *Ptf1a* and *Pdx1*, perhaps with some threshold dependency. We are now also setting up for genetically testing the possibility that the Ptf1a-Pdx1 inter-regulation, and the recruitment of second- and third-tier pro-pancreatic instructors, is countermanded by competing gene regulatory programs such as those run by Sox2. After an initial phase of suppressed Sox2 levels throughout Ptf1a^{EDD}-endoderm, normal Sox2 levels were then reasserted in the non-pancreas-convertible anterior endoderm, such as the presumptive forestomach, esophagus, and lung. It is also plausible that there is an early-established more repressive epigenetic packaging effect on the *Pdx1*, *Ptf1a*, and other member genes of the pro-pancreatic GRN in the non-convertible regions, as compared to conversion-susceptible regions. During embryogenesis, *Sox2* expression starts in the rostral foregut and spreads posteriorly towards the caudal stomach (Sherwood et al., 2009). Following the normal embryogenesis strategy of the mammalian embryo, wherein rostral/anterior regions are older, the more-anterior endoderm could receive a more-extended and stronger conditioning by Sox2 (for example, more anti-pancreatic chromatin remodeling), making cells resistant to Ptf1a^{EDD}-initiated pancreatic respecification. We expect that the endoderm-specific elimination of Sox2 expression would allow testing for destabilization in the assembly of competing programs, indirectly rendering these regions sensitive to Ptf1a-mediated pancreatic respecification. Shh

signaling is active in anterior endoderm, and has been connected to the resistance to pancreatic respecification (Kim and Melton, 1998; Hebrok et al., 1998). Possibly, the reason for the pancreas-proximate liver escaping full Ptf1a^{EDD}-induced conversion to pancreas could be somewhat different. Being required for embryonic viability, mechanisms could have arisen to ensure its early and robust commitment to a defined program.

Spatial Precision of Normal Pancreatic Specification

In endodermal development, therefore, it is clearly critical to restrain tightly the distribution of Ptf1a, to confine the area of pancreatic specification, and the delimiting mechanisms must presumably be very precise in the posterior ventral foregut where several tissues (EHBS, ventral pancreas, gall bladder) emerge from a relatively compact progenitor group (Spence et al., 2009). It remains to be seen if such 'pinpoint precision' is accomplished by overlapping activity gradients of a few secreted factors, or if they work together with tightly regulated inductive tissue juxtapositions.

The mesoderm-endoderm interaction is important for pancreatic growth and survival (for review, Pan and Wright, 2011), but little is known about how the pancreatic mesoderm, specifically, might be patterned or specified. After Ptf1a^{EDD}, the prospective mesodermal components of what would have normally been stomach, duodenum, and EHBS adopted a phenotype indistinguishable from that of normal pancreatic mesoderm. Therefore, respecified endodermal MPCs were able to communicate locally with the adjacent mesoderm, and control the mesodermal differentiation pathway. With the more-limited ability of later Ptf1a^{EDD} to produce only an acinar conversion (and which became progressively more focal as embryogenesis progressed), the mesoderm became resistant to transformation. These findings indicate that during an early developmental period, the mesoderm is sensitive to the local

specification state of the endoderm. This period of development may be associated with substantial communication back and forth between endoderm-mesoderm, in which congenital defects (such as biliary, duodenal, or gastric atresia) could arise from altered specification states of the endoderm or mesoderm. The factors produced by respecified endoderm that then switch the regional character of the mesoderm would be worthy to explore, and could involve retinoic acid, Wnt, FGF, Shh, and other pathways (Pan and Wright, 2011). Aiding in such studies would be the identification of spatiotemporally resolved genes that imbue distinct regionalized character to the mesoderm of the primordial gut tube.

Using *Ptf1a/Pdx1* co-expression to mark the achievement of a 'pancreatic commitment' state has been partially applied in hESC directed-differentiation paradigms (Kroon et al., 2008): tissue with a *Ptf1a/Pdx1* co-expression state in vitro, after transplantation into mice, underwent maturation into apparently fully differentiated pancreas tissue. Our results suggest possible substantial improvements in the derivation and authenticity of material for human therapies based not on single-fate cells (e.g., pure beta cells), but on deriving tissues or organoids *in vitro* from embryonic or induced pluripotent stem cells. The limited, transient expression of exogenous Ptf1a in appropriately staged tissue could prompt self-regulating assembly of a pancreas-generating program, conceivably including the co-specification of supportive tissues such as the pancreatic mesenchyme. Induction of Ptf1a could divert more cells down the pancreas track, but its timing would be crucial. Initiating Ptf1a expression after cells have moved past MPC competency, or enforcing expression too long, would lead to acinar specification at the expense of endocrine islet lineages (our results; Jarikji et al., 2007; Schaffer et al., 2010).

CHAPTER IV

THE ROLE OF PTF1A IN TIP CELLS OF THE DEVELOPING PANCREATIC EPITHELIUM

Introduction

The post-specification pancreatic buds undergo a dramatic re-organization from what appears as a largely homogenous population of pseudo-stratified epithelial progenitor cells into a dense epithelial plexus. Coinciding with the beginning of this epithelial remodeling, which leads to the establishment of the pancreatic epithelial tree, is the formation of two progenitor populations, tip and trunk, within the pancreatic epithelium.

Tip MPCs (multipotent progenitor cells) are a highly proliferative population of cells that grow into the surrounding pancreatic mesenchyme and leave behind progeny that give rise to other tips or trunk cells. Tip cells were first characterized by their production of the primary MPC markers Ptf1a and Pdx1 in addition to c-Myc and Cpa1 (Zhou et al., 2007). The pancreatic mesenchyme is thought to promote tip cell identity by providing key signaling molecules and extracellular matrix components (for integrin signaling, etc). When formation of the epithelial plexus is disrupted by removing the function of the Rho-GTPase Cdc42, the mesenchyme and ECM environment normally enriched around the tip domain become more evenly distributed throughout the pancreatic epithelium. Increased acinar-cell gene expression is seen at the expense of endocrine-cell gene expression in these mutants (Kesavan et al., 2009).

Tip cells were identified as a multipotent progenitor population through the use of genetic lineage tracing with CreER. Cells expressing *Ptf1a* or *Cpa1* (which is a direct target gene of Ptf1a) are able to give rise to all pancreatic lineages as late as E14.5. The MPC numbers are,

however, rapidly declining by this time as estimated by the decreased proportional labeling of the endocrine and duct cells compared to the acinar cells that maintain *Ptf1a* and *Cpa1* expression. By E15.5, the cells located in the tip domains largely exist as a unipotent, acinar-restricted progenitor (because they are mitotic) and precursor population (Pan et al., 2013; Zhou et al., 2007). The change in progenitor behavior of tip cells from multipotent to unipotent corresponds with the timing of molecular changes in the PTF1 complex. In primary MPCs and early tip MPCs, the trimeric PTF1 complex contains RBPJκ (PTF1-κ), the downstream mediator of Notch signaling. As tip cells transition to an acinar-lineage restricted progenitor population, the PTF1 complex replaces RBPJκ with RBPJL (PTF1-J), a Notch-independent paralog of *RBPJκ*. *RBPJL* is a direct target gene of the PTF1-κ complex in tip cells, and as the levels of RBPJL increase, it replaces RBPJκ in the PTF1 complex (Beres et al., 2006; Masui et al., 2008).

While the change in molecular character of the PTF1 complex coincides with the change in progenitor behavior of tip cells, recruitment of RBPJL into the PTF1 complex is, perhaps surprisingly, not functionally required for tip cells to change from multipotent to unipotent, pro-acinar behavior. Genetic deletion of *RBPJL* causes no change in tip-cell behavior and only leads to minor changes in the terminal differentiation of acinar cells (Masui et al., 2010). Biochemical interrogation of *RBPJL* mutants suggests that RBPJκ can functionally replace RBPJL in the PTF1 complex and largely maintain the differentiation program of committed acinar cells. The minor changes in acinar cell differentiation seen in the RBPJL-deletion tissue compared to wild-type tissue are thought to arise from subtle differences in DNA-binding potential between the PTF1-J and PTF1-κ complexes. While most developmental and early acinar-specific target genes appear to have binding sites compatible with both PTF1-κ and PTF1-J binding, some later-stage acinar-specific targets appear to require explicitly the PTF1-J complex for full-scale activation.

It is possible that acinar cells programmed by PTF1-κ complexes are more functionally inferior than we know from current analyses.

Gain-of-function experiments using Ptf1a and Nkx6.1 have helped establish genetic relationships between the tip and trunk cell gene regulatory programs during the formation of these domains at E9.5/E10.5. Constitutive misexpression of Ptf1a in all pancreatic progenitors from the onset of pancreatic development leads to the expansion of tip cell markers, such as Cpa1, across the pancreatic epithelium and suppression of trunk cell markers such as Nkx6.1 and Sox9. In contrast, constitutive production of Nkx6.1 in all pancreatic progenitors causes the expansion of trunk-cell markers and suppression of Ptf1a. These experiments implicate Ptf1a as a high level member of the transcriptional network that establishes tip cell identity – first MPC, then acinar – during early development (Schaffer et al., 2010).

Current models place the PTF1 complex as a major regulatory molecule controlling tip-cell behavior throughout pancreatic development. Neither the *RBPJk* nor *RBPJL* knockout illuminated the role of the PTF1 complex in tip cells. To continue to explore the function of PTF1 in tip cells, I have focused on Ptf1a. The role of *Ptf1a* in the maintenance and function of tip cells has not been examined because *Ptf1a* null (described in the introduction to this thesis) and hypomorphic mutants have severe defects in pancreatic specification and morphogenesis. Mice with hypomorphic *Ptf1a* levels have hypoplastic pancreatic buds, with a substantial amount of pancreatic progenitors not specified to the pancreatic lineage similar to *Ptf1a* null embryos, and therefore significant alterations in overall pancreatic morphogenesis. Consequently, acinar differentiation is delayed and the hypomorphic mice are glucose intolerant due to decreased endocrine-cell specification (Fukuda et al., 2008).

In order to study the role of *Ptf1a* in tip cells, I developed a novel genetic tool: a *Ptf1a* conditional null allele (*Ptf1a* floxed allele or $Ptf1a^{Flox}$). Combining $Ptf1a^{Flox}$ with a tamoxifen-inducible Cre allele, such as $Ptf1a^{CreER}$ or $Cpa1^{CreER}$, allows conditional removal of *Ptf1a* function from tip cells at various stages of pancreatic development. In combination with a *ROSA26* lineage-tracing allele, the progeny of tip cells could then be observed for changes in progenitor behavior and cell fate upon the loss of *Ptf1a* function. The results section in this chapter will detail the generation of the *Ptf1a* floxed allele and experiments to conditionally remove Ptf1a function from tip progenitor cells.

In addition to the experiments mentioned in this thesis, $Ptf1a^{Flox}$ is useful to study *Ptf1a* function during development, homeostasis, and disease in many other organs. In the pancreas, collaborations have been set up to study the role of Ptf1a in adult acinar cells with Dr. Ray MacDonald at the University of Texas, Southwestern (Dallas). *Ptf1a* expression is maintained in adult acinar cells and may play an important role in adult acinar-cell function. Adult acinar cells are an interesting cell type to study because they can be reprogrammed into pancreatic β-cells using three transcription factors (Pdx1, Ngn3 and MafA) (Zhou et al., 2008). We are collaborating with Dr. Mark Magnuson at Vanderbilt University to test if destabilizing the acinar-cell state using $Ptf1a^{Flox}$ is able to increase the efficiency of transcription factor-enforced acinar-cell reprogramming. In human pancreatic cancer, pancreatic acinar cells are now becoming established as the primary cell-of-origin for this disease. We are collaborating with Dr. Charles Murtaugh at the University of Utah to test if destabilizing the acinar-cell state by removing *Ptf1a* function, in the background of other oncogenic mutations, increases cancer susceptibility and/or progression. Outside of the pancreas, the role of *Ptf1a* is being investigated in dorsal spinal cord interneurons with Dr. Julia Kaltschmidt at Memorial Sloan-Kettering

Cancer Center. *Ptf1a*^{Flox} will also be useful to study the role of *Ptf1a* in the retina, cerebellum, and other areas of the central nervous system, where Ptf1a is expressed in diverse groups of GABAergic interneurons.

Ptf1a^{Flox} will also be useful for the generation of *Ptf1a* heterozygous and homozygous null mutants in any tissue, using an appropriate Cre driver to convert the *Ptf1a*^{Flox} allele to a null. The only previously available *Ptf1a* null allele was *Ptf1a*^{Cre}, which had limited uses in many genetic experiments because it also produces Cre. *Ptf1a*^{Flox} crossed to a germ-line Cre driver, such as EIIA^{Cre}, would generate a "global" *Ptf1a* null allele, *Ptf1a*^{Null}, avoiding this caveat.

Results

Generation of *Ptf1a*^{Flox}

The overall strategy for generating the *Ptf1a* floxed allele was to create a targeting vector for homologous recombination in mouse embryonic stem (ES) cells by using BAC (Bacterial Artificial Chromosome) recombineering. BACs are large pieces of mouse genomic DNA (usually 90-200 kb) cloned into a plasmid backbone, based on a bacterial fertility or F-plasmid, that propagate at low copy number (1 or 2 copies) in bacterial cells. Fertility plasmids have partition genes that promote dispersal of the BAC into both bacterial cells upon cell division. BAC recombineering is useful for making modifications (insertions, deletions, point mutations, or combinations thereof) in large pieces of genomic DNA while leaving limited, if any, unwanted changes in the modified DNA. The modified pieces of genomic DNA can then be retrieved, using a so-called retrieval vector, to generate a much smaller plasmid called the targeting vector, which is able to be grown at much higher copy number to increase yield for use in transgenesis or homologous recombination in ES cells.

The bacterial strain that were used in to modify the *Ptf1a* BAC contained a heat-shock-inducible gene cassette that leads to the expression of the RED recombination system from the λ bacteriophage (Lee et al., 2001). Note that other BAC recombineering systems are available, but will not be described here. RED proteins facilitate the efficient recombination in bacteria between short stretches of identical DNA sequences carried on separate DNA molecules. In addition to the RED system, an *E. coli* strain (SW106 - derived from the DH10B *E. coli* strain; Warming et al., 2006) that contains all the components of the *gal* operon except the *galK* (galactokinase) was used. Bacterial strains lacking *galK* can be used for positive-negative selection using galactokinase substrates – provided when the *galK* cassette is brought in on the exogenous BAC that will be engineered, for example.

In order to generate the *Ptf1a* floxed allele, a BAC was ordered from BAC PAC Resources at C.H.O.R.I (https://bacpac.chori.org/). Because the Vanderbilt Transgenic Mouse/Embryonic Stem Cell Shared Resource (TMESCSR) uses a 129/Sv-derived ES cell line for homologous recombination, care was taken to order a BAC clone from a 129/Sv BAC library. The RP22-251-E16 clone was selected because it contained a large genomic region centered on the *Ptf1a* locus. Extensive restriction-digest fingerprinting and DNA sequencing verified that the genomic region contained in the BAC clone included the *Ptf1a* locus and the necessary 5´ and 3´ regions required to generate the derived *Ptf1a* floxed targeting vector.

Insertion of the 5' LoxP Site

Briefly, the general strategy to insert the 5´ loxP site was to place a *galK* cassette in the desired location for the loxP site using positive selection and then to replace this *galK* cassette with the loxP site using negative selection. A non-conserved region, identified by examining the

sequence conservation between rat and mouse, 1.7 kb 5′ of the *Ptf1a* transcriptional start site (TSS) was selected as the insertion site for the 5′ loxP site (Fig. 4.1). Two 500 bp homology regions (so-called 5′ and 3′ HRs) surrounding the location selected for 5′ loxP site were subcloned into a plasmid (pGALK) containing an *em7*-promoter-driven *galK* gene cassette. Restriction digests were performed to excise a DNA fragment from the modified pGALK plasmid containing the 5′ and 3′ HRs and the *galK* cassette, which was gel-purified and ethanol-precipitated before further preparation for electroporation. The 5′HR–*galK*–3′HR DNA fragment was electroporated into *SW106* bacteria containing the RP22 Ptf1a BAC clone and heat shocked (20 minutes) to induce the RED proteins. Bacteria recovered from the heat shock were grown on minimal medium plates lacking all carbon sources except galactose, and therefore bacteria require galactokinase to phosphorylate galactose for carbon utilization. Bacteria containing a BAC clone that properly underwent insertion of *galK* cassette in the BAC by homologous recombination will become competent to grow on galactose-only minimal medium. Clones that grew on the galactose-only agar were screened by PCR and diagnostic restriction digests for the correct insertion of the *galK* cassette. DNA sequencing of PCR products generated from the modified 5′ LoxP region of the BAC identified correctly modified clones.

To start negative selection, the pGALK plasmid that contained the 5' HR, *galK* cassette, and 3′ HR was modified to replace the *galK* cassette with a single loxP site that was flanked with restriction sites. The 5′HR-loxP-3′HR DNA fragment was excised from the pGALK plasmid and electroporated into *SW106* bacteria containing the RP22 *galK* Ptf1a BAC clone. The bacteria

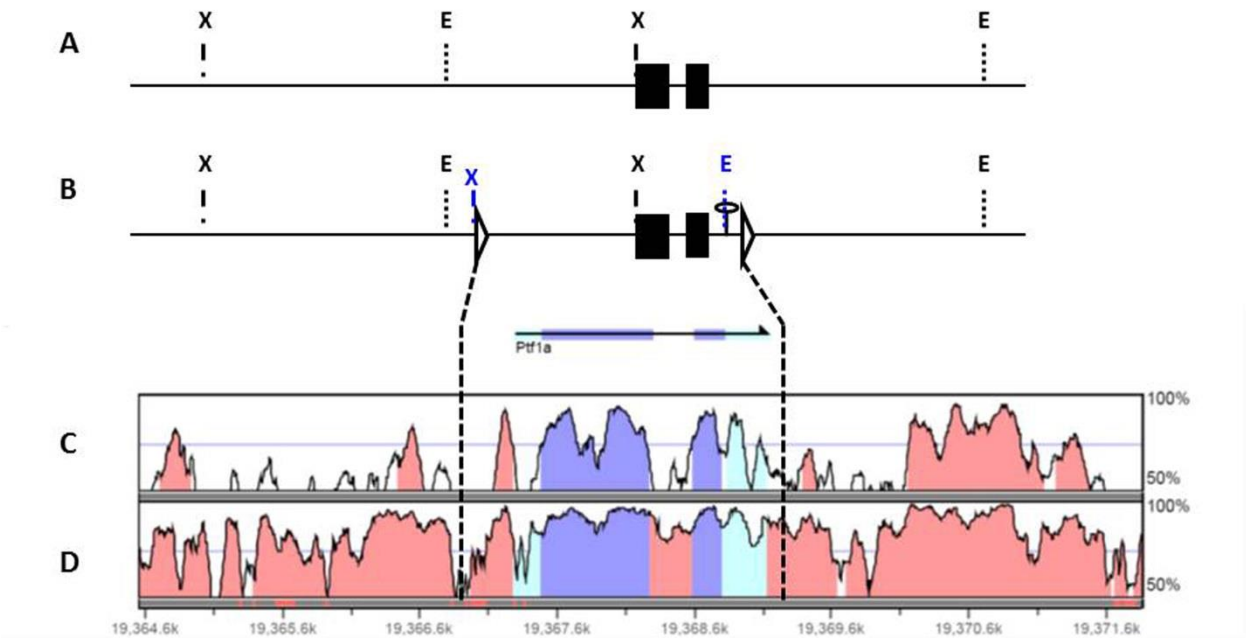

Fig. 4.1 Location of the loxP sites in the *Ptf1a*^{Flox} locus. (A) The endogenous *Ptf1a* locus. Black boxes signify exons. Relevant restriction sites are indicated by dashed lines: X, *Xba*I; E, *Eco*RI. (B) Hypothetical configuration of *Ptf1a*^{Flox}. Restriction sites added by BAC recombineering are indicated in blue. loxP sites are represented by triangles, FRT sites by line with a circle on top. (C, D) Vista genome browser sequence conservation plot. X-axis, kilo-bases 5′ to 3′ (left to right); Y-axis, percent conservation. A higher ~~the~~ peak on the plot equals higher inter-species sequence conservation. Non-coding regions, red; untranslated regions, light blue; coding regions, darker blue. (C) Relative DNA-sequence conservation in the *Ptf1a* locus between mouse and human, and (D) mouse and rat. Dashed lines indicate the approximate location of 5′ and 3′ loxP sites in the *Ptf1a*^{Flox} locus. A non-conserved region 5′ of the *Ptf1*a coding region was selected for the location of the 5′ loxP site (note the absence of conservation peaks). DNA sequences 3′ of the *Ptf1a* coding region were highly conserved between mouse and rat. A region poorly conserved between mouse and human was chosen for the location of the 3′ loxP site.

were heat shocked to induce the RED proteins, recovered, and grown on agar plates containing 2-deoxy-galactose (2-DOG). Bacterial cells containing galactokinase grown in the presence of 2-DOG causes the production of 2-deoxy-galactose-1-phosphate, a toxic intermediate, and leads to cell death. Bacterial cells can only grow on 2-DOG agar if they modify or remove the *galK* cassette inserted into the Ptf1a BAC clone. Clones that grew on the 2-DOG minimal agar were screened by PCR and diagnostic restriction digest analysis for the correct insertion of the loxP site and the loss of the *galK* cassette in the BAC. Correctly modified clones were finally screened by DNA sequencing of PCR products produced from the modified BAC. The correctly targeted 5´ loxP Ptf1a BAC clone contained only the loxP sites and 4 restriction sites used in cloning or for Southern-blotting analysis after homologous recombination in mouse ES cells.

Insertion of the 3´ LoxP Site

Similar to the 5´ loxP site location, a non-conserved location 1 kb 3´ of the *Ptf1a* TSS was used as the insertion location for FRT-flanked neo^R cassette and 3´ loxP site (Fig. 4.1). Two 500 bp HRs surrounding the genomic region selected for insertion of the 3´ loxP site were subcloned into a plasmid (PL451) containing a FRT-flanked PGK-em7- promoter-driven neo^R cassette and loxP site. The loxP site is located 3´ to both FRT sites so that after homologous recombination and derivation of the *Ptf1a* floxed mouse line, the FRT-flanked neo^R cassette can be removed by crossing to FlpE-expressing mouse strains. Recombination between the FRT sites by FlpE resulted in removal of one FRT site and the neo^R gene cassette and left one FRT site and the 3´ loxP site of the *Ptf1a* floxed allele.

The 5´HR-FRT-flanked neo^R cassette-3´loxP-3´HR DNA fragment was electroporated into *SW106* bacteria containing the 5´ loxP RP22 BAC clone and the bacteria were heat shocked

to induce the RED system, recovered, and plated on agar with kanamycin (the *neo*^{R} cassette provides bacterial resistance to kanamycin). The correctly targeted 5′ loxP, FRT-flanked *neo*^{R} cassette, 3′ loxP site Ptf1a BAC clones were identified by PCR, diagnostic restriction digest analysis, and DNA sequencing of PCR products.

Retrieval of the Targeting Vector

Targeting vectors contain modified genomic DNA with a positive selection marker (in this case, *neo*^{R}) with a vector backbone containing a negative-selection marker (diphtheria toxin A) and are used for homologous recombination in eukaryotic cells. In addition to the modified genomic DNA, targeting vectors contain large pieces of genomic DNA (called homology arms), located 5′ and 3′ of the modified DNA, which initiate homologous recombination. Prior to the generation of the targeting vector, it is important to generate synthetically the proposed targeting vector using DNA-sequence analysis software to identify a restriction site that will be usable in the future linearization step to prepare the targeting vector for electroporation into ES cells – linearization being necessary for efficient homologous recombination. The restriction enzyme must linearize the targeting vector by cutting in the pBS (Bluescript™; Stratagene) vector backbone outside of the diphtheria toxin A gene cassette or the regions retrieved from the modified *Ptf1a* BAC.

The *Ptf1a*^{Flox} targeting vector was retrieved from the modified 5′ loxP, FRT-flanked *neo*^{R} cassette, 3′ loxP site *Ptf1a* BAC clone by using dual-drug selection and homologous recombination to re-circularize a linearized plasmid backbone. The plasmid backbone used to retrieve the targeting vector contains 500 bp 5′ and 3′ HRs, an ampicillin-resistance gene cassette, and a diphtheria toxin A gene cassette (pBS.DTA). All DNA sequences intervening

between the 5´ HR and 3´ HRs were retrieved from the modified BAC clone to re-circularize the plasmid. The 5´ HR was located 12.3 kb 5´ of the *Ptf1a* TSS, while the 3' HR was located 6.3 kb 3' of the *Ptf1a* TSS. The spacing of the 5' and 3' HR regions in the retrieval vectors permits the generation of large homology arms for the Ptf1a targeting vector to try to increase the efficiency of homologous recombination in ES cells. When subcloning the 5´ and 3´ HR into the pBS.DTA vector, special consideration was taken to ensure there is a restriction enzyme located between the 5' and 3' HR that would be able to linearize (single cut) the pBS.DTA 5´ and 3´ HR plasmid. It is important that the restriction enzyme cuts between the HRs and not in the plasmid backbone, because the plasmid backbone needs to re-circularize and propagate the targeted DNA that has been retrieved from the modified BAC clone.

The linearized pBS.DTA 5´ and 3´ HR plasmid was electroporated into *SW106* bacteria containing the modified 5´ loxP, FRT-flanked neo^R cassette, 3´ loxP site *Ptf1a* BAC clone. The electroporated bacteria were heat shocked to induce RED recombination and plated on agar containing kanamycin and ampicillin. Only bacteria that contain the re-circularized pBS.DTA plasmid with the modified DNA containing the neo^R gene cassette retrieved from the BAC grow on the dual-drug agar. The targeting vector was thoroughly screened by PCR, diagnostic restriction digest analysis, and DNA sequencing to ensure no errors were contained in the DNA sequence of the finalized targeting vector.

Homologous Recombination and Southern Blot Screening of Targeted ES Cell Clones

Linearized targeting vector was supplied to the Vanderbilt TMESCSR for ES-cell electroporation. ES clones that underwent homologous recombination were selected using positive-negative selection. The neo^R gene cassette contains a eukaryotic promoter (PGK) and provides resistance to the drug G418, which inhibits peptide synthesis. The DTA gene cassette in

the pBS.DTA backbone kills any cell that incorporates DTA in the genome, and therefore should kill any randomly integrated, non-homologously recombined transgenic integrants.

ES cell clones that grew in G418 medium were picked and grown in small quantities for large-scale Southern-blot screening (see Fig 4.2 for an overview of the Southern blot strategy). During the design of the *Ptf1a*^{Flox} targeting vector, restriction enzyme sites had been preplanned in the 5´ and 3´ homology arms to allow for accurate Southern-blot analysis of the final targeted *Ptf1a*^{Flox} locus. An *Eco*RI restriction site was added adjacent to the 3´ loxP site. Incorporation of this exogenous *Eco*RI site into the *Ptf1a* locus by homologous recombination changes the size of a restriction digest fragment that can be identified by the 3´ Southern blot probe from 10.1 kb to 8.2 kb (Fig. 4.2 D). An *Xba*I restriction digest site was added 5´ side of the 5´ loxP site. Incorporation of this exogenous *Xba*I site into this location changes the size of a restriction digest fragment identified by the 5´ Southern-blot probe from 13.6 kb to 11.6 kb. After initially screening 600 potential targeted clones by *Eco*RI digestion of genomic DNA and the 3´ Southern-blot probe, seven clones (14 clones were identified in total from the initial screen) were expanded for additional screening. All seven clones were screened by *Eco*RI digestion with the 3´ Southern-blot probe and *Xba*I digestion with the 5´ Southern-blot probe. Importantly, both probes were located in regions external to the targeting vector. All seven clones were identified as properly targeted by the 5´ and 3´ Southern-blot probes, and two independent clones were selected for blastocyst injection. Several high-percentage (>60%) male chimeras were produced

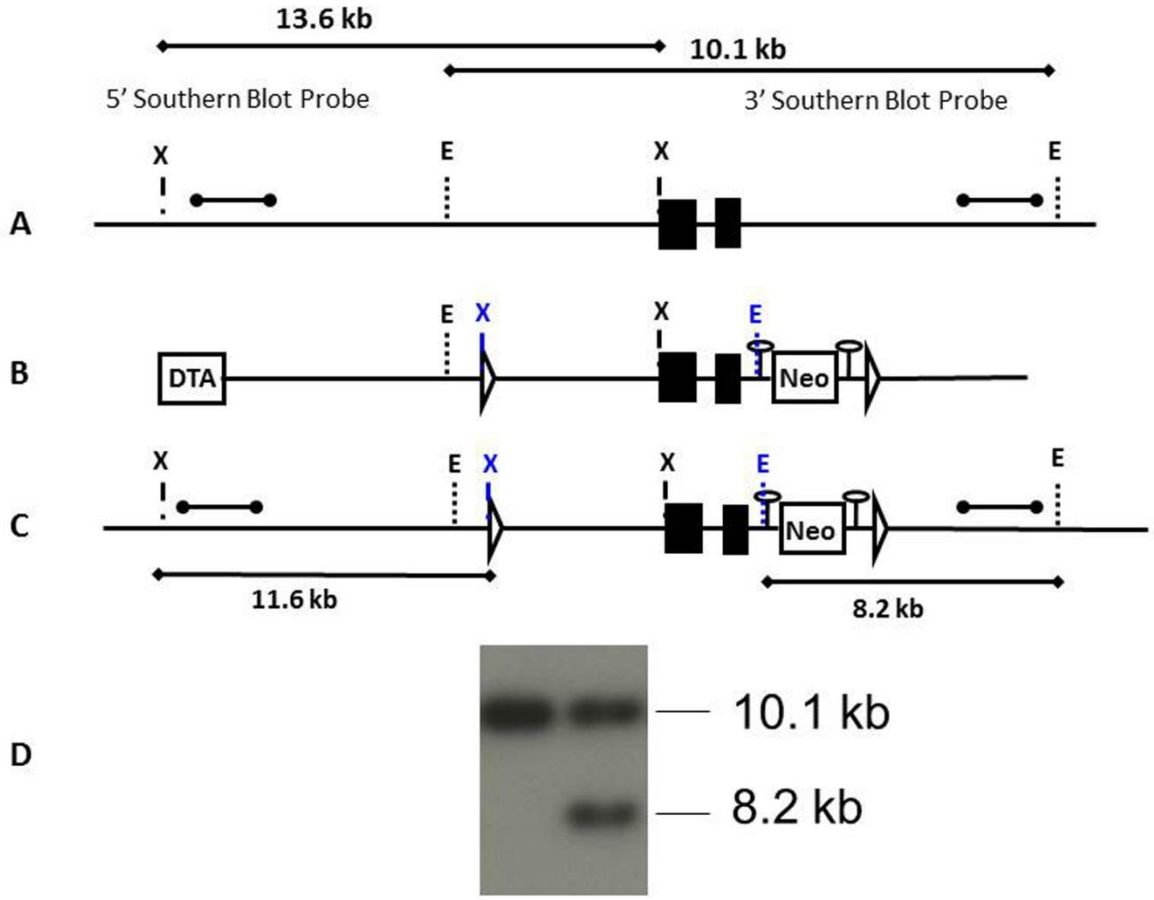

Fig. 4.2. Southern Blot Strategy for *Ptf1a*^{Flox}. (A) Schematic of the endogenous *Ptf1a* locus with the approximate location of the 5´ and 3´ Southern-blot probes (SBP). Digestion of genomic DNA with *Xba*I (X) and performing a Southern blot with the 5´ SBP reveals a 13.6 kb DNA fragment. Digestion of genomic DNA with *Eco*RI (E) and Southern blot analysis with the 3´ SBP reveals a 10.1 kb DNA fragment. (B) Schematic of the *Ptf1a*^{Flox} targeting vector. loxP sites are indicated by triangles, FRT sites are indicated by lines with a circle on top. DTA, diphtheria toxin A; Neo, neomycin resistance cassette. (C) Schematic of the *Ptf1a*^{FloxNEO} targeted locus. Addition of new *Xba*I and *Eco*RI restriction sites via BAC recombineering changes the size of the DNA fragments in the *Ptf1a* locus revealed by the 5´ and 3´ SBPs. (D) Example Southern blot with the 3´ SBP and *Eco*RI digestion. Targeted ES cells (lane 2) produced the predicted DNA fragment size of 8.1 kb suggesting that the exogenous *Eco*RI site was incorporated into the *Ptf1a* locus.

from the blastocyst injections of the ES clones. The high-percentage male chimeras were mated to Black Swiss (an outbred strain) mice. All progeny derived from the chimeras had the coat color (agouti) of the

injected, modified 129/Sv ES cells instead of the host blastocyst C57BL/6 (black) cells, indicating an unusually high, and near-100% incorporation of the targeted ES cells in the germline of the chimeras (the 129/Sv cells carry a dominant *Agouti* allele). F1 progeny from the chimera x Black Swiss cross were genotyped for the presence of the *Ptf1a* floxed allele (*Ptf1a*^{floxNEO}, not having yet had the *neo*^{R} cassette removed). *Ptf1a*^{floxNEO} F1 progeny were mated to *FlpE* mice to remove the FRT-flanked *neo*^{R} cassette. *Ptf1a*^{floxNEO}, *FlpE*-positive progeny were identified by genotyping and mated back to Black Swiss mice. In mice containing the FlpE allele, FLP-recombinase expression is driven mosaically throughout development and in adult tissues, indicating variegated expression from the β-actin promoter (Lakso et al., 1996). Because of mosaic expression, not all progeny from *Ptf1a*^{FloxNEO}, FlpE-positive mice will inherit *Ptfla*^{FloxNEO} without the FRT-flanked *neo*^{R} cassette (*Ptf1a*^{flox}). Progeny from the *Ptf1a*^{FloxNEO}, FlpE-positive mice were systematically screened using PCR analysis to identify progeny containing *Ptf1a*^{Flox}, and to validate the loss of the *neo*^{R} cassette and breed away the *FlpE* allele (Fig. 4.3). *Ptf1a*^{Flox} mice used in subsequent experiments were maintained on a mixed background of C57BL/6 and 129/Sv.

Ptf1a^{CreER} deletion of Ptf1a^{Flox}

The *Ptf1a*^{CreER} allele of Pan et al. (2013) is a knock-in allele. In the absence of tamoxifen, *Ptf1a*$^{CreER/Flox}$ mice are normal heterozygous animals. After the addition of tamoxifen, cells that express *Ptf1a* would recombine the *Ptf1a* floxed allele and in effect become *Ptf1a*-null cells (Fig.

4.3). In order to follow cells that activate CreER in the presence of tamoxifen, a genetic lineage-tracing allele such as *ROSA26*^{YFP} is generally bred into the *Ptf1a*$^{CreER/Flox}$ mice.

In order to validate that *Ptf1a* was conditionally deleted from tip progenitor cells, it must be verified that Ptf1a protein production can be removed from the lineage-traced cell population. Genetic crosses were set up to generate *Ptf1a*^{CreER}/^{Flox}; *ROSA26*^{YFP}/+ embryos. A single 3.0 mg dose of tamoxifen was given by intraperitoneal injection to pregnant dams at E12.5 of gestation and embryos were collected at E15.5.

In this cross, *Ptf1a* is deleted from *Ptf1a*-expressing tip cells. Loss of Ptf1a can be shown by immunofluorescence analysis compared to the lineage-tracing indicator, YFP. In control embryos (*Ptf1a*^{CreER}/+; *ROSA26*^{YFP}/+), the majority of lineage-traced cells should remain in the tip and produce Ptf1a protein. It is important to keep in mind that some tip cells lose expression of *Ptf1a* because they become non-Ptf1a-expressing progenitor-like trunk cells.
In conditional-mutant embryos injected with tamoxifen at E12.5 (*Ptf1a*$^{CreER/Flox}$; *ROSA26*^{YFP}/+), it is expected that there will be an increased population of YFP-positive, Ptf1a-negative cells in tissue analyzed at E15.5.

Ptf1a^{CreER}/+; *ROSA26*^{YFP}/+ and *Ptf1a*^{CreER}/^{Flox}; *ROSA26*^{YFP}/+ embryos at E15.5 were cryosectioned and immunostained for Ptf1a and YFP. Unexpectedly, a large number of Ptf1a-expressing cells residing in the tip domain were lineage-traced (YFP-positive) in *Ptf1a*^{CreER}/^{Flox}; *ROSA26*^{YFP}/+ embryos. These data indicate that, under my conditions for tamoxifen administration, the *Ptf1a*^{CreER} allele was largely inefficient at recombining both *ROSA26*^{YFP} and

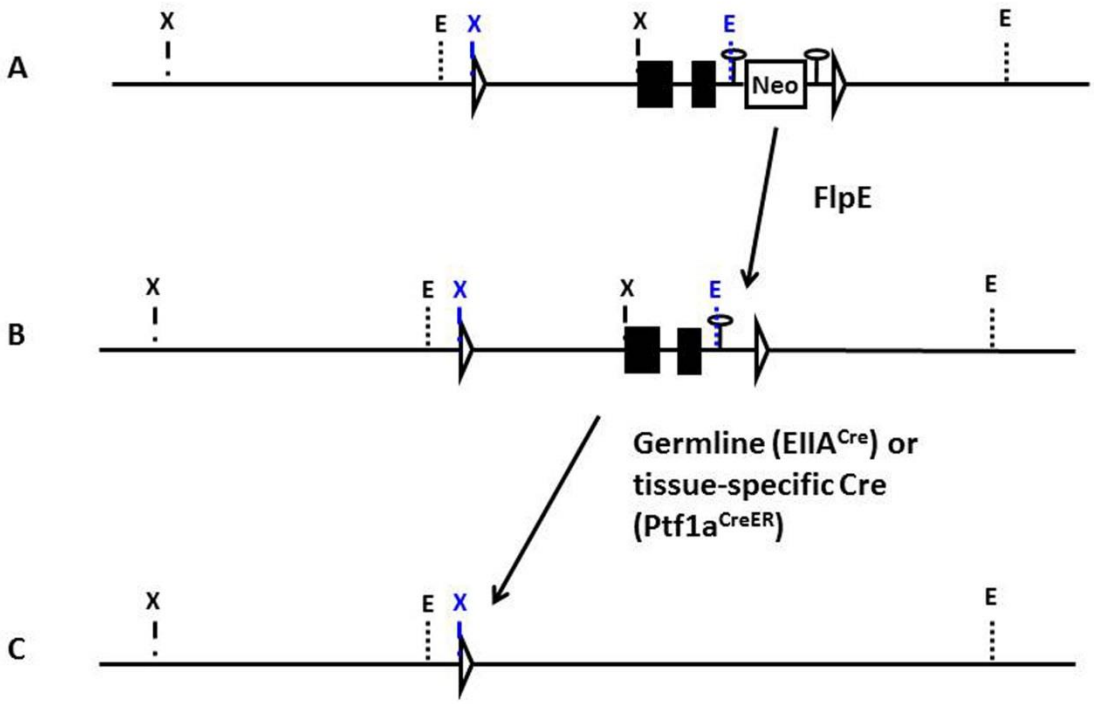

Fig 4.3. Modification of the *Ptf1a*^{flox} locus. (A) Schematic of the *Ptf1a*^{FloxNEO} locus. Mating the *Ptf1a*^{FloxNEO} allele to a *FlpE*-deleter strain causes recombination between the FRT sites. This leads to the deletion of the *neo*^{R} cassette and generates the *Ptf1a*^{Flox} allele, (B). Mating the *Ptf1a*^{Flox} allele to a germline-deleter strain, such as EIIA^{Cre}, causes recombination between the loxP sites, removes the entire Ptf1a coding region, and generates a novel Ptf1a^{Null} allele. Triangle, loxP; line-circle, FRT; Neo, neomycin resistance cassette; E, *Eco*R1; X, *Xba*1.

Ptf1a^{Flox} in a large number of cells. Because *Ptf1a*^{Flox} is a true, functional conditional-null allele (validated by crossing *Ptf1a*^{Flox} to EIIA^{Cre}), we assume that non-parallel recombination (described below) is leading to appearance of YFP^{+} cells that are still Ptf1a^{+} (Liu et al., 2013).

In separate work that I contributed to (Liu et al., 2013), we showed that low Cre activity (when driven by a weak promoter or undergoing low activation of CreER with tamoxifen) leads to a high incidence of non-parallel recombination – that is, recombination of Ptf1a^{Flox} but not *ROSA26*^{YFP} (*Gt(ROSA)26Sor*$^{tm1(EYFP)Cos}$) or vice versa, in individual *Ptf1a*-expressing cells. We came to this conclusion by using mice that were trans-heterozygous for different lineage-tracing alleles at the *ROSA26* locus. These *ROSA26* alleles (such as *ROSA26*^{YFP}and *ROSA26*^{AI9}) produce different fluorescent proteins after recombination, allowing the direct visualization of the recombination pattern of each allele. In the presence of low Cre activity, many cells activated only one of the *ROSA26* alleles. From this study, we also speculated that other variables that potentially contribute to the non-parallel recombination of independent floxed alleles include the "openness" of the genetic locus (one locus could be in a closed or repressed state while another could be more open to recombination), and/or the distance between the loxP sites. A larger distance between loxP sites appears to cause a substantially lower frequency of recombination. My preliminary data, in combination with the study by Liu et al. (2013) indicate that *Ptf1a*^{CreER}-driven mosaic recombination of the *Ptf1a*^{Flox} is not a robust enough system to study the functional role of *Ptf1a* in tip progenitor cells due to the high degree of non-parallel recombination.

Discussion

It is important to determine functionally the direct role of *Ptf1a* in tip progenitor cells. Because of non-parallel recombination, I was unable to use *Ptf1a*^{CreER} for the efficient conditional removal of *Ptf1a* function in tip cells, and to follow the progeny of those cells during organogenesis. To overcome these technical problems, a more robust genetic system will need to be developed that can efficiently link gene inactivation and lineage tracing. One potential approach would be to engineer a lineage-tracing tool directly into the *Ptf1a*^{Flox} allele. By directly linking the loss of *Ptf1a* function to lineage-tracing initiated from the same locus, one would prevent the need for an independent lineage-tracing allele, and avoid the problem of non-parallel recombination. However, the design of such an allele, towards tracing cells that move into a non-*Ptf1a*-expressing state, would require somehow engineering a change in the behavior of the *Ptf1a* promoter, from cell-type specific to cell-type independent, occurring concomitant with removing *Ptf1a* function. Cell-type independent promoters (like *ROSA26* promoter) are active regardless of the cell state while the *Ptf1a* promoter is only active in Ptf1a-expressing cells. There is currently no way that has been invented to change a promoter from cell-type-specific to cell-type-independent – such as using split promoters that are restored to function after removal of a floxed sequence. Currently there are techniques, such as the generation of COIN (Conditional by Inversion) alleles, which incorporate reporter tools into conditional null alleles. These alleles turn on the reporter upon functional inactivation by Cre-driven inversion, but are far from ideal. They require heavy modification of the endogenous locus, potentially altering important *cis*-regulatory modules, and would rely on the gene's own cell-type specificity, therefore not allowing one to follow progeny if they moved into a cell fate that did not express that gene. Note that some short-term lineage tracing might be possible, which would be highly dependent upon the longevity of the marker (for example a fluorescent protein) that is produced after inversion.

Elsewhere in this thesis (see chapter III), I used a tetracycline-inducible system to activate gene expression at various stages of embryogenesis and organogenesis. This system can also be used for gene inactivation, and it has some benefits over CreER-based systems. Tetracycline-inducible systems allow for efficient gene activation during early development because the toxicity of tetracycline analogs (such as doxycycline) is low compared to tamoxifen. Tamoxifen is an abortifacient and therefore cannot be given at high doses to pregnant dams during early to mid-gestation. A *Ptf1a*^{rtTA} allele has been made available within the community and it could be used with a tetO-Cre allele, *Ptf1a*^{Flox}, and a *ROSA26* lineage-tracing allele to generate a system where high levels of Cre activity would be achieved to drive parallel recombination of both *Ptf1a*^{Flox} and *ROSA26*^{YFP} within more cells. This system introduces more complexity with the additional allele. Another potential system that could be used to drive conditional but mosaic deletion of Ptf1a and allow tracing of cell progeny is an in vitro organ culture system, bringing Cre activity in on a dilute viral vehicle. In order to this method to be viable, long-term in vitro culture systems to study pancreas development must be developed to allow tracking of the behavior of infected progenitor cells during subsequent differentiation stages.

CHAPTER V

ANTIBODIES TO DETECT CRE AND MCHERRY PROTEIN LOCALIZATION

Introduction

Current molecular genetic techniques, especially those using fluorescent proteins and DNA recombinases to trace cells for analysis in situ, or for flow-cytometry-based isolation and analysis, rely heavily on antibodies to select the specific populations of cells. Fluorescent proteins are also frequently used as a surrogate of the direct visualization of transcriptional activity from promoters, or for the very important determination of the sub-cellular localization of fusion proteins as part of determining molecular mechanisms. In these conditions, Cre and mCherry often have to be visualized by indirect methods, such as antibody detection. In many instances, while the endogenous fluorescence of the GFP and dsRed family members are useful readouts, under many circumstances there are fixation conditions that are optimized for detecting other proteins but that reduce or eliminate the endogenous fluorescence. For these and multiple other applications, such as co-immunoprecipitation of fluorescently tagged protein complexes, it was decided that it would be helpful to produce additional antibody reagents that would specifically detect these proteins, particularly because my research was possibly going to use multiple types of fluorescent mouse strains to label different cell populations. Analytical flexibility afforded by these novel antibody reagents would increase the number and type of experimental approaches possible with the genetic tools.

GFP and its derivatives (i.e. YFP, CFP, etc.) are the most commonly used fluorescent proteins within the scientific community. There are a limited number of widely available high-quality antibodies to detect these proteins in fixed tissue samples, and their relatedness allows the

same antibodies to detect many of the color variants. The dsRed family (i.e. mCherry, mApple, tdTomato, etc.) is another group of highly used fluorescent proteins. Molecular evolution of dsRed has produced several variant proteins, including a slow-maturing oligomer and a fast-maturing monomeric fluorescent protein, and the latter has a wide variety of spectral variants useful for imaging. The amino-acid sequence alterations that stabilize the monomeric form of dsRed were achieved by a type of 'modular replacement', changing the N-terminal and C-terminal regions of dsRed with the respective parts of GFP (Shaner et al., 2008). Because of this 'domain sharing', many of the currently available antibodies directed against GFP therefore cross-react with the altered dsRed family members, which limits their usefulness in imaging settings if both classes of fluorescent proteins were to be used. The generation of antibodies solely against antigenic regions that represent non-shared, dsRed-specific sequences would allow specific protein detection in various experimental contexts.

Cre recombinase seems to be the prevalent DNA recombinase in use today in mouse molecular genetics and other genetic manipulations used in cell lines, likely far outweighing the use of the Flp-FRT system. Cre and its ligand-activated derivative, CreER, are used to manipulate the genome of live mice in a spatiotemporally controlled manner. Of several commercially available Cre antibodies that the Wright lab tested, almost all were found to be of poor quality, suggesting that new approaches should be used to generate antibodies against this protein. Only one Cre antibody gave meaningful analytical data, and even then it seemed to work sporadically with seemingly little conclusive information arising over the correct type of fixation conditions or antibody titer to use. In many instances it would be useful to detect Cre in tissues, or detect the period of nuclear-residency of tamoxifen-activated CreER, as it could

provide fundamental insight into the time window during which CreER is active and allow direct visualization of the cell populations that are being targeted in these experiments.

With this rationale in hand, I therefore designed and generated fusion proteins containing predicted solvent-exposed, antigenic regions of the protein mCherry, which is a bright-red monomeric variant of dsRed, or Cre. These regions were fused to the C-terminus of a carrier protein glutathione S-transferase (GST). GST is a useful carrier protein for fusion proteins because of its high affinity for glutathione (Smith and Johnson, 1988), and when produced as a fusion protein with regions that antibodies are trying to be made against, it is thought that it might act to enhance any immunogenic response. In my case, the fused mCherry or Cre domains could be thought of as essentially acting as 'haptenized' immunogenic regions. GST fusion proteins can be bound with high affinity to glutathione that is covalently immobilized on beads, allowing essentially a simple 'one-step' extraction of soluble fusion proteins from lysates that are prepared from the bacterial hosts. Using online algorithms (www.expasy.org), I combined antigenicity-prediction and hydrophilicity/hydrophobicity plots to predict likely regions that would either be hydrophilic, or represented moderately hydrophobic regions flanked by more hydrophilic regions. These criteria were employed to try to maximize the likelihood of both a good solubility of the final GST fusion protein under non-denaturing sonication conditions, and when possible – using additional guidance from the 3-D structures of the proteins – that these regions would form 'external' parts of the protein, rather than being more buried, hydrophobic internal regions that would be much less accessible in future antibody-binding applications.

Results and Discussion

Predicting likely solvent-exposed, 'surface regions' of Cre and mCherry

Many of the currently available antibodies generated against Cre or dsRed family members have used the full-length proteins as the antigens. Often these full-length proteins have poor solubility. Using fragments of the selected protein that are hydrophilic, or likely external regions, can help improve solubility of the antigen during production and immunization. Otherwise one has to resort to relatively harsh denaturation and solubilization conditions, such as chaotropic agents, followed by sequential dialysis to remove these agents. These harsh conditions can have an uncertain effect on the protein and often the protein turns insoluble again during the dialysis steps. To identify likely soluble regions of Cre and mCherry, I used the Hopp-Wood algorithm to plot the hydrophobicity of Cre (Fig. 5.1 A) and mCherry (Fig 5.1 C). The selected hydrophilic regions of Cre and mCherry were attached to the C-terminus of GST. In between GST and the fused antigen was a glycine-rich linker sequence, which should allow GST and the antigen to fold independently and improve presentation of the antigen during immunization (Fig 5.1 E).

The most hydrophilic region of Cre was between amino acids 100-158. Additionally, amino acids 17-100 and 270-343 have a largely hydrophilic profile. Based on this plot I sub-cloned four different peptide fragments of Cre into the plasmid pGEX-KG to generate GST fusion proteins: a.a. 17-100 (C1), 17-158 (C2), 100-158 (C3), and 270-343 (C4) (Fig. 5.1 B). The Hopp-Wood hydrophobicity plot for mCherry suggested hydrophilic regions near its N and C terminus (Fig 5.1 C). I sub-cloned three different peptide fragments of mCherry into pGEX-KG: a.a. 136-190 (FG1), 151-190 (FG2), and 23-57 (FGC) (Fig 5.1 D). As mentioned above, the N-

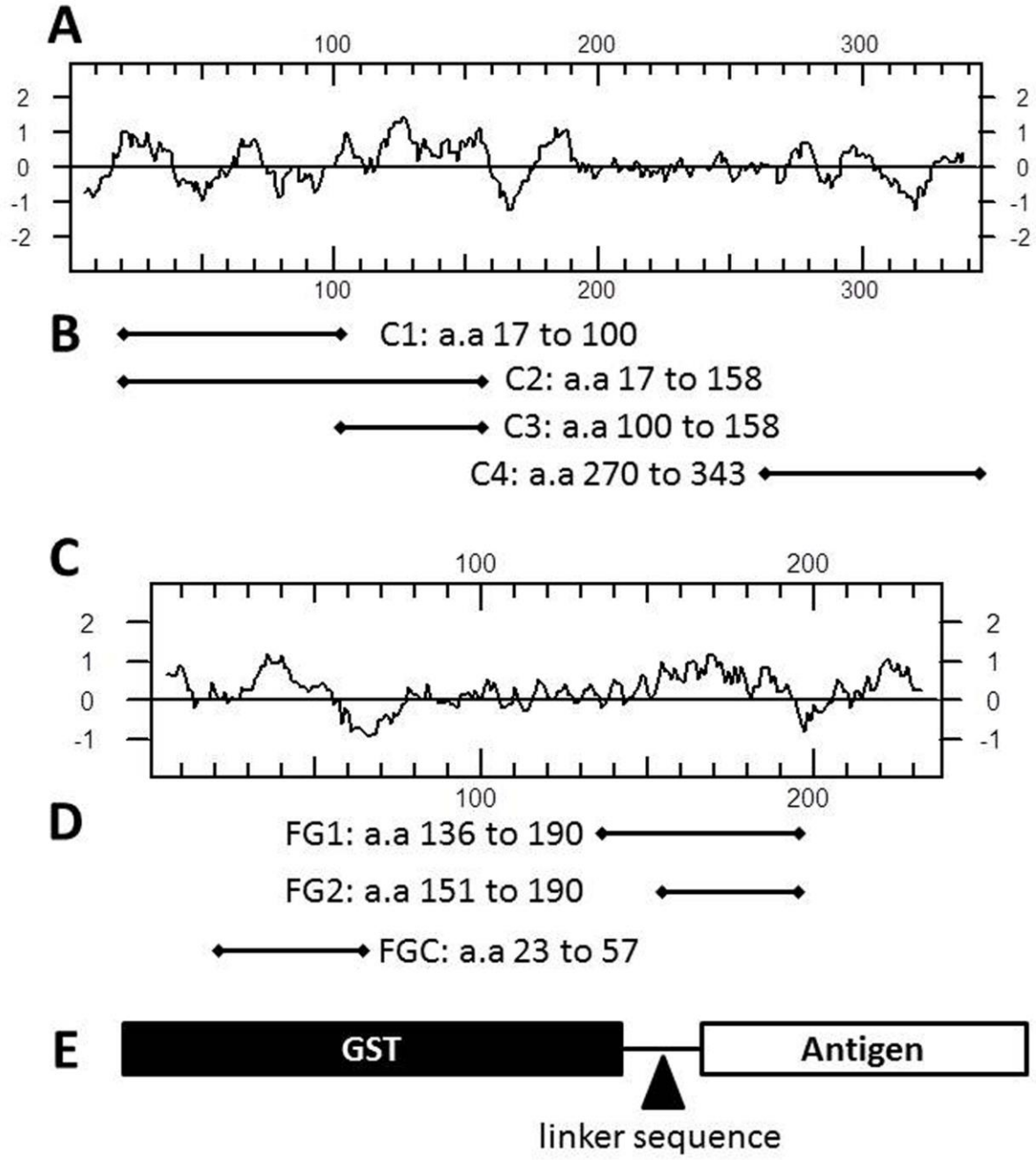
A
100
200
300
2
1
0
-1
-2
B
C1: a.a 17 to 100
C2: a.a 17 to 158
C3: a.a 100 to 158
C4: a.a 270 to 343
C
D
FG1: a.a 136 to 190
FG2: a.a 151 to 190
FGC: a.a 23 to 57
E
GST
Antigen
linker sequence

Figure 5.1 Hydrophobicity Plots of Cre and mCherry and Amino Acid selection for GST Fusion proteins. Plot of (A) Cre and (C) mCherry using the Hopp-Wood algorithm. The *y*-axis is a logarithmic representation of hydrophobicity (positive values, more hydrophilic; negative values, more hydrophobic); the *x*-axis is the amino-acid sequence of the respective proteins. (A) Amino-acid residues 100-158 represented the largest stretch of hydrophobic sequences in Cre, with smaller regions of largely hydrophobic character near the N- and C-termini. (B) The peptide sequence regions of Cre selected for individual GST-Cre fusion proteins. (C) For mCherry, two regions of hydrophilic character were indicated near the N- and C-terminus. (D) Indication of mCherry peptide sequence selected for individual GST fusion proteins. (E) Structure of all GST-fusion proteins. The selected antigen regions of Cre and mCherry were attached to the C-terminus of GST in the plasmid expression vector pGEX-KG, immediately after a short $(Gly)_5$ linker sequence (discussed in methods).

terminal residues 1-12 and C-terminal residues 223-231 of mCherry were omitted from these fusion proteins because of their peptide sequence identity to GFP –we required reagents that would be specific for mCherry that could be used in mCherry and GFP co-expressing tissues.

GST Fusion Proteins for Cre and mCherry

Fusion proteins were generated using a standard GST fusion protein preparation, which is generally done at 37°C (and sometimes at 32°C as explained below). At all steps of fusion protein production the temperatures and incubation times can be altered depending on the behavior of the fusion protein (for extensive detail on fusion protein production, please see the Wright lab "fusion protein" manual). Sometimes the fusion protein is produced slower at lower temperatures, with less of it becoming packed into an insoluble form inside bacterial inclusion bodies. Thus, while the overall protein yield per bacterium might be lower at 32°C, the soluble proportion might be higher, allowing higher yield from the glutathione-agarose purification step. Cre and mCherry pGEX-KG fusion-protein plasmids were transformed into JM109 *E. coli.* Prior to large-scale protein preparations, small-scale protein preparations with sonication release from the bacteria into a simple low-salt buffer were performed to determine the general solubility of each fusion protein. The small-scale protein preparation protocol is similar to the large-scale method mentioned below, except the bacterial culture volumes are only 1.5 mL for both the overnight and the next day's IPTG-induced culture. Duplicates of the "protein miniprep" were included to determine the total protein (sample not sonicated, just centrifugation-collected and then boiled in SDS-PAGE sample buffer) and soluble protein (that released by sonication). The total-protein fractions for Cre and mCherry fusion proteins indicated that good amounts of each were induced. Substantial amounts of IPTG-induced protein were observed at or near the predicted size (Fig 5.2 A). Of the four GST-Cre fusion proteins, C1 had the highest soluble-

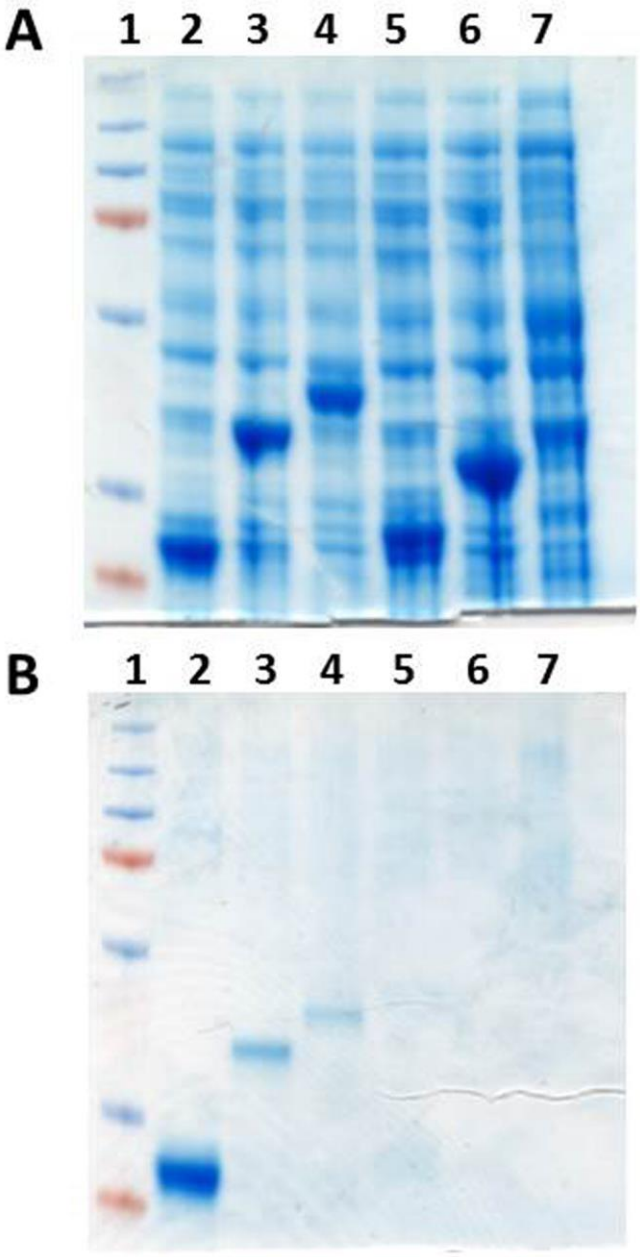
A
1 2 3 4 5 6 7
B
1 2 3 4 5 6 7
C
1 2 3 4

Figure 5.2. Small-scale preparation of Cre and mCherry GST-fusion proteins. (A) Total protein preparation of Cre fusion proteins detected by **Coomassie** Brilliant Blue R-250 staining on SDS-PAGE gels. "Protein Minipreps" were done to induce fusion-protein production of either GST alone (Lane 2, 26 kDa), GST-C1 (lane 3, 35 kDa), GST-C2 (Lane 4, 41.5 kDa), GST-C3 (Lane 5, 32.4 kDa), GST-C4 (Lane 6, 34 kDa), or without induction by IPTG (Lane 6). Intense protein bands were detected at or close to the predicted size for each GST-Cre fusion protein. (B) Soluble protein fractions, same lane assignments as in (A). C1 and C2 GST-Cre fusion proteins were more soluble than the C3 and C4 fusions. (C) Soluble protein fractions of mini-preparations of mCherry fusion proteins. All three GST-mCherry fusion proteins were highly soluble: GST-FG1 (lane 2, 32 kDa); GST-FG2 (lane 3, 30 kDa), GST-FGC (lane 4, 30 kDa).

protein yield with C2 appearing slightly less soluble **(**Fig 5.2 B). Fusion proteins C3 and C4 did not appear in the soluble fraction. All GST-mCherry fusion proteins (FG1, FG2, and FGC) were highly soluble (Fig 5.2 C). Fusion proteins C1, C4, and FG1 were therefore chosen for large-scale protein preparation. C4 was selected to determine if the small-scale "protein miniprep" was accurately depicting the solubility of the fusion proteins.

Independent bacterial colonies representing C1, C4, and FG1 were used to inoculate 200 mL overnight starter-cultures. Next morning, the starter-cultures were used to inoculate large cultures of 4 to 8 L, which were then grown for 2-4 hours before protein production was induced by adding Isopropyl β-D-1-thiogalactopyranoside (IPTG). IPTG binding to the lac repressor protein releases it from the *lac* operator sequence, initiating transcription from the associated transcription unit. The pGEX-KG plasmid contains a *lac* repressor gene cassette and a separate GST-fusion-protein gene cassette controlled by the *lac* operator. Induced bacteria were grown for a further two hours, collected by centrifugation, resuspended and sonicated. The sonicated bacterial solution was then centrifuged and the soluble supernatant gathered for affinity purification of the GST fusion proteins.

The soluble proteins were bound to glutathione-agarose with rotation on a hematological mixer for several hours at room temperature, or up to overnight. The next morning the beads/lysate mixture was loaded into a plastic/glass column assembly with a sintered glass bottom. The column was washed with a lot of volume and then several aliquots of freshly made 5.0 mM reduced glutathione were run over the column to compete the fusion protein off the glutathione-Sepharose beads, usually releasing the bulk of the bound GST fusion protein within close to the void volume of the settled matrix in the column. Ten 1.0 ml factions were collected during the elution process and examined for protein content by Bradford reagent. High-content

protein fractions were analyzed by SDS-PAGE (Sodium Dodecyl Sulfate Polyacrylamide Gel Electrophoresis) on preformed 10% gels to determine the quality and concentration of the fusion proteins in each fraction.

Consistent with the small-scale preparations, large-scale C1 and FG1 preparations contained large amounts of soluble protein (Fig 5.3). The most-concentrated protein-containing fractions were combined and stored at -20°C. The large-scale C4 GST-Cre preparation demonstrated a significantly higher solubility than indicated by the small-scale protein miniprep (Fig 5.3). The SDS-PAGE analysis of C4 showed two major bands: a larger one present in the minority that corresponded to the full-length fusion protein and a more major band that was slightly larger than GST alone. Adding protease inhibitors during the bacterial sonication and protein preparation did not significantly alter the ratio of these two bands (full-length and the smaller one that we presumed was undergoing proteolytic clipping).

The pooled high-protein content fractions from the C1 and FG1 preparations were sent to the BCBC antibody core in Denmark (directed by Dr. Ole Madsen). Each fusion protein was used to immunize two rabbits and guinea pigs. Several test and production bleeds were gathered, in addition to an exsanguination bleed. Samples of approx. 1.0 ml of each bleed, from each species and fusion protein were sent to the Wright lab for our testing on tissue samples. To date, testing of each antibody's characteristics was only done with the raw anti-serum; no affinity purification was attempted.

No positive reaction to mCherry on fixed tissue sections was detected with the rabbit or guinea pig antiserum derived from FG1 mCherry immunization. One guinea pig immunized with

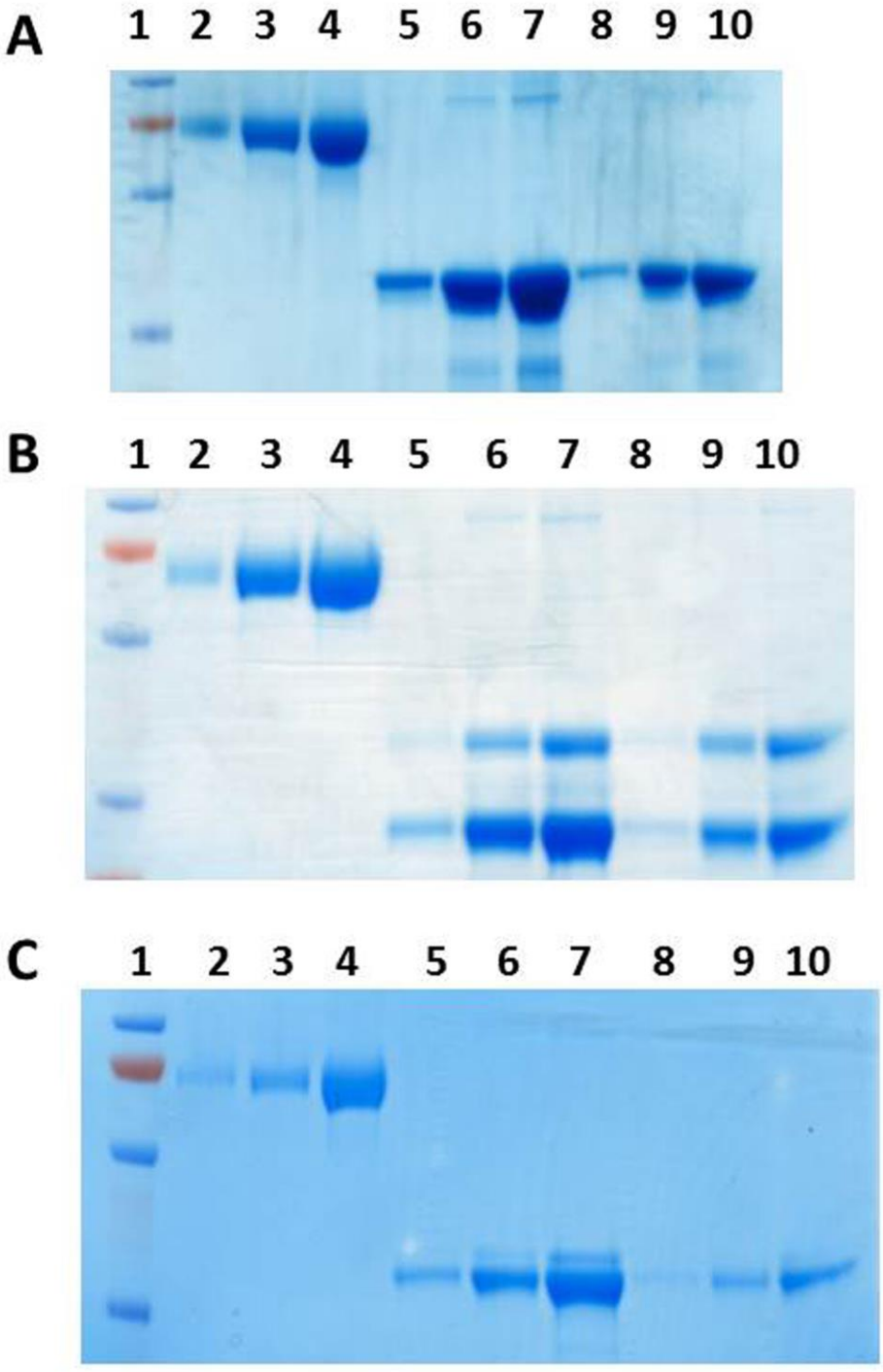
A
1 2 3 4 5 6 7 8 9 10
B
1 2 3 4 5 6 7 8 9 10
C
1 2 3 4 5 6 7 8 9 10

Figure 5.3. Large-scale fusion protein preparations of GST-C1, GST-C4, and FG1. Soluble protein preparation of GST-C1 (A), GST-C4 (B), and FG1 (C) fusion proteins detected by **Coomassie** Brilliant Blue R-250 staining on SDS-PAGE gels. For each gel: Lane 1, protein marker ladder; lane 2, 1.0 mg Bovine Serum Albumin (BSA); lane 3, 5.0 mg BSA; lane 4, 10.0 mg BSA. Lanes 4-7 and 8-10 are serial dilutions of the two highest protein-content fractions for each fusion protein. (A) GST-C1 is a highly soluble well-behaved fusion protein. (B) GST-C4, which was very insoluble based on the small-scale fusion protein preparation (comparing solubilized protein between the sonicated and centrifugation-cleared lysate and the protein remaining in the pelleted material). Large-scale protein preparation revealed that GST-C4 is mildly soluble, but the fusion protein runs on the gel as a large protein band (full-length fusion protein) and smaller "clipped" band (mostly GST). Addition of a cocktail of protease inhibitors (Complete mini, Roche) did not alter the ratio of "clipped" fusion protein to full-length fusion protein (not shown). (C) FG1 was highly soluble, consistent with the first indications from the small-scale protein preparation.

the C1 Cre fusion protein produced raw antiserum detected Cre in fixed samples. Adult murine pancreas tissue containing CreER under the control of the *Ptf1a* cis-regulatory regions (from the *Ptf1a*^{CreER} knock-in strain) was used to test the antiserum. A *Ptf1a*^{CreER} animal was injected with tamoxifen and sacrificed 12-hours post-injection to capture the nuclearly translocated CreER. The tamoxifen-treated *Ptf1a*^{CreER} mice were compared to *Ptf1a*^{CreER}-positive mice not treated with tamoxifen (should give a cytoplasmic signal), and adult pancreas tissue from animals with no CreER production (Fig. 5.4). Antiserum in the dilution range 1:500-1:2000 on CreER-negative tissue gave no signal in any pancreatic cells. The *Ptf1a*$^{CreER+}$ (no tamoxifen) samples showed diffuse cytoplasmic signal restricted to the acinar cells. Tamoxifen-treated *Ptf1a*$^{CreER+}$ samples produced strong nuclear signal only in Cpa1^{+} acinar cells. These data show that this raw Cre antiserum detects Cre or CreER selectively under these conditions; future affinity purification could clean the reagent up even more.

When generating antibodies, it is often necessary to affinity purify the antibodies in order to reduce the background signal, making signal-to-noise higher and detecting lower amounts of protein more effective. Often there are cross-reacting Abs against the GST and other contaminating bacterial proteins, and there are autoimmune reactions in the animals that can create problems in producing 'specific but not desired' signals on mammalian tissues. Often a specific reagent is masked, and affinity purification of a GST-fusion protein column with previous depletion steps (see Wright lab antibody manual). For all the antisera that I generated, so far only the raw antiserum was tested. In the case of the C1 Cre antiserum, an even cleaner, more specific signal might have been achieved with affinity purification. If the antiserum from this guinea pig is affinity purified, I believe that this Cre antibody could be a useful tool for the scientific community to detect Cre protein on fixed tissue sections.

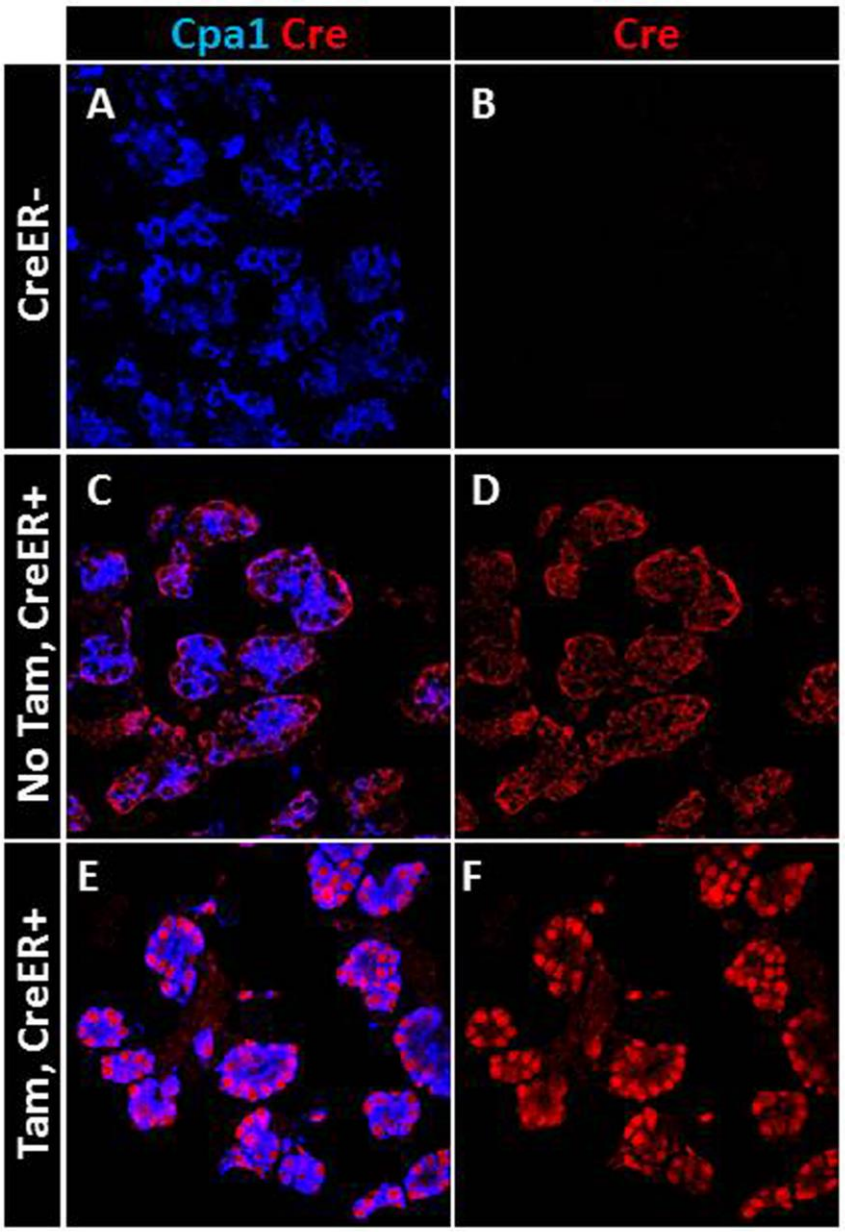

Figure 5.4 Validation of the behavior of antiserum derived from a guinea pig immunized with GST-C1. (A, B) GST-C1 antiserum tested on *Ptf1a*^{CreER}-negative cryo-embedded, fixed-tissue; no positive signal is detected. (C, D) On *Ptf1a*^{CreER}-positive tissue that was not administered tamoxifen, GST-C1 antiserum produced diffuse cytoplasmic signal in Cpa1-positive acinar cells. In the absence of tamoxifen, CreER should localize to the cytoplasm of acinar cells in *Ptf1a*^{CreER} tissue. (E, F) After tamoxifen administration, CreER translocates to the nucleus. In this condition, GST-C1 anti-serum produced strong nuclear signal in Cpa1-positive acinar cells. These findings indicate that this new GST-C1 antiserum can detect the localization of Cre or CreER in cryo-embedded, fixed-tissue samples.

CHAPTER VI

CONCLUSIONS AND FUTURE AIMS

Conclusions

There have been extensive studies of endodermal progenitor competence in model organisms (like chick, zebrafish, and *Xenopus)* using tissue recombination experiments. One interesting pertinent example to this thesis involves the specification of the glandular stomach (reviewed by Yasugi, 1993) in the chick. When glandular stomach mesenchyme was placed adjacent to gizzard endoderm, the gizzard endoderm adopted a glandular stomach phenotype and expressed markers such as pepsinogen (a marker specific to the glandular stomach). Follow-up studies placed the glandular stomach mesenchyme adjacent to other regions of the endoderm. When glandular stomach mesenchyme was placed adjacent to the allantoic or intestinal epithelium, the endoderm does not initiate expression of glandular stomach markers. These findings suggested that there are regional differences in the ability of the endoderm to adopt specific organ phenotypes. Tissue adjacent to the glandular stomach, like the gizzard, retained competence to interconvert organ fates when placed next to the glandular stomach mesenchyme, while distant regions of the endoderm did not. Further studies suggested that one mechanism by which the mesenchyme alters organ phenotype was through the regulation of key transcription factors. For example, gizzard mesenchyme induced high levels of *Sox2* in glandular stomach endoderm (leading to a gizzard endodermal phenotype), while glandular stomach mesenchyme caused gizzard endoderm to express low levels of *Sox2* (Ishii et al., 1998).

Loss-of-function or gene-dosage studies on key transcription factors (e.g., Sox2, Sox17, Ptf1a, and Cdx2) in the mouse further confirmed the role of transcription factors in specifying

regional and organ-specific progenitor character in the endoderm. Removing or reducing the function of these transcription factors caused endodermal progenitors to acquire another region or organ identity (Que et al., 2007; Gao et al., 2009; Spence et al., 2009; Kawaguchi et al., 2002). These studies suggested that even during organ specification, endodermal progenitors retain competence to adopt other organ fates and that transcription factors are important regulators of progenitor specification and commitment.

Less is understood in the field about how the timing of activation of organ-specific gene regulatory networks leads to or facilitates to organ commitment. Pioneering studies by Wandzioch and Zaret (2009) detailed that the response of progenitors in the ventral posterior foregut to specific signaling pathways is highly dependent on timing. Using an in vitro culture method and small molecules to inactivate BMP signaling, the Zaret lab was able to show the response of pancreatic progenitors to BMP signaling changes within a two hour window during development. During the 3-4 somite stage, BMP signaling initially limits expression of Pdx1 expression in the posterior ventral foregut, but at the 5-6 somite stage BMP signaling promotes Pdx1 expression. While these studies did not directly determine the commitment state of these altered progenitors after treatment, they at least suggested that the process of progenitor commitment could be extremely dynamic during development. It would be interesting to enact the same alterations in BMP signaling in an intact embryo to determine if there are functional changes in commitment (i.e. do these progenitors adopt different organ fates depending on when BMP signaling is altered?). It is also unclear what cause the progenitor to change their response to BMP signaling.\

There is no single model for how key transcription factors establish and maintain organ-specific gene regulatory networks. A potential model for the role of Ptf1a during establishment

of the pancreatic gene regulatory network is extrapolated from the role of c-Myc, a basic helix-loop-helix transcription factor similar to Ptf1a, during reprogramming adult cell types into a pluripotent state (Soufi et al., 2012). In contrast to Sox2, Oct4, and Klf4 (the other reprogramming factors), which were shown to bind to enhancers distant from promoters and act as pioneer factors (reviewed by Zaret and Carroll, 2011) during early reprogramming, c-Myc was shown to preferentially bind to promoter regions of the genome that were active in the fibroblast state. 48 hours later, c-Myc was shown to bind to new regions of the genome made accessible through the pioneer activity of Sox2, Oct4, and Klf4. c-Myc was also shown to enhance the recruitment of the other factors to genomic region where it was located (Soufi et al., 2012).

Other important inferences to the behavior of Ptf1a can be derived from NeuroD and MyoD. NeuroD, MyoD, and Ptf1a are highly similar basic helix-loop-helix proteins (more-so even than to c-Myc). Both NeuroD and MyoD have been classically described as determinants of the neuogenic and myogenic lineages, respectively. When NeuroD was expressed in pluripotential mouse embryonal carcinoma cell line (P19 cells), these cells are converted into neurons. When MyoD was expressed in mouse embryonic fibroblasts (MEFs), these cells were converted into myoblasts. Interestingly, NeuroD cannot convert MEFs into neurons and MyoD cannot convert P19 cells into myoblasts (Fong et al., 2012; reviewed by Buckingham and Rigby, 2014). Similar to c-Myc, NeuroD and MyoD are only able to bind to open chromatin, and are, thus, limited in their ability to activate direct targets without other transcription factors opening the chromatin for them.

One difference between NeuroD and MyoD that was thought to contribute to their cell-specific ability to act instructively is their DNA-sequence recognition. NeuroD and MyoD bind

to different unique E-box sequences in addition to the canonical E-box (Fong et al., 2012). The binding of the NeuroD or MyoD to the unique E-box sequences was associated with transcriptional activation. These finding are interesting with regards to Ptf1a, because Ptf1a forms a trimeric complex (with RBPJk or RBPJL) with a highly specific 14 base-pair recognition sequence (6 base-pair E-box; 8 base-pair TC-box) (Masui et al., 2009). This highly specific recognition sequence could confer ability of Ptf1a to act within the pancreatic gene regulatory network.

The field is extremely limited in our overall understanding of the chromatin landscape of early endodermal progenitors, in contrast to ground state pluripotent cells and terminally differentiated cell types. The most thorough description of the chromatin landscape of early endodermal progenitors is derived from in vitro directed differentiation (Xie et al., 2013). It is unclear how well these cells compare to the in vivo progenitor state. This study found that as progenitors transition from naïve foregut progenitors to organ-specified progenitors, there is a transition of the epigenetic state from bivalent (reviewed by Vastenhouw and Schier, 2012) to active. This study specifically implicated the removal of marks laid down by Polycomb group (PcG) during this transition. The Wright lab has attempted to remove the function of PRC2 during endodermal development. Preliminarily, there does not appear to be alterations in the patterning of the posterior foregut endoderm (Pdx1, Ptf1a, Gata4 and Sox2 appear to respect their normal expression territories) when Ezh2 function (essential for PRC2 function) is removed from the early endoderm (Reick and Wright, unpublished data). This is in contrast to previous studies by the Zaret lab (Xu et al., 2011), which implicated PcG in controlling the Pdx1 expression domain. Additional description of the epigenetic landscape of naïve foregut

progenitors and organ-specified progenitors will be needed to continue to interrogate the role of epigenetic modifiers during the process of organ specification and commitment.

Potentially during early endodermal development, pioneer factors in the endoderm (FoxAs and GATAs) establish "open" regions of genome, which are bivalent at this time (Xie et al., 2013). Binding of Ptf1a to chromatin would then potentially promote the recruitment of epigenetic modifiers to maintain activation marks and remove repressive marks to cause full-scale activation of the locus. Ptf1a has been shown to recruit histone acetyl-transferases (P/CAF) to specific loci in acinar cells (Rodolosse et al., 2009). The binding of Ptf1a to the chromatin could also increase the binding of other factors to the chromatin. Recent data has suggested that there is a genetic interaction between Ptf1a and Foxa2 during development (Meredith et al., 2014). The ability of Ptf1a to change the distribution of Foxa2 on chromatin could help shape the pancreas-specific gene regulatory network. This type of model would predict that in a gain-of-function experiment, Ptf1a would only be able to re-specify progenitors which contain the correct complement of pioneer factors that establish the right "open" chromatin for Ptf1a to access important direct target genes. In the absence of these pioneer factors, Ptf1a would not be able to access the genome, initiate transcription, and establish the pancreatic gene regulatory network.

In the following paragraph prior to the Future Directions section, I will briefly summarize my finding from Chapter III. The findings of my thesis work make important contributions to the field by precisely defining the regions (entire glandular stomach, extra hepatic biliary system, and anterior duodenum) of the endoderm that have pancreatic competence. While Ptf1a has been misexpressed in other model organisms (*Xenopus;* Afelik et al., 2006), the territories that are competent to be respecified have never been described in such precise spatial detail as in this

thesis. Additionally, I attempted to define the time window in which these progenitors are competent to be respecified as pancreatic progenitors. I have described that territories like the glandular stomach retained the ability to be respecified as pancreatic cell types as late as E15.5 (the last stage I tested). These findings demonstrate that competence to access pancreatic fate persists far later during development than previously appreciated in the posterior foregut. I was also able to interrogate, for the first time, what factors are controlled by Ptf1a during the initiation of pancreatic respecification. I describe that Ptf1a strongly induces Pdx1 expression, indicating that Ptf1a and Pdx1 act inter-dependently during this time. Finally, I describe the ability of the endoderm to change the specification state of the mesoderm. These findings suggest that there is a level of plasticity in the endoderm-associated mesoderm that has not been properly appreciated previously and the endoderm and mesoderm have interdependent specification programs.

Our tetracycline-based transient *Ptf1a* misexpression system permitted us to determine the consequence of broad *Ptf1a* misexpression in early mammalian endodermal progenitors, testing for its dominance as an organ-fate instructor. Our findings revealed that Ptf1a is a context-specific dominant trigger of pancreatic specification, and revealed new information about its region-specific potency in recruiting expression from their endogenous loci of additional members of the pro-pancreatic gene regulatory network. *Ptf1a* misexpression dramatically induced a broader expression territory of *Pdx1* in the early endoderm.

Only the endodermal territories that retained $Ptf1a^{+}Pdx1^{+}$ progenitors at later stages went on to undergo differentiation as pancreatic progenitors. Some areas such as the prospective rostral-most stomach, esophagus and even lung bud, were induced to express *Pdx1* from the endogenous locus, but then wound down *Ptf1a* and *Pdx1* expression, and restored the normal organ-fate

program for those regions. Our observations suggest that maintaining the $Ptf1a^{+}Pdx1^{+}$ state above a particular threshold or for long enough is likely an important gateway into establishing and maintaining the pancreatic fate, in competition with pre-existing gene regulatory networks that assign other organ fates.

We further defined quality of pancreatic respecification changed over time. Only early respecification (dox injections from E9.5-11.5) converted these territories into complete pancreas with representatives of all cell types – exocrine and most importantly endocrine cells – while the later-stage (E12.5 and after) Ptf1a induction only induced acinar-cell-specific respecification, and in a more mosaic/focal manner (clusters of acinar cells).

An important observation regarding the reciprocal instruction of cell/tissue fate between endoderm and mesoderm was the observation that when the Ptf1a-induced pancreatic respecification was towards complete pancreas, the mesodermal progenitors of the prospective glandular-stomach region changed their organ phenotype from stomach (thick mesenchyme located beneath the endodermal epithelium) to pancreas (interdigitated within the endodermal epithelium). These observations suggest that Ptf1a-based conversion of endodermal fate can, at least within a specific early period of organogenesis, have non-autonomous effects on instructing mesodermal tissue fates. It is therefore possible that defects in the mesenchyme could contribute to the almost complete failure of pancreas specification in Ptf1a null mutants.

Future Directions

There are many unanswered questions and future directions relating to the Ptf1a misexpression project. Possible future directions that are elaborated in greater detail following this listing include:

(1) Generating tools to misexpress Ptf1a and Pdx1 together as a way of testing if, in combination, these factors are more potent at driving pancreatic specification – they might act more effectively in achieving a specific threshold activation value for the Ptf1a-Pdx1 feedforward loop proposed in Chapter III.

(2) An exploratory project of high interest to me is the investigation of the molecular pathways that control the specification of pancreatic mesenchyme, and describing the changes in mesenchymal specification following Ptf1a misexpression.

(3) Another exploratory project of great significance in my opinion would be to use *Sox17*^{GFPCre} to manipulate other factors controlling endodermal patterning (Sox2 and Cdx2, for example). Combining Ptf1a misexpression with genetic conditions that are expected to alter early stages of endodermal patterning could be used to develop a molecular understanding of the factors that restrict or support pancreatic competence in the endoderm. One type of genetic alteration I began to study towards the end of my thesis research was the endodermal deletion of Sox2, which is known to be expressed broadly and has known functions from studies of hypomorphs to be involved with the development of the stomach, esophagus, and trachea.

Other smaller follow-up projects from the results presented in Chapter III include:

(4) Pervious studies (Schaffer et al., 2009) have described findings about persistent misexpression of Ptf1a in the endogenous pancreatic epithelium. The inducible misexpression system described in Chapter III of my thesis can be used to explore how the role of *Ptf1a* in controlling progenitor behavior and differentiation changes over time within the pancreatic epithelium.

(5) Transdifferentiating adult cell types into disease relevant cell populations is a potential therapeutic avenue for treating human disease conditions. Ptf1a misexpression can be used to test if Ptf1a is able to reprogram fully differentiated adult non-pancreatic cell types (such as parietal and chief cells in the glandular stomach). Potentially, Ptf1a can covert these cell types (by itself or in combination with other genetic or epigenetic factors) into pancreatic acinar cells, which can be further transdifferentiated into pancreatic endocrine cells.

Below, I now briefly speculate on some of these future directions.

Conditional Misexpression of both Ptf1a and Pdx1 in the Early Endoderm

Transient misexpression of *Ptf1a* in the early endoderm drastically expanded the expression territory of *Pdx1*. Pancreas-adjacent progenitor domains that were respecified maintained expression of both Pdx1 and Ptf1a. More distant endodermal territories that were not respecified could show a temporary expression of *Pdx1*, but, slightly later in embryogenesis, *Pdx1* and *Ptf1a* expression from their endogenous loci was extinguished, as discussed below, and these territories proceeded with their normally expected organ-fate program for that region. These observations suggest that stabilizing a $Pdx1^{+}Ptf1a^{+}$ progenitor state is an essential intermediate to initiating the pancreatic program following Ptf1a misexpression.

One potential reason why these distant organ territories are not converted into pancreatic cell types is because either the duration, or the protein level per cell, of transient Ptf1a was not sufficient to promote the establishment of the feed-forward cross-regulatory relationships with Pdx1 through activation of the endogenous *Pdx1* and *Ptf1a* loci. In adjacent resistant organ territories such as the forestomach, esophagus, or liver, there is potentially a more repressive genetic and/or epigenetic state that blunts or offsets the limited-duration Ptf1a from accessing or

properly activating the endogenous *Ptf1a* and *Pdx1* loci or other targets downstream targets of these genes. A new speculation that we are proposing is that the co-misexpression of Ptf1a/Pdx1 at the same time might be more effective at initiating the pancreatic gene regulatory network, rather than relying on activation of *Pdx1*, and autoactivation of endogenous *Ptf1a*, by the doxycycline-activated $Ptf1a^{EDD}$. Under the idea that regional or organ-specific GRNs work competitively with each other, we are thus designing ways of enforcing the transient co-misexpression of both Pdx1 and Ptf1a. Because I propose that activating the $Pdx1^{+}Ptf1a^{+}$ expression state during intermediate stages of development is crucial to initiating and maintaining the pancreatic program, I would predict that triggering of both factors in non-pancreatic progenitor domains resistant pancreatic conversion from Ptf1a misexpression alone (forestomach, esophagous, lung, and liver) would lead to pancreatic respecification.

The prediction in the previous paragraph could be tested by comparing the phenotype of Ptf1a misexpression alone to misexpression of Ptf1a and Pdx1 to two stages of analysis presented in Chapter III of this thesis (E12.5 and P0). At E12.5, I would interrogate changes in the expression domain of Ptf1a and Pdx1. Maintenance of these factors in different territories of the endoderm would indicate that misexpression of both factors at the same time is more efficient at activating their endogenous loci. Failure to expand the domain of expression of Ptf1a and Pdx1 at E12.5 would indicate that activation of the Pdx1/Ptf1a co-expression state is not the limiting factor controlling the activation of the Pdx1 and Ptf1a loci. Perhaps, other genetic (permissive/repressive factor) or epigenetic (closed chromatin) mechanisms prevent the activation of these loci following Ptf1a or Ptf1a/Pdx1 misexpression.

Ultimately, the most important comparison is whether misexpression of Ptf1a and Pdx1 together cause a change in the distribution of ectopic pancreatic cell types at P0. Finding ectopic

pancreatic cell types in organs not converted by Ptf1a misexpression alone would indicate misexpression of Pdx1 and Ptf1a is more efficient at establishing and maintaining the pancreatic gene regulatory network during development. If Pdx1/Ptf1a misexpression produces an identical or nearly identical phenotype at P0 to Ptf1a misexpression alone, this would again indicate that activation of the Pdx1/Ptf1a co-expression state is not the limiting factor leading to pancreatic respecification.

One way of achieving this goal would be to create a new tetO-driven transgene that could be used in the tri-genic misexpression system described in Chapter III (together with *Sox17*^{GFPCre} and *ROSA26*$^{rtTA.IRES.EGFP}$). The design currently under discussion in the Wright lab is a Ptf1a/Pdx1 co-producer allele that uses peptide-2A breaker sequences, rather than the more unpredictable IRES method. The peptide-2A system should produce initially equivalent amounts of Ptf1a and Pdx1.

The studies described above would further define the nature of pancreatic competence in the endoderm. Potentially all endodermal progenitors are competent to access pancreatic fates, provided they can be pushed – early enough, to access a stable pancreatic-MPC-specifier Ptf1a^{+}Ptf1a^{+} coexpression state. On the other hand, regardless of whether the correct levels of Pdx1 and Ptf1a are present at the right time, or if the two factors begin to activate the expression of downstream-tier propancreatic genes, some areas of the endoderm may still be extremely resistant to an artificial push towards a pancreatic fate. Learning how the endoderm might be subdivided according to either of these possibilities would provide a primary new level of insight.

Molecular Pathways Underlying Pancreatic Mesenchyme Specification

My studies using Ptf1a as a dominant trigger of pancreatic specification suggest that there is a developmental time window in which mesenchymal progenitor cells surrounding the prospective glandular stomach, EHBS, and anterior duodenum are competent to respond to the specification status of the adjacent endodermal progenitors. For example, glandular stomach has a thick multi-layered submucosal mesenchyme (Fig 3-8) containing multiple cells types such as smooth muscle cells, in stark contrast to the less structured, interdigitated pancreatic mesenchyme with the entire organ surrounded by the coelomic epithelium.

The implication of my finding that the mesenchyme of the prospective stomach is dramatically switched to a pancreatic character after Ptf1a^{EDD} induction is that there is a direct or indirect but rapid activation of expression of some factor(s) in the endoderm that then instructs mesenchymal cell identity. Identification of such factor(s) would shed light on the pathways that regionalize the mesenchyme surrounding the endoderm. It is important to explore the molecular mechanisms that lead to the specification of pancreatic mesenchyme because this cell population plays important instructive and permissive roles during pancreatic organogenesis. Understanding the molecular pathways that control the specification of pancreatic mesenchyme would be useful in directed differentiation protocols. Making bona fide pancreatic mesenchyme alongside pancreatic endoderm could substantially improve the quality and efficiency of complete pancreatic organoid or organ differentiation.

Currently, very little is known about the pathways that control the differentiation endoderm-associated mesenchyme in the posterior foregut. We also only have speculative candidates for potential endodermally expressed targets of Ptf1a that could signal instructively to the mesenchyme (Eph/Ephrins, Netrins, FGFs), and direct its developmental program differentially

compared to the adjacent organ regions. Very few markers of regionally distinct mesenchymal progenitor populations are known. Markers that are known, such as Nkx3.2 or Isl1, have poorly described spatiotemporal expression characteristics. Additionally, neither of the above markers has been linked to instructing organ-specific mesenchymal identity. Below I will describe a set of preliminary experiments, with and without the Ptf1a misexpression system, to explore the molecular mechanisms that lead to dominant specification of pancreatic mesenchyme.

A suitable approach to exploring the mechanisms that control the regionalization of the endoderm-associated mesenchyme in the posterior foregut would be to profile the expression of genes within the developing endoderm-associated mesenchyme and early organ-specified endodermal progenitors. For example, this could be accomplished by isolating, sorting, and RNA profiling the mesenchyme of each organ domain in the posterior foregut during early development (i.e. E9.5 or E10.5). Without suitable cell surface markers that qualitatively subdivide the mesenchyme associated with the various organ fates, manual micro-dissection is a suitable initial approach to gather reasonably pure mesenchyme progenitor populations for each organ. Cell numbers are a huge concern when performing RNA profiling of progenitor populations at stages of development such as E9.5 and E10.5. If numerous wild-type matings, say ten or more, were to be set up in parallel, it would be feasible to attempt flow cytometry to gather enough endoderm and mesenchymal progenitors. For some organ domains, like the EHBS and anterior duodenum, the number of collectable cells would likely be insufficient for RNA profiling even with multiple litters for pooling samples. The stomach is, however, the largest organ at these stages and does have a substantial number of associated mesenchymal cells. Micro-dissecting the E10.5 stomach and sorting with the endodermal-specific marker EpiCAM would allow the isolation of two cell populations: one being the $EpiCAM^{+}$ endodermal epithelial

cells, and the other (EpiCAM$^-$) population being the mesoderm (the cell population of interest), together with the accompanying endothelial cells, and any neural crest-derived cells. In such a preliminary, exploratory design, RNA profiling of the mesenchyme/endothelium/neural crest pool would still be able to detect potential interesting targets. In parallel, I would sort and RNA-profile the pancreatic endoderm and mesenchyme (by sorting later-stage tissues because of cell number concerns, E12.5 or E13.5) to identify genes enriched in pancreatic organogenesis and mesenchymal development.

Using these four data sets (pancreatic mesenchyme and endoderm; stomach mesenchyme and endoderm), I would hope to generate a candidate list of transcription factors and signaling molecules that are differentially expressed in the stomach and pancreas endoderm/mesenchyme. It is possible that there are no qualitatively differentially expressed genes that identify the mesenchyme of either organ. In this case, quantitative methods will need to be used. However, this is unlikely as it is known that Hox genes are expressed in a sequential order down the mesoderm/ectoderm and endoderm, although the latter is more poorly characterized.

Using the data sets described above, I would then explore expression of these genes in E10.5 Ptf1a^{EDD} embryos by whole-mount in situ hybridization. I would specifically examine the respecified stomach territory for acute changes in gene expression in the endoderm and mesenchyme following Ptf1a misexpression. I would attempt to identify genes that become acutely ectopically expressed in the respecified stomach endoderm and/or mesenchyme. The most interesting candidates should be explored with genetic tools (for example, *Sox17*^{GFPCre}-based conditional deletion if the factor is endodermally expressed) to determine the direct role in pancreatic development and mesenchyme specification. Given the speculative nature of these experiments, it will be difficult to predict whether a specific gene that is induced in the stomach

endoderm after Ptf1a misexpression has a role in assembling the pancreatic gene regulatory network in the endoderm or communicating with the adjacent mesoderm.

The data sets generated from profiling the developing stomach and pancreatic mesenchyme would also be useful to investigate the spatiotemporal expression characteristics of uncharacterized genes using in situ hybridization. Potentially, genes could be identified that are useful for genetic investigation of the development of mesenchyme (i.e. the spatiotemporal expression characteristics of their promoter might be useful for the generation of Cre drivers or fluorescent tools).

Endodermal Patterning

One prediction from studies described in Chapter III is that competence to adopt the pancreatic fate in relatively distant endodermal progenitor domains (anterior foregut, midgut, and hindgut) is restricted by the encoding of their normal organ programs, which concurrently place, genetically and epigenetically, the loci that are involved in the propancreatic program into a more-suppressed state. I therefore propose that an important future direction would be to explore what factors control organ specification and commitment in non-pancreatic endoderm. The emerging knowledge would further two goals: (1) Better understanding of the processes that control specification and commitment in the endoderm as a whole. (2) Increased knowledge of how to re-direct progenitors that are initially non-pancreatic (that is, having been regionally specified as either nearby or more-distant endoderm) towards a propancreatic state, with or without misexpression of Ptf1a (± Pdx1), or suppression of a small number of selected transcription factor genes that operate as high-level instructors of other regional or organ fates.

One such attractive factor that has been implicated in the development of anterior endodermal fates, including forestomach and esophagus, is *Sox2*. Sox2 is a critically important transcription factor involved in a variety of essential developmental processes including specification of the epiblast, neural progenitors, and retinal progenitors (Avilion et al., 2003; Ferri et al., 2004; Taranova et al., 2006). *Sox2* is also one of the four transcription factors that were first reported in the induced pluripotency from adult cell types, creating iPS cells (Takahashi et al., 2006). In addition to these well-studied functions, *Sox2* is expressed in the anterior definitive endoderm. Hypomorphic *Sox2* embryos have defects in the development of the esophagus and trachea, mimicking human disease conditions (anopthalmiaesophageal-genital syndrome) (Que et al., 2007). The expression pattern of *Sox2* suggests that *Sox2* has an important role in patterning the early anterior foregut. There has been no attempt (due to a lack of suitable genetic tools) to completely remove *Sox2* function from the endoderm. *Sox17*$^{GFP.Cre}$ is an appropriate tool to conditionally inactivate *Sox2* broadly throughout the endoderm, before it begins to exert any of its patterning functions. The timing and broad expression characteristics of the new *Sox17*$^{GFP.Cre}$ tool make it even better than, say, Foxa3^{Cre} (which would inactivate after Sox2 expression begins, be mosaic, and not target the very anterior foregut where Sox2 is expressed). *Sox17*$^{GFP.Cre}$-based endoderm-specific *Sox2* conditional inactivation could therefore reveal several putative levels of novel information. There could be a loss of the proper location of the glandular stomach-forestomach boundary. This boundary is especially pertinent to my thesis research because it seems to mark the limit of pancreatic competence identified under the challenge of Ptf1a^{EDD} (the prospective glandular stomach region being convertible, but forestomach not). I found that while Ptf1a misexpression was able to suppress *Sox2* transiently in the prospective forestomach and esophagus, just a little later in development the Sox2

expression returned to levels indistinguishable from wild type – even though the final differentiation was not normal, the forestomach and esophageal endoderm did not convert to pancreatic tissue. In contrast, the Ptf1a^{EDD}-converted progenitors of the putative glandular stomach region did not reactive *Sox2* and remained fully diverted to the pancreatic fate.

I have begun these initial studies with *Sox17*$^{GFP.Cre}$-based elimination of endodermal *Sox2* function. I acquired a *Sox2* null allele (*Sox2*^{EGFP}) and conditional null allele (*Sox2*^{COND}) (Taranova et al., 2006), and initially studied neonatal (P0) *Sox17*$^{GFP.Cre}$/+; *Sox2*$^{EGFP/COND}$ pups (termed Sox2$^{\Delta EDD}$). In these Sox2$^{\Delta EDD}$ pups, *Sox2* was inactivated in specified definitive endoderm and endothelial cells, but because *Sox2* is not expressed in endothelial cells, endothelial dysfunction will not complicate or contribute to this knockout model. The P0 Sox2$^{\Delta EDD}$ pups were stillborn and were observed as immediately not breathing, likely because of the morphological changes in endoderm described below. Dissection of Sox2$^{\Delta EDD}$ pups revealed large-scale disruptions in the normal wild-type morphology and tissue histology of the stomach, esophagus, and trachea, and dramatically distinct from the phenotype in *Sox2* hypomorphic embryos described in Que et al. (2007). The stomach size was drastically reduced in Sox2$^{\Delta EDD}$ pups (Fig. 6.1), whereas there was no such stomach size phenotype reported for *Sox2* hypomorphic mice (Que et al., 2007). Sox2$^{\Delta EDD}$ pups contained a single trachea-esophageal tube

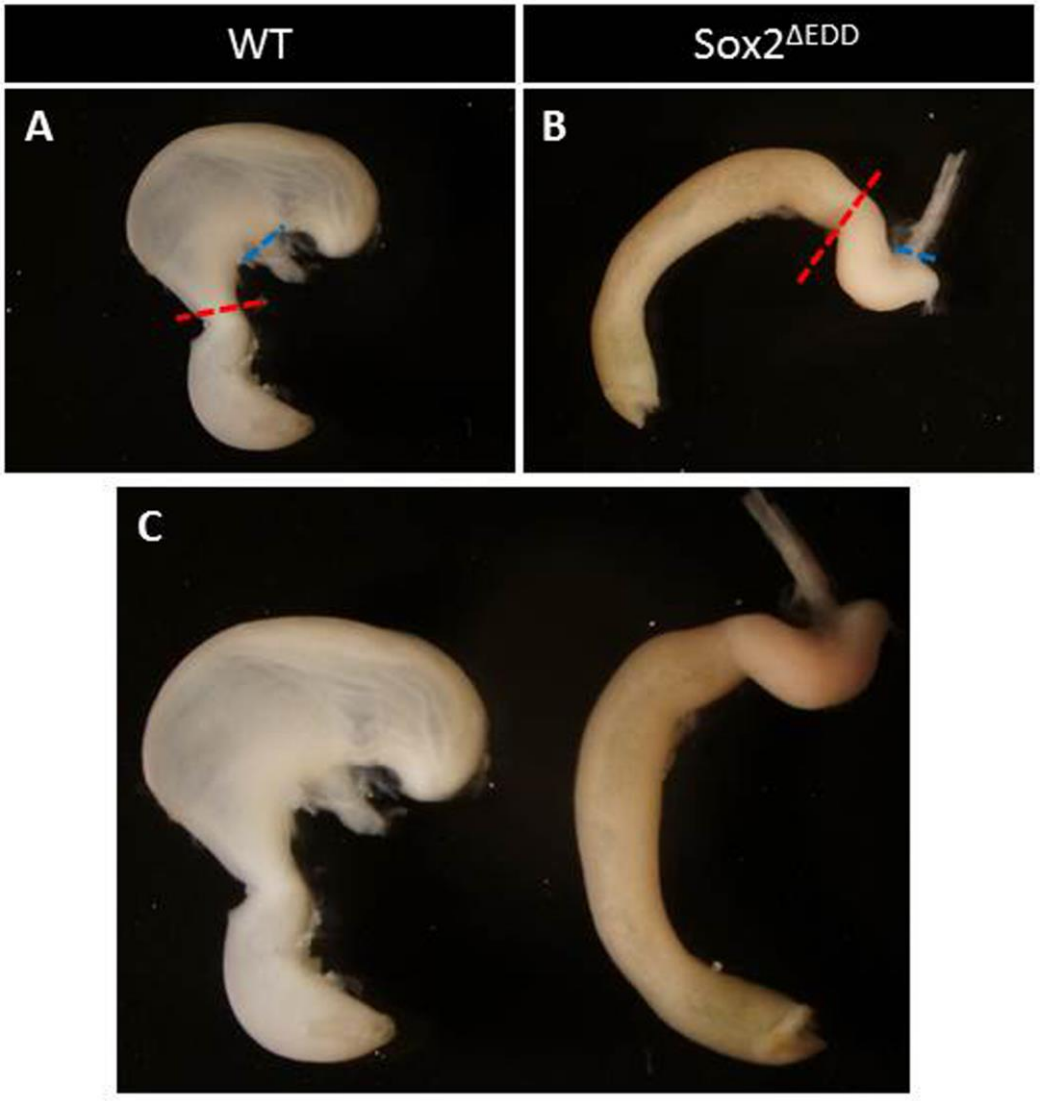

Figure 6.1. Morphological alterations in the stomach of Sox2$^{\Delta EDD}$ pups. (A) Dissected wild-type P0 stomach and anterior duodenum. Junction between the duodenum and stomach (pylorus) is indicated by the dashed red line; between esophagus and forestomach by the dashed blue line. (B) Sox2$^{\Delta EDD}$ stomach and anterior duodenum. Sox2$^{\Delta EDD}$ stomachs are significantly hypoplastic compared to wild-type stomachs. (C) Direct size comparison of wild-type and Sox2$^{\Delta EDD}$ stomachs.

that extended from the stomach up to the oral endoderm. The large bronchioles of the lung connected directly to this single tube (Fig. 6.2). The lack of separation of trachea and esophagus, as well as potential structural abnormalities in the pharynx (at least the epiglottis is missing) may cause $Sox2^{\Delta EDD}$ embryos to suffocate on amniotic fluid during gestation or these animals are simply incapable of coordinated breathing.

The phenotypic changes in $Sox2^{\Delta EDD}$ endoderm differentiation were examined further by histology, and by an initial survey of the effects on important regionally restricted transcription factors. Confirming that endodermal Sox2 was completely eliminated by $Sox17^{GFPCre}$, Sox2 was not immunodetectable in proximal lung samples of $Sox2^{\Delta EDD}$ pups (Fig. 6.3). Sox2 was also absent from the single trachea-esophageal tube, and the putative forestomach and glandular stomach (not shown). Additional studies would be needed to determine if *Sox2* expression is always lacking from the endoderm, by analyzing stages focused at and just after formation of the nascent definitive endoderm.

One potential outcome of the complete removal of *Sox2* in the endoderm is that the boundaries of other important regionally expression transcript factors will change. This finding would suggest that *Sox2* has important role in defining these territories. One important early-acting gene that needs to be considered strongly, knowing its role in endodermal patterning (Gao et al., 2009) is *Cdx2*. The expression territories of *Cdx2* and *Sox2* are non-overlapping (see the introductory chapter of this thesis), with the *Sox2* domain ending in the caudal stomach, adjacent to the anterior limit of *Cdx2* expression in the rostral-most anterior duodenal endoderm. Endoderm-selective removal of *Cdx2* function causes the expansion of *Sox2* throughout the posterior endoderm. Under a cross-repression model, removing *Sox2* function would lead to expanded *Cdx2* throughout the anterior endoderm. In my $Sox2^{\Delta EDD}$ analysis so far, none of the

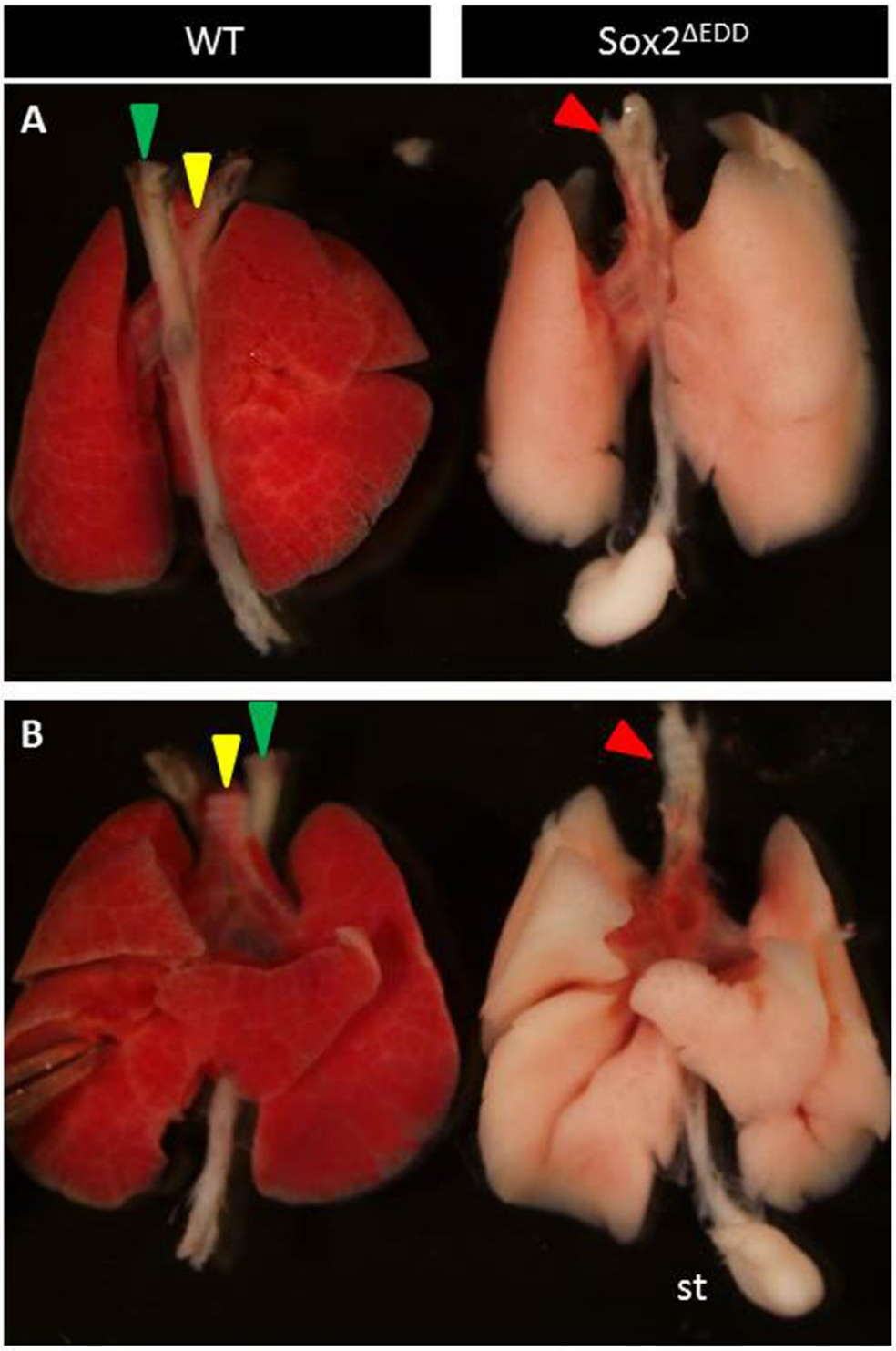

Figure 6.2. Morphological alterations in esophagus and trachea of Sox2$^{\Delta EDD}$ pups. Wild-type (left) and Sox2$^{\Delta EDD}$ (right) trachea, esophagus, and lung. (A) Dorsal view, (B) Ventral view. Wild-type tissue has distinct tracheal (yellow arrowhead) and esophageal tubes (green arrowhead). Sox2$^{\Delta EDD}$ tissue has one tube structure throughout (red arrowhead). The anterior portion of this tube appears to resemble the trachea (cartilage rings indicated by red arrowhead).

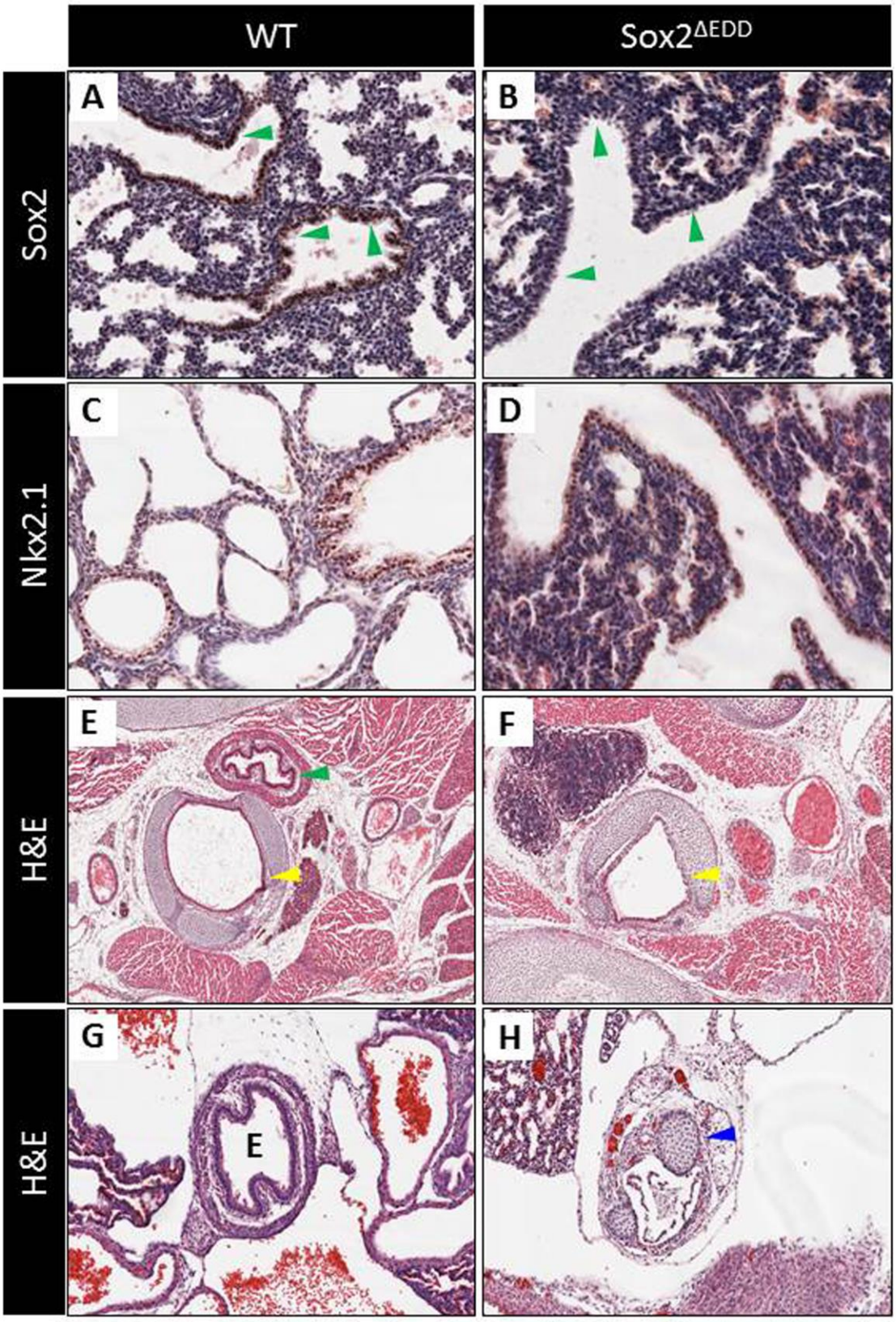
WT
Sox2ΔEDD
Sox2
Nkx2.1
H&E
H&E
A
B
C
D
E
F
G
H
E

Figure 6.3. Histology and gene expression alterations in Sox2$^{\Delta EDD}$ tissue. (A, B) Sox2 immunohistochemistry. (A) Sox2 signal in wild-type proximal lung (green arrowheads). (B) Sox2 production is lost in the proximal lung (green arrowheads) and the entire endoderm (not shown) of Sox2$^{\Delta EDD}$ pups. (C, D) Nkx2.1 immunohistochemical analysis. (C) Nkx2.1 in wild-type lung in both the proximal (yellow arrowhead) and distal lung (green arrowhead) (B) Nkx2.1 in the lung of Sox2$^{\Delta EDD}$ pups. Nkx2.1-positivity supports the idea that this tissue is lung, where Sox2 is normally expressed. The loss of Sox2 in the lung in (B) indicates that *Sox17*^{GFPCre}-based deletion efficiently removes *Sox2* from the endoderm. (E, F) Hematoxylin and eosin staining of wild-type (E) or Sox2$^{\Delta EDD}$ (F) tissue located anterior of the lung, around the thymus/thyroid. In this area of the endoderm there should be independent tracheal (yellow arrowhead) and esophageal tubes (green arrowhead). Sox2$^{\Delta EDD}$ tissue contains one tube resembling a trachea (yellow arrowhead). No squamous epithelium can be identified. (G, H) Hematoxylin and eosin staining of wild-type (G) compared to Sox2$^{\Delta EDD}$ (H) tissue between the lung and stomach. In this region of endoderm, there should be one tube with a squamous epithelium (esophagus, E). The single tube in Sox2$^{\Delta EDD}$ tissue (H) contains no squamous epithelium. The Sox2$^{\Delta EDD}$ epithelium in this location is much more columnar. The mesenchyme contains small pieces of cartilage (blue arrowhead) which would normally only surround the trachea.

endodermal cells in the glandular stomach or any other anterior endodermal territory showed Cdx2 positivity, thus indicating the absence of a fundamental change to an intestinal character. Preliminarily, therefore, it appears that *Sox2* is not the only factor involved in limiting the expression territory of *Cdx2*. Another gene potentially regulated by *Sox2* is *Pdx1*. *Pdx1* and *Sox2* are co-expressed in the antral stomach and *Sox2* could potentially set this *Pdx1* expression boundary. However, the P0 analysis of *Sox2*$^{\Delta EDD}$ tissue showed that the Pdx1-positive tissue domain exhibited a similar anterior boundary compared to controls.

In *Sox2*$^{\Delta EDD}$ pups, the normal stratified squamous epithelium of the forestomach and esophagus was replaced by a simple columnar epithelium. There was no apparent stratification or keratinization of cells within the forestomach and esophagus. Because the columnar epithelium in the esophagus/forestomach was reminiscent of the type of epithelium seen in the wild-type proximal lung and trachea, I tested if there was a wide broadening of the expression domain of *Nkx2.1*. Endodermal *Nkx2.1* is found in the lung, trachea, and thyroid and is required for the proper development of all of these organs (Minoo et al., 1999). Interestingly, Nkx2.1-positive tissue was found throughout the columnar epithelium replacing the esophagus and forestomach in the *Sox2*$^{\Delta EDD}$ tissues (Fig. 6.4). These findings suggest strongly that *Sox2* is a potent suppressor of *Nkx2.1* expression in the prospective forestomach and esophagus during development. Further studies should address if the columnar epithelial cells within the esophagus and forestomach express any of the differentiated cell markers of the trachea or proximal lung, to help identify the nature of this altered epithelium. Histological analysis also indicated significant changes in the development of the pharynx, which also appeared to be altered to a simple columnar epithelium with relatively uniform Nkx2.1-positivity.

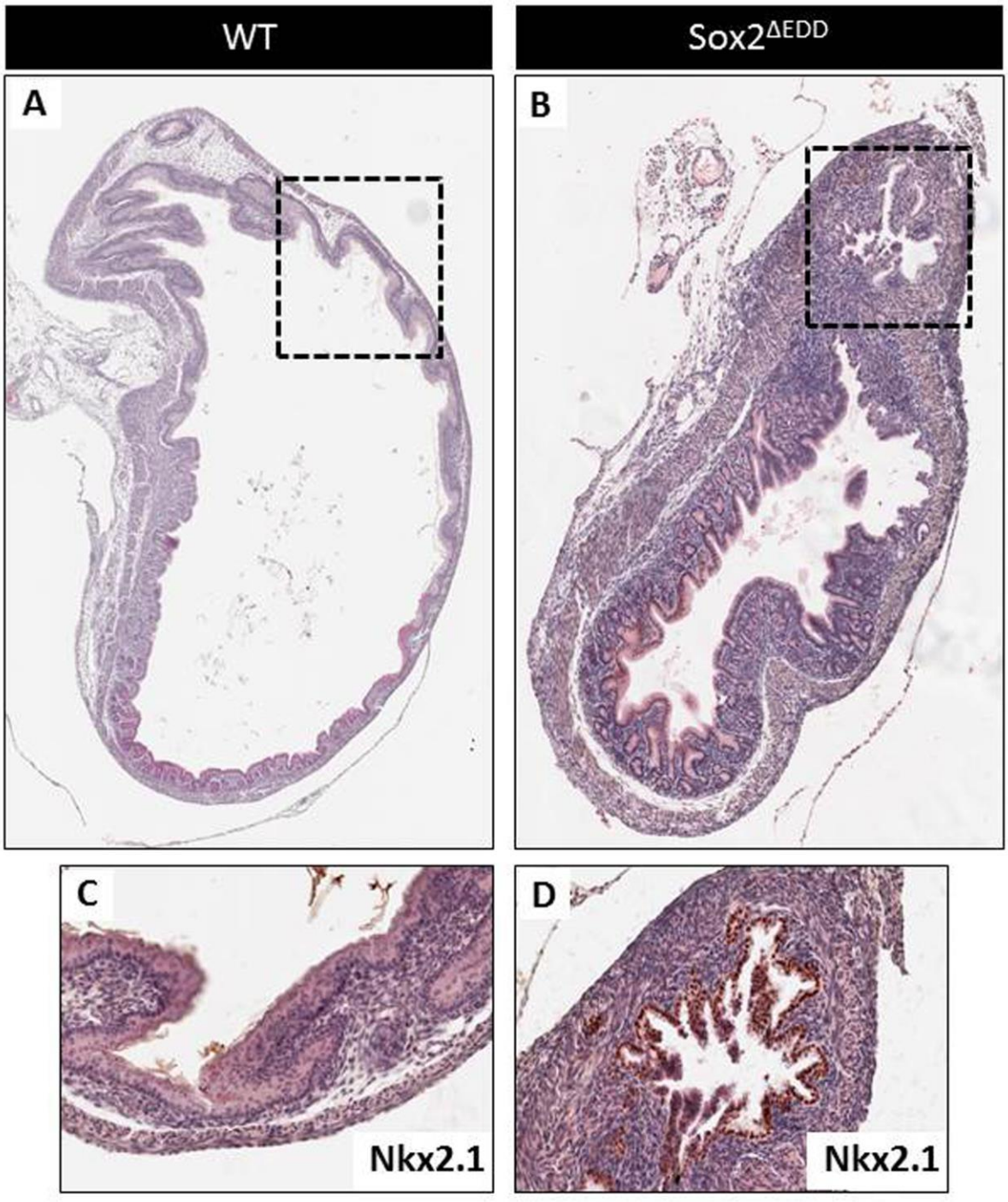
WT
Sox2ΔEDD
A
B
C
Nkx2.1
D
Nkx2.1

Figure 6.4. Histology and gene expression alterations in the forestomach of endodermal *Sox2*-null mice. (A, B) Hematoxylin and eosin staining of wild-type (A) compared to $Sox2^{\Delta EDD}$ (B) stomach. The forestomach of $Sox2^{\Delta EDD}$ pups (B) does not resemble the stratified squamous epithelium of control embryos, but is columnar. (C, D) Immunohistochemical detection of Nkx2.1, which is not produced in wild-type forestomach (C), but is expressed throughout the $Sox2^{\Delta EDD}$ forestomach (D). This finding suggests that the $Sox2^{\Delta EDD}$ forestomach is likely being regionally converted into trachea/proximal lung-like cell fates.

My preliminary data suggests that in the absence of *Sox2* function the forestomach, esophagus, and pharynx somehow are subject to a misallocation process, diverting them from their expected normal organ fates. By including transient Ptf1a^{EDD} (± Pdx1) misexpression into the context of the Sox2$^{\Delta EDD}$ deficiency, one could test is now a time window during which these organ territories show competence to access the pancreatic fate. Expansion of pancreatic cell types into the forestomach and esophagus after in the Ptf1a misexpresison, Sox2$^{\Delta EDD}$ background would indicate that Sox2, through programming the endogenous gene regulatory networks of the esophagus and forestomach, prevents these progenitors from accessing the pancreatic fate. Failure to convert the esophagus and forestomach into pancreatic cell types in the background of Sox2^{EDD} would indicate the programming of the endogenous forestomach and esophagus gene regulatory network does not restrict pancreatic competence. Other genetic (permissive/repressive factors) or epigenetic (differences in the chromatin landscape) mechanisms would need to be explored to explain the lack of pancreatic competence in the anterior endoderm. Competence to undergo conversion should also focus on whether or not such re-regionalization and organ fate reprogramming might need to occur prior to the action of Nkx2.1 in beginning to direct cells to tracheal and proximal lung fates.

My analysis quickly revealed that *Sox2* also shows expression in the most caudally located endodermal derivatives, which is in agreement with data shown in the GUDMAP (http://www.gudmap.org/). Sox2^{+} progenitors contribute to the urethra and anus, both of which develop into tissue with some squamous epithelial structure. Based on my observations of alterations in the squamous epithelia of the anterior endoderm in *Sox2*$^{\Delta EDD}$ tissue, it is possible that *Sox2* is a key determinant, in general, of a squamous epithelial phenotype in all endodermally derived organ anlagen. Clearly, further investigation of *Sox2* hypomorphic and

Sox2$^{\Delta EDD}$ tissue would be required to determine if *Sox2* has deterministic tissue-instructive roles, rather than just determining a general epithelial structure, in caudal-most endoderm.

Cell Lineage Allocation in the Endogenous Pancreas Following Ptf1a Misexpression

In addition to the extra-pancreatic tissue alterations (see Chapter III), Ptf1a misexpression did cause substantial changes in the developmental program within the "endogenous" pancreas. Misexpression of Ptf1a within the pancreas was partially explored by Schaffer et al. (2010). They used chronic, not transient, Ptf1a expression from a transgene made in the Wright lab, in which expression was controlled by the *Pdx1* promoter that activates within the developing pancreatic epithelium starting at E8.5. They studied the effects of prolonged Ptf1a production within Pdx1-expressing epithelium up until E14.5, which was the only stage of analysis reported. These studies demonstrated that such chronic misexpression of Ptf1a caused pancreatic progenitors to adopt a tip cell, pro-acinar state, and to suppress the movement to a 'trunk state' Nkx6.1-positive epithelium that could produce endocrine-directed progeny. In contrast, our system allows stage-controlled *Ptf1a* misexpression, wherein we can alter the timing and duration of Ptf1a to test its ability to determine the progenitor state of later stage pancreatic progenitors.

My initial scanning of the effects within the pancreas of mid-organogenesis application of Ptf1a^{EDD} (E12.5) suggested that there were changes in the relative specification of endocrine and ductal cell lineages, when scored in early post-natal tissue. In contrast, when initiating transient Ptf1a^{EDD} in the early pancreatic buds (at approx. E9.5-10.5), the early progenitors do not alter differentiation by the end of gestation. Exploring the reason why early progenitors fail to alter their behavior after exogenous Ptf1a misexpression might uncover novel genetic relationships

that could help illuminate the molecular pathways that distinguish and propagate the different lineages that emerge from the tip vs. trunk domains, how these domains are initially segregated, and the degree of commitment or plasticity in the later stages of embryogenesis. Gene expression profiling could be helpful direction, because of the currently limited number of genes known as direct targets of Ptf1a in early pancreatic progenitors.

Reprogramming Adult Cell Types into Pancreatic Acinar or Other Cell Types

The transdifferentiation and/or reprogramming of adult cell types into clinically relevant cell types is an emerging field of study. I have shown in my thesis work that *Ptf1a* can exert dominant effects leading to the functional respecification of non-pancreatic progenitors into pancreatic cell types during development. A follow-up study based on my findings would be to test if *Ptf1a* could transdifferentiate adult non-pancreatic cell types into pancreatic cell types. Transdifferentiation of adult cell types into disease relevant cell populations is a potential therapeutic avenue for treating human disease conditions. Potentially, Ptf1a can convert adult non-pancreatic cell types (such as chief or parietal cell in the glandular stomach) into pancreatic acinar cells that could then be turned into pancreatic endocrine cells with further genetic manipulation such as those presented in Zhou et al. (2008).

The use of CreER lines such as *H/K ATPase*^{Cre} (Syder et al., 1999) and *Mist1*^{CreER} (Shi et al., 2009) in combination with *ROSA26*$^{rtTA.IRES.EGFP}$ and tetO$^{Ptf1a.IRES.lacZ}$ would allow misexpression of Ptf1a in parietal and chiefs cells of the adult stomach, respectively. Other less specific CreER lines such as *Sox9*^{CreER} could also be useful. Sox9 is generally expressed in most endodermal organs (lung, stomach, intestine, liver, etc…) within the adult stem cell compartment and some differentiated cell progeny (Furuyama et al., 2011). There are well established in vitro organoid

culture conditions for the glandular stomach. Such an in vitro system would allow easy further manipulation of these cell types with small molecules and siRNA knockdown in background of Ptf1a misexpression.

Perhaps, Ptf1a misexpression is sufficient to transdifferentiate parietal or chief cells into acinar cells. This type of outcome would indicate that even after terminal differentiation, the glandular stomach retains competence to access pancreatic cell fates. Another potential outcome is that Ptf1a may only be able to convert parietal cells and not chief cells, or vice versa. This type of outcome would indicate that during the differentiation of these adult cell types, the ability of access pancreatic cell fates only lost during specific differentiation programs. This is a particular attractive outcome because it allows the direct comparison of competence and non-competent adult cell types at genetic and epigenetic levels. This could potentially reveal important target, pathways, and co-regulators that necessary for pancreatic respecificaiton in adult cell types. While during development Ptf1a was sufficient to respecify glandular stomach progenitors to pancreatic progenitors, in the adult, another possible outcome is that Ptf1a alone is not sufficient to elicit this type of outcome. It may be necessary to misexpress Ptf1a with other factors, like Pdx1 for example, in order to promote any adult stomach cell to access the pancreatic fate. Other fruitful avenues could include using small molecules to inhibit epigenetic enzymes. This type of manipulation may relax the resistance of terminally differentiated cell types to conversion.

REFERENCES

Afelik, S., Chen, Y., and Pieler, T. (2006). Combined ectopic expression of Pdx1 and Ptf1a/p48 results in the stable conversion of posterior endoderm into endocrine and exocrine pancreatic tissue. *Genes Dev.* **20**, 1441-1446.

Ahnfelt-Rønne, J., Jørgensen, M.C., Klinck, R., Jensen, J.N., Füchtbauer, E.M., Deering, T., MacDonald, R.J., Wright, C.V., Madsen, O.D., and Serup, P. (2012). Ptf1a-mediated control of Dll1 reveals an alternative to the lateral inhibition mechanism. *Development* **139**, 33-45.

Ang, S.L., and Rossant, J. (1994). HNF-3 beta is essential for node and notochord formation in mouse development. *Cell* **78**, 561–574.

Antonica, F., Kasprzyk, D. F., Opitz, R., Iacovino, M., Liao, X. H., Dumitrescu, A. M., Refetoff, S., Peremans, K., Manto, M., Kyba, M., and Costagliola, S. (2012). Generation of functional thyroid from embryonic stem cells. *Nature* **491**, 66-71.

Avilion, A.A., Nicolis, S.K., Pevny, L.H., Perez, L., Vivian, N., and Lovell-Badge, R. (2003) Multipotent cell lineages in early mouse development depend on SOX2 function. *Genes Dev.* **17**, 126-140.

Belteki, G., Haigh, J., Kabacs, N., Haigh, K., Sison, K., Costantini, F., Whitsett, J., Quaggin, S. E., and Nagy, A. (2005). Conditional and inducible transgene expression in mice through the combinatorial use of Cre-mediated recombination and tetracycline induction. *Nucleic Acids Res.* **33**, e51.

Beres, T.M., Masui, T., Swift, G.H., Shi, L., Henke, R.M., and MacDonald, R.J. (2006). PTF1 is an organ-specific and Notch-independent basic helix-loop-helix complex containing the mammalian Suppressor of Hairless (RBP-J) or its paralogue, RBP-L. *Mol. Cell Biol.* **26**, 117-130.

Bort, R., Martinez-Barbera, J. P., Beddington, R. S. & Zaret, K. S. (2004) Hex homeobox gene-dependent tissue positioning is required for organogenesis of the ventral pancreas. *Development* **131**, 797–806.

Branda, C.S. and Dymecki, S.M. (2004). Talking about a revolution: The impact of site-specific recombinases on genetic analyses in mice. *Dev. Cell* **6**, 7-28.

Buckingham, M. and Rigby. P.W. (2014). Gene regulatory networks and transcriptional mechanisms that control myogenesis. *Dev Cell.* **28**, 225-38.

Burlison, J. S., Long, Q., Fujitani, Y., Wright, C. V., and Magnuson, M. A. (2008). Pdx-1 and Ptf1a concurrently determine fate specification of pancreatic multipotent progenitor cells. *Dev. Biol.* **316**, 74-86.

Carrasco, M., Delgado, I., Soria, B., Martín, F., and Rojas, A. (2012). GATA4 and GATA6 control mouse pancreas organogenesis. *J. Clin. Invest.* **122**, 3504-3515.

Choi, E., Kraus, M. R., Lemaire, L. A., Yoshimoto, M., Vemula, S., Potter, L. A., Manduchi, E., Stoeckert, C. J. Jr., Grapin-Botton, A., and Magnuson, M. A. (2012). Dual lineage-specific expression of Sox17 during mouse embryogenesis. *Stem Cells* **10**, 2297-2308.

Engert, S., Liao, W. P., Burtscher, I., and Lickert, H. (2009). Sox17-2A-iCre: a knock-in mouse line expressing Cre recombinase in endoderm and vascular endothelial cells. *Genesis* **47**, 603-610.

Ferri A.L., Cavallaro, M., Braida, D., Di Cristofano, A., Canta, A., Vezzani, A., Ottolenghi, S., Pandolfi, P.P., Sala, M., DeBiasi, S., and Nicolis, S.K. (2004) Sox2 deficiency causes neurodegeneration and impaired neurogenesis in the adult mouse brain. *Development* **131**, 3805-3819.

Fong, A.P., Yao, Z., Zhong, J.W., Cao, Y., Ruzzo, W.L., Gentleman, R.C., and Tapscott, S.J. (2012). Genetic and epigenetic determinants of neurogenesis and myogenesis. *Dev. Cell* 22, 721-735.

Friedman, J.R., and Kaestner, K.H. (2006). The Foxa family of transcription factors in development and metabolism. *Cell Mol. Life Sci.* **63**, 2317-2328.

Fujitani, Y., Fujitani, S., Luo, H., Qiu, F., Burlison, J., Long, Q., Kawaguchi, Y., Edlund, H., MacDonald, R.J., Furukawa, T., et al. (2006) Ptf1a determines horizontal and amacrine cell fates during mouse retinal development. *Development* **133**, 4439-4450.

Fukuda, A., Kawaguchi, Y., Furuyama, K., Kodama, S., Horiguchi, M., Kuhara, T., Kawaguchi, M., Terao, M., Doi, R., Wright, C.V., Hoshino, M., Chiba, T., and Uemoto, S. (2008). Reduction of Ptf1a gene dosage causes pancreatic hypoplasia and diabetes in mice. Diabetes **57**, 2421-2431.

Furuyama, K., Kawaguchi, Y., Akiyama, H., Horiguchi, M., Kodama, S., Kuhara, T., Hosokawa, S., Elbahrawy, A., Soeda, T., Koizumi, M., et al. (2011). Continuous cell supply from a Sox9-expressing progenitor zone in adult liver, exocrine pancreas and intestine. *Nat. Genet.* **43**, 34-41.

Gannon, M., Gamer, L.W., and Wright, C.V. (2001). Regulatory regions driving developmental and tissue-specific expression of the essential pancreatic gene pdx1. *Dev. Biol.* **238**, 185-201.

Gao, N., LeLay, J., Vatamaniuk, M.Z., Rieck, S., Friedman, J.R., Kaestner, K.H. (2008). Dynamic regulation of Pdx1 enhancers by Foxa1 and Foxa2 is essential for pancreas development. *Genes Dev.* **22**, 435-448.

Gao, N., White, P., and Kaestner, K. H. (2009). Establishment of intestinal identity and epithelial-mesenchymal signaling by Cdx2. *Dev. Cell* **16**, 588-599.

Gerrish, K., Cissell, M. A., and Stein, R. (2001). The role of hepatic nuclear factor 1 alpha and PDX-1 in transcriptional regulation of the pdx-1 gene. *J. Biol. Chem.* **276**, 47775-47784.

Gerrish, K., Van Velkinburgh, J. C., and Stein, R. (2004). Conserved transcriptional regulatory domains of the pdx-1 gene. *Mol. Endocrinol.* **18**, 533-548.

Glasgow, S.M., Henke, R.M., Macdonald, R.J., Wright, C.V., and Johnson, J.E. (2005) Ptf1a determines GABAergic over glutamatergic neuronal cell fate in the spinal cord dorsal horn. *Development* **132**, 5461-5469.

Gu, G., Dubauskaite, J., and Melton, D.A. (2002). Direct evidence for the pancreatic lineage: NGN3+ cells are islet progenitors and are distinct from duct progenitors. *Development* **129**, 2447-2457.

Gustafsson, E,, Brakebusch, C., Hietanen, K., and Fässler, R. (2001). Tie-1-directed expression of Cre recombinase in endothelial cells of embryoid bodies and transgenic mice. *J. Cell Sci.* **114**, 671-676.

Hale, M.A., Kagami, H., Shi, L., Holland, A.M., Elsässer, H.P., Hammer, R.E., and MacDonald, R.J. (2005). The homeodomain protein PDX1 is required at mid-pancreatic development for the formation of the exocrine pancreas. *Dev Biol.* **286**, 225-237.

Hale, M.A., Swift, G.H., Hoang, C.Q., Deering, T.G., Masui, T., Lee, Y.K., Xue, J., and MacDonald, R.J. (2014) The nuclear hormone receptor family member NR5A2 controls aspects of multipotent progenitor cell formation and acinar differentiation during pancreatic organogenesis. *Development* **141**, 3123-33.

Hart, A.H., Hartley, L., Sourris, K., Stadler, E.S., Li, R., Stanley, E.G., Tam, P.P., Elefanty, A.G., and Robb, L. (2002). Mixl1 is required for axial mesendoderm morphogenesis and patterning in the murine embryo. *Development* **129**, 3597–3608.

Haumaitre, C., Barbacci, E., Jenny, M., Ott, M.O., Gradwohl, G., and Cereghini, S. (2005). Lack of TCF2/vHNF1 in mice leads to pancreas agenesis. *Proc Natl Acad Sci USA* **102**, 1490–1495.

Hebrok, M., Kim, S. K., and Melton, D. A. (1998). Notochord repression of endodermal Sonic hedgehog permits pancreas development. *Genes Dev.* **12**, 1705-1713.

Hebrok, M., Kim, S.K., St Jacques. B., McMahon, A.P., and Melton, D.A. (2000). Regulation of pancreas development by hedgehog signaling. *Development* **127**, 4905-4913.

Holland, A. M., Hale, M. A., Kagami, H., Hammer, R. E., and MacDonald, R. J. (2002). Experimental control of pancreatic development and maintenance. *Proc. Natl. Acad. Sci. U.S.A.* **99**, 12236-12241.

Holmstrom, S.R., Deering, T., Swift, G.H., Poelwijk, F.J., Mangelsdorf, D.J., Kliewer, S.A., and MacDonald, R.J. (2011). LRH-1 and PTF1-L coregulate an exocrine pancreas-specific transcriptional network for digestive function. *Genes Dev.* **25**, 1674-1679.

Huang, M., Huang, T., Xiang, Y., Xie, Z., Chen, Y., Yan, R., Xu, J., and Cheng, L. (2008). Ptf1a, Lbx1 and Pax2 coordinate glycinergic and peptidergic transmitter phenotypes in dorsal spinal inhibitory neurons. *Dev Biol.* **322**, 394-405.

Hoshino, M., Nakamura, S., Mori, K., Kawauchi, T., Terao, M., Nishimura, Y.V., Fukuda, A., Fuse, T., Matsuo, N., Sone, M., et al. (2005) Ptf1a, a bHLH transcriptional gene, defines GABAergic neuronal fates in cerebellum. *Neuron* 47, 201-213.

Ishii, Y., Rex, M., Scotting, P.J., and Yasugi, S. (1998). Region-specific expression of chicken Sox2 in the developing gut and lung epithelium: regulation by epithelial-mesenchymal interactions. *Dev. Dyn.* **213**, 464-475.

Jacobsen, C.M., Narita, N., Bielinska, M., Syder, A.J., Gordon, J.I., and Wilson, D.B. (2002). Genetic mosaic analysis reveals that GATA-4 is required for proper differentiation of mouse gastric epithelium. *Dev. Biol.* **241**, 34–46.

Jacquemin, P., Lemaigre, F.P., and Rousseau, G.G. (2003). The Onecut transcription factor HNF-6 (OC-1) is required for timely specification of the pancreas and acts upstream of Pdx-1 in the specification cascade. *Dev Biol*. **258**, 105–116.

Jarikji, Z. H., Vanamala, S., Beck, C. W., Wright, C. V., Leach, S. D., and Horb, M. E. (2007). Differential ability of Ptf1a and Ptf1a-VP16 to convert stomach, duodenum and liver to pancreas. *Dev. Biol.* **304**, 786-799.

Johansson, K. A., Dursun, U., Jordan, N., Gu, G., Beermann, F., Gradwohl, G., and Grapin-Botton, A. (2007). Temporal control of neurogenin3 activity in pancreas progenitors reveals competence windows for the generation of different endocrine cell types. *Dev. Cell* **12**, 457-465.

Jonsson, J., Carlsson, L., Edlund, T., and Edlund, H. (1994). Insulin-promoter-factor 1 is required for pancreas development in mice. *Nature* **371**, 606-609.

Jusuf, P.R., Almeida, A.D., Randlett, O., Joubin, K., Poggi, L., and Harris, W.A. (2011). Origin and determination of inhibitory cell lineages in the vertebrate retina. J Neurosci. 31, 2549-2562.

Kanai-Azuma, M., Kanai, Y., Gad, J. M., Tajima, Y., Taya, C., Kurohmaru, M., Sanai, Y., Yonekawa, H., Yazaki, K., Tam, P. P., and Hayashi, Y. (2002). Depletion of definitive gut endoderm in Sox17-null mutant mice. *Development* **129**, 2367-2379.

Kawaguchi, Y., Cooper, B., Gannon, M., Ray, M., MacDonald, R., and Wright, C. V. (2002). The role of the transcriptional regulator Ptf1a in converting intestinal to pancreatic progenitors. *Nat. Genet*. **32**, 128-134.

Kesavan, G., Sand, F.W., Greiner, T.U., Johansson, J.K., Kobberup, S., Wu, X., Brakebusch, C., Semb, H. (2009). Cdc42-mediated tubulogenesis controls cell specification. *Cell* **139**, 791-801.

Kim, D.G., Kang, H.M., Jang, S.K., and Shin, H.S. (1992). Construction of a bifunctional mRNA in the mouse by using the internal ribosomal entry site of the encephalomyocarditis virus. *Mol. Cell Biol.* **12**, 3636-3643.

Kim, S.K., Hebrok, M., and Melton, D.A. (1997). Notochord to endoderm signaling isrequired for pancreas development. *Development* **124**, 4243–4252.

Kim, S.K., and Melton, D.A. (1998) Pancreas development is promoted by cyclopamine, a hedgehog signaling inhibitor. *Proc Natl Acad Sci USA* **95**, 13036-13041.

Kopp, J.L., Dubois, C.L., Schaffer, A.E., Hao, E., Shih, H.P., Seymour, P.A., Ma, J., and Sander, M. (2011). Sox9+ ductal cells are multipotent progenitors throughout development but do not produce new endocrine cells in the normal or injured adult pancreas. *Development* **138**, 653-665.

Krapp, A., Knöfler, M., Ledermann, B., Bürki, K., Berney, C., Zoerkler, N., Hagenbüchle, O., and Wellauer, P. K. (1998) The bHLH protein PTF1-p48 is essential for the formation of the exocrine and the correct spatial organization of the endocrine pancreas. *Genes Dev*. **12**, 3752-3763.

Kroon, E., Martinson, L. A., Kadoya, K., Bang, A. G., Kelly, O. G., Eliazer, S., Young, H., Richardson, M., Smart, N. G., Cunningham, J. et al. (2008). Pancreatic endoderm derived from human embryonic stem cells generates glucose-responsive insulin-secreting cells in vivo. *Nat. Biotechnol.* **26**, 443-452.

Kwon, G.S., Viotti, M., Hadjantonakis, A.K. (2008). The endoderm of the mouse embryo arises by dynamic widespread intercalation of embryonic and extraembryonic lineages. *Dev. Cell* 15, 509-520.

Lakso, M., Pichel, J.G., Gorman, J.R., Sauer, B., Okamoto, Y., Lee, E., Alt, F.W., and Westphal, H. (1996). Efficient in vivo manipulation of mouse genomic sequences at the zygote stage. *Proc Natl Acad Sci U S A* **93**, 5860-5865.

Lawson, A., and Schoenwolf, G.C. (2003). Epiblast and primitive-streak origins of the endoderm in the gastrulating chick embryo. *Development* **130**, 3491-3501.

Lawson, K.A., Meneses, J.J., and Pedersen RA. (1986). Cell fate and cell lineage in the endoderm of the presomite mouse embryo, studied with an intracellular tracer. *Dev. Biol.* 115:325-339.

Lee, E. R., Trasler, J., Dwivedi, S., and Leblond, C. P. (1982). Division of the mouse gastric mucosa into zymogenic and mucous regions on the basis of gland features. *Am. J. Anat.* **164**, 187-207.

Lee, E.C., Yu, D., Martinez de Velasco, J., Tessarollo, L., Swing, D.A., Court, D.L., Jenkins, N.A., and Copeland, N.G. (2001). A highly efficient Escherichia coli-based chromosome engineering system adapted for recombinogenic targeting and subcloning of BAC DNA. *Genomics* **73**, 56-65.

Lelièvre, E.C., Lek, M., Boije, H., Houille-Vernes, L., Brajeul, V., Slembrouck, A., Roger, J.E., Sahel, J.A., Matter, J.M., Sennlaub, F., Hallböök, F., Goureau, O., and Guillonneau X. (2011). Ptf1a/Rbpj complex inhibits ganglion cell fate and drives the specification of all horizontal cell subtypes in the chick retina. *Dev. Biol.* **358**, 296-308.

Liu, J., Willet, S.G., Bankaitis, E.D., Xu, Y., Wright, C.V., and Gu, G. (2013) Non-parallel recombination limits Cre-LoxP-based reporters as precise indicators of conditional genetic manipulation. *Genesis.* **51**, 436-442.

McCracken, K. W. and Wells, J. M. (2012). Molecular pathways controlling pancreas induction. *Semin. Cell Dev. Biol.* **23**, 656-662.

Marshak, S., Benshushan, E., Shoshkes, M., Havin, L., Cerasi, E., and Melloul, D. (2000). Functional conservation of regulatory elements in the pdx-1 gene: PDX-1 and hepatocyte nuclear factor 3beta transcription factors mediate beta-cell-specific expression. *Mol. Cell Biol*. **20**, 7583-7590.

Masui, T., Long, Q., Beres, T. M., Magnuson, M. A., and MacDonald, R. J. (2007). Early pancreatic development requires the vertebrate suppressor of hairless (RBPJ) in the PTF1 bHLH complex. *Genes Dev.* **21**, 2629–2643.

Masui, T., Swift, G. H., Hale, M. A., Meredith, D. M., Johnson, J. E., and Macdonald, R. J. (2008) Transcriptional autoregulation controls pancreatic Ptf1a expression during development and adulthood. *Mol. Cell Biol.* **28**, 5458-5468.

Masui, T., Swift, G.H., Deering, T., Shen, C., Coats, W.S., Long, Q., Elsässer, H.P., Magnuson, M.A., and MacDonald, R.J. (2010) Replacement of Rbpj with Rbpjl in the PTF1 complex controls the final maturation of pancreatic acinar cells. *Gastroenterology* **139**, 270-280.

Meredith, D.M., Borromeo, M.D., Deering, T.G., Casey, B.H., Savage, T.K., Mayer, P.R., Hoang, C., Tung, K.C., Kumar, M., Shen, C., Swift, G.H., Macdonald, R.J., and Johnson, J.E. (2014). Program specificity for Ptf1a in pancreas versus neural tube development correlates with distinct collaborating cofactors and chromatin accessibility. *Mol. Cell Biol.* **33**, 3166-3179.
Minoo, P., Su, G., Drum, H., Bringas, P., and Kimura, S. (1999). Defects in tracheoesophageal and lung morphogenesis in Nkx2.1(-/-) mouse embryos. *Dev. Biol*. **209**, 60-71.

Morrisey, E.E., Tang, Z., Sigrist, K., Lu, M.M., Jiang, F., Ip, H.S., Parmacek, M.S. (1998). GATA6 regulates HNF4 and is required for differentiation of visceral endoderm in the mouse embryo. *Genes Dev.* **12**, 3579–3590.

Morrisey, E. E. and Hogan, B. L. (2010). Preparing for the first breath: genetic and cellular mechanisms in lung development. *Dev. Cell* **18**, 8-23.

Offield, M. F., Jetton, T. L., Labosky, P. A., Ray, M., Stein, R. W., Magnuson, M. A., Hogan, B. L., and Wright, C. V. (1996). PDX-1 is required for pancreatic outgrowth and differentiation of the rostral duodenum. *Development* **122**, 983-995.

Oliver-Krasinski, J. M., Kasner, M. T., Yang, J., Crutchlow, M. F., Rustgi, A. K., Kaestner, K. H., and Stoffers, D. A. (2009). The diabetes gene Pdx1 regulates the transcriptional network of pancreatic endocrine progenitor cells in mice. *J. Clin. Invest.* **119**, 1888-1898.

Pan, F. C., Bankaitis, E. D., Boyer, D., Xu, X., Van de Casteele, M., Magnuson, M. A., Heimberg, H., and Wright, C. V. (2013). Spatiotemporal patterns of multipotentiality in Ptf1a-expressing cells during pancreas organogenesis and injury-induced facultative restoration. *Development* **140**, 751-764.

Pan, F. C. and Wright, C. (2011). Pancreas organogenesis: from bud to plexus to gland. *Dev. Dyn.* **240**, 530-65.

Pedersen, J. K., Nelson, S. B., Jorgensen, M. C., Henseleit, K. D., Fujitani, Y., Wright, C. V., Sander, M., Serup, P.; Beta Cell Biology Consortium. (2005). Endodermal expression of Nkx6 genes depends differentially on Pdx1. *Dev. Biol.* **288**, 487-501.
Pikaart, M.J., Recillas-Targa, F., and Felsenfeld, G. (1998). Loss of transcriptional activity of a transgene is accompanied by DNA methylation and histone deacetylation and is prevented by insulators. *Genes Dev.* **12**, 2852-2862.

Pin, C.L., Rukstalis, J.M., Johnson, C., Konieczny, S.F. (2001). The bHLH transcription factor Mist1 is required to maintain exocrine pancreas cell organization and acinar cell identity. *J. Cell Biol.* **155**, 519-530.

Que, J., Okubo, T., Goldenring, J. R., Nam, K. T., Kurotani, R., Morrisey, E. E., Taranova, O., Pevny, L. H., and Hogan, B. L. (2007). Multiple dose-dependent roles for Sox2 in the patterning and differentiation of anterior foregut endoderm. *Development* **134**, 2521-2531.

Rodolosse, A., Campos, M.L., Rooman, I., Lichtenstein, M., and Real, F.X. (2009). p/CAF modulates the activity of the transcription factor p48/Ptf1a involved in pancreatic acinar differentiation. *Biochem. J.* **418**, 463-473.

Rodríguez, C.I., Buchholz, F., Galloway, J., Sequerra, R., Kasper, J., Ayala, R., Stewart, A.F., and Dymecki, S.M. (2000). High-efficiency deleter mice show that FLPe is an alternative to Cre-loxP. *Nat Genet.* **25**, 139-140.

Sasaki, H., and Hogan, B.L. (1993). Differential expression of multiple forkhead related genes during gastrulation and axial pattern formation in the mouse embryo. *Development* **118**, 47–59.

Schaffer, A. E., Freude, K. K., Nelson, S. B., and Sander, M. (2010). Nkx6 transcription factors and Ptf1a function as antagonistic lineage determinants in multipotent pancreatic progenitors. *Dev. Cell* **18**, 1022-1029.

Seymour, P.A., Shih, H.P., Patel, N.A., Freude, K.K., Xie, R., Lim, C.J., and Sander M. (2012). A Sox9/Fgf feed-forward loop maintains pancreatic organ identity. *Development* **139**, 3363-3372.

Shaner, N.C., Lin, M.Z., McKeown, M.R., Steinbach, P.A., Hazelwood, K.L., Davidson, M.W., and Tsien, R.Y. (2008). Improving the photostability of bright monomeric orange and red fluorescent proteins. Nat. Methods **5**, 545-51.

Sherwood, R.I., Chen, T.Y., and Melton, D.A. (2009) Transcriptional dynamics of endodermal organ formation. *Dev. Dyn.* **238**, 29-42.

Smith, D.B. and Johnson, K.S. (1988). Single-step purification of polypeptides expressed in Escherichia coli as fusions with glutathione S-transferase. *Gene*. **67**, 31-40.

Shi, G., Zhu, L., Sun, Y., Bettencourt, R., Damsz, B., Hruban, R.H., and Konieczny, S.F. (2009). Loss of the acinar-restricted transcription factor Mist1 accelerates Kras-induced pancreatic intraepithelial neoplasia. *Gastroenterology* **136**, 1368-1378.

Solar, M., Cardalda, C., Houbracken, I., Martín, M., Maestro, M.A., De Medts, N., Xu, X., Grau, V., Heimberg, H., Bouwens, L., and Ferrer, J. (2009). Pancreatic exocrine duct cells give rise to insulin-producing beta cells during embryogenesis but not after birth. *Dev. Cell* **17**, 849-660.

Soufi, A., Donahue, G., and Zaret, K.S. (2012). Facilitators and impediments of the pluripotency reprogramming factors' initial engagement with the genome. *Cell* **151**, 994-1004.

Spence, J. R., Lange, A. W., Lin, S. C., Kaestner, K. H., Lowy, A. M., Kim, I., Whitsett JA, and Wells JM. (2009). Sox17 regulates organ lineage segregation of ventral foregut progenitor cells. *Dev. Cell* **17**, 62-74.

Srinivas, S., Watanabe, T., Lin, C.S., William, C.M., Tanabe, Y., Jessell, T.M., and Costantini, F. (2001). Cre reporter strains produced by targeted insertion of EYFP and ECFP into the ROSA26 locus. *BMC Dev Biol.* Epub 2001 Mar 27.

Syder, A.J., Guruge, J.L., Li, Q., Hu, Y., Oleksiewicz, C.M., Lorenz, R.G., Karam, S.M., Falk, P.G., and Gordon, J.I. (1999). Helicobacter pylori attaches to NeuAc alpha 2,3Gal beta 1,4 glycoconjugates produced in the stomach of transgenic mice lacking parietal cells. *Mol. Cell* **3**, 263-274

Takahashi, K. and Yamanaka, S. (2006) Induction of pluripotent stem cells from mouse embryonic and adult fibroblast cultures by defined factors. *Cell* **126**, 663-676.

Talchai, C., Xuan, S., Lin, H. V., Sussel, L., and Accili, D. (2012). Pancreatic β cell dedifferentiation as a mechanism of diabetic β cell failure. *Cell* **150**, 1223-1234.

Taranova, O.V., Magness, S.T., Fagan, B.M., Wu, Y., Surzenko, N., Hutton, S.R., and Pevny, L.H. (2006) SOX2 is a dose-dependent regulator of retinal neural progenitor competence. *Genes Dev.* **20**, 1187-1202.

Thompson, N., Gésina, E., Scheinert, P., Bucher, P., and Grapin-Botton, A. (2012). RNA profiling and chromatin immunoprecipitation-sequencing reveal that PTF1a stabilizes pancreas progenitor identity via the control of MNX1/HLXB9 and a network of other transcription factors. *Mol. Cell Biol.* **32**, 1189-1199

Vastenhouw, N.L. and Schier, A.F. (2012) Bivalent histone modifications in early embryogenesis. *Curr. Opin. Cell Biol.* **24**, 374-386.

Villasenor, A., Chong, D.C., Henkemeyer, M., Cleaver, O. (2010) Epithelial dynamics of pancreatic branching morphogenesis. *Development* **137**, 4295-4305.

Wandzioch, E. and Zaret, K. S. (2009). Dynamic signaling network for the specification of embryonic pancreas and liver progenitors. *Science* **324**, 1707–1710.

Wang, J., Kilic, G., Aydin, M., Burke, Z., Oliver, G., and Sosa-Pineda, B. (2005). Prox1 activity controls pancreas morphogenesis and participates in the production of "secondary transition" pancreatic endocrine cells. *Dev Biol.* **286**, 182-194.

Warming, S., Costantino, N., Court, D.L., Jenkins, N.A., and Copeland, N.G. (2006). Simple and highly efficient BAC recombineering using galK selection. *Nucleic Acids Res.* **33**, e36.

Watt, A.J., Zhao, R., Li, J., and Duncan, S.A. (2007). Development of the mammalian liver and ventral pancreas is dependent on GATA4. *BMC Dev. Biol.* 7:37.

Wiebe, P. O., Kormish, J. D., Roper, V. T., Fujitani, Y., Alston, N. I., Zaret, K. S., Wright, C. V., Stein, R. W., and Gannon, M. (2007). Ptf1a binds to and activates area III, a highly

conserved region of the Pdx1 promoter that mediates early pancreas-wide Pdx1 expression. *Mol. Cell Biol.* **27**, 4093-4104.

Willet, S.G., Hale, M.A., Grapin-Botton, A., Magnuson, M.A., MacDonald, R.J., and Wright C.V.E. (2014). Dominant and Context-Specific Control of Endodermal Organ Allocation by Ptf1a. *Development*, In Press

Xie, R., Everett, L.J., Lim, H.W., Patel, N.A., Schug, J., Kroon, E., Kelly, O.G., Wang, A., D'Amour, K.A., Robins, A.J., Won, K.J., Kaestner, K.H., and Sander, M. (2013) Dynamic chromatin remodeling mediated by polycomb proteins orchestrates pancreatic differentiation of human embryonic stem cells. *Cell Stem Cell.* 12, 224-237.

Xu, C.R., Cole, P.A., Meyers, D.J., Kormish, J., Dent, S., and Zaret, K.S. (2011). Chromatin "prepattern" and histone modifiers in a fate choice for liver and pancreas. *Science* **332**, 963-966.

Xuan, S., Borok, M.J., Decker, K.J., Battle, M.A., Duncan, S.A., Hale, M.A., Macdonald, R.J., and Sussel, L. (2012) Pancreas-specific deletion of mouse Gata4 and Gata6 causes pancreatic agenesis. *J. Clin. Invest.* **122**, 3516-3528.

Yasugi S. (1993) Role of Epithelial-Mesenchymal Interactions in Differentiation of Epithelium of Vertebrate Digestive Organs. *Develop. Growth & Differ.* **35,** 1-9

Yoshitomi, H., and Zaret, K.S. (2004). Endothelial cell interactions initiate dorsal pancreas development by selectively inducing the transcription factor Ptf1a. *Development* **131**, 807–817.

Zaret, K.S. and Carroll, J.S. (2011) Pioneer transcription factors: establishing competence for gene expression. *Genes Dev.* **25**, 2227-2241.

Zhou, Q., Law, A. C., Rajagopal, J., Anderson, W. J., Gray, P. A., and Melton, D. A. (2007). A multipotent progenitor domain guides pancreatic organogenesis. *Dev. Cell* **13**, 103-14.

Zhou, Q., Brown, J., Kanarek, A., Rajagopal, J., and Melton, D.A. (2008). In vivo reprogramming of adult pancreatic exocrine cells to beta-cells. *Nature* **455**, 627-632.